Max Planck Institute for Molecular Plant Physiology

Prof. Dr. Lothar Willmitzer

Characterization of a *Chlamydomonas* protein involved in cell division and autophagy

Dissertation
zur Erlangung des akademischen Grades
Doctor rerum naturalium
(Dr. rer. nat.)
in der Wissenschaftsdisziplin
"Pflanzenphysiologie"

Eingereicht an der
Mathematisch-Naturwissenschaftlichen Fakultät
der Universität Potsdam

Yehezkel Tenenboim

Januar 2014

Published online at the
Institutional Repository of the University of Potsdam:
URL http://opus.kobv.de/ubp/volltexte/2014/7065/
URN urn:nbn:de:kobv:517-opus-70650
http://nbn-resolving.de/urn:nbn:de:kobv:517-opus-70650

Selbständigkeitserklärung

Hiermit erkläre ich, dass ich die vorliegende Arbeit selbständig und unter Verwendung keiner anderen als den von mir angegebenen Quellen und Hilfsmitteln verfasst habe. Ferner erkläre ich, dass ich bisher weder an der Universität Potsdam noch anderweitig versucht habe, eine Dissertation einzureichen oder mich einer Doktorprüfung zu unterziehen.

Yehezkel Tenenboim Januar 2014

Parts of this dissertation were published in:

Tenenboim H, Smirnova J, Willmitzer L, Steup M, Brotman Y. VMP1-deficient *Chlamydomonas* exhibits severely aberrant cell morphology and disrupted cytokinesis. Submitted.

Scenario One was more heroic and romantic. Two more prosaic and businesslike. The trouble was that the real world was not committed to behaving in either style but went on its way indifferently.

—From *Berserkers* by Fred Saberhagen

Table of contents

List of figures

List of tables

List of abbreviations

aa	Amino acids
bp	Base pairs
BSA	Bovine serum albumin
cDNA	Complementary DNA
CIAP	Calf intestine alkaline phosphatase
CV	Contractile vacuole
Ct	Threshold cycle
DNA	Deoxyribonucleic acid
ER	Endoplasmic reticulum
GC	Guanine/cytosine
HSM	High-salt medium
kDa	Kilodalton
LB	Lysogeny broth
MPIMP	Max Planck Institute for Molecular Plant Physiology, Potsdam, Germany
mRNA	Messenger RNA
MS	Mass spectrometry/spectrometer
nt	Nucleotides
PCA	Principal component analysis
PBS	Phosphate-buffered saline
PCR	Polymerase chain reaction
PE	Phosphatidylethanolamine
PI3P	Phosphatidylinositol 3-phosphate
PNK	Polynucleotide kinase
qRT-PCR	Quantitative real-time reverse-transcription PCR
RNA	Ribonucleic acid
RT	Room temperature
TAG	Triacylglyceride
TAP	Tris-acetate-phosphate
TOF	Time of flight
UCLA	University of California, Los Angeles, USA
UPLC	Ultra-performance liquid chromatography
UPPC	Department of Physical Chemistry, Universität Potsdam, Germany
YFP	Yellow fluorescent protein

Zusammenfassung

Die kontraktile Vakuole ist ein osmoregulatorisches Organell, das ausschließlich in Algen und Protisten vorkommt. Zusätzlich zu ihrer Rolle als Ausstoßer überflüßigen Wassers aus der Zelle heraus, stößt sie auch Ionen und andere Metaboliten aus, und trägt dabei zur metabolischen Homöostase der Zelle bei. Das Interesse an der kontraktilen Vakuole erstreckt sich über seine unmittelbare zelluläre Rolle hinaus. Die Funktion der kontraktilen Vakuole ist mit einigen grundsätzlichen zellulären Verfahren, wie Membrandynamik und Vesikelknospung und -fusion, verwandt; einige physiologische Verfahren in Tieren, zum Beispiel synaptische Neurotransmission und das Filtrieren des Blutes in den Nieren, sind mit der Funktion der Vakuole eng verwandt; und einige Pathogene—der Ursacher der Schlafkrankheit als Beispiel—besitzen kontraktile Vakuolen, die als Ziele von Medikamenten dienen könnten. Die grüne Alge *Chlamydomonas reinhardtii* verfügt über zwei Vakuolen. Sie sind die kleinsten bekannten in der Natur, und bleiben bisher verhältnismäßig unerforscht. Viele Gene, die in anderen Organismen als kontraktile-Vakuole-bezogen erwiesen wurden, haben Homologe in *C. reinhardtii*. Wir versuchten, diese Gene auszuschalten und den Einfluss auf die Vakuole zu beobachten. Die Ausschaltung eines unserer Gene, VMP1, verursachte starke, beachtliche Phänotype. Die Zellen zeigten gestörte Zytokinese und aberrante Zellformen. Die kontraktile Vakuole blieb jedoch verschont. Des Weiteren zeigten Mutantzellen einige Hinweise auf gestörte Autophagie. Einige wichtige Gene des Zellzyklus und der Autophagie waren unterexprimiert in Mutantzellen. Lipidomische Analyse zeigte mehrere bedeutsame Unterschiede zwischen Wildtyp und Mutant, die die Beobachtungen der gestörten Autophagie verstärkten. VMP1 ist ein singularisches Protein, mit Homologen in zähligen eukaryotischen Organismen (jedoch nicht in Pilzen), aber üblicherweise ohne Verwandte in den jeweiligen Genomen. Seit seiner Erstcharakterisierung 2002 wurde es mit etlichen zellulären Verfahren, wie Autophagie, programmiertem Zelltod, Sekretion, Zelladhäsion, und Biogenese der Organellen, assoziiert. Es wurde auch mit einigen menschlichen Krankheiten wie Diabetes, Pankreatitis, und einigen Arten von Krebs in Verbindung gebracht. Unsere Ergebnisse wiederholen einige Beobachtungen in anderen Organismen, zeigen dennoch zum ersten Mal eine Beteiligung von VMP1 an der Zellteilung. Die unterliegenden Mechanismen dieser Beteiligung in *Chlamydomonas*, sowie andere wichtige Aspekte, etwa die subzelluläre Lokalisierung von VMP1 und dessen Interaktionspartner, warten noch auf Aufklärung.

Summary

The contractile vacuole (CV) is an osmoregulatory organelle found exclusively in algae and protists. In addition to expelling excessive water out of the cell, it also expels ions and other metabolites and thereby contributes to the cell's metabolic homeostasis. The interest in the CV reaches beyond its immediate cellular roles. The CV's function is tightly related to basic cellular processes such as membrane dynamics and vesicle budding and fusion; several physiological processes in animals, such as synaptic neurotransmission and blood filtration in the kidney, are related to the CV's function; and several pathogens, such as the causative agents of sleeping sickness, possess CVs, which may serve as pharmacological targets. The green alga *Chlamydomonas reinhardtii* has two CVs. They are the smallest known CVs in nature, and they remain relatively untouched in the CV-related literature. Many genes that have been shown to be related to the CV in other organisms have close homologues in *C. reinhardtii*. We attempted to silence some of these genes and observe the effect on the CV. One of our genes, VMP1, caused striking, severe phenotypes when silenced. Cells exhibited defective cytokinesis and aberrant morphologies. The CV, incidentally, remained unscathed. In addition, mutant cells showed some evidence of disrupted autophagy. Several important regulators of the cell cycle as well as autophagy were found to be underexpressed in the mutant. Lipidomic analysis revealed many meaningful changes between wild-type and mutant cells, reinforcing the compromised-autophagy observation. VMP1 is a singular protein, with homologues in numerous eukaryotic organisms (aside from fungi), but usually with no relatives in each particular genome. Since its first characterization in 2002 it has been associated with several cellular processes and functions, namely autophagy, programmed cell-death, secretion, cell adhesion, and organelle biogenesis. It has been implicated in several human diseases: pancreatitis, diabetes, and several types of cancer. Our results reiterate some of the observations in VMP1's six reported homologues, but, importantly, show for the first time an involvement of this protein in cell division. The mechanisms underlying this involvement in *Chlamydomonas*, as well as other key aspects, such as VMP1's subcellular localization and interaction partners, still await elucidation.

1. Introduction

1.1 The contractile vacuole

1.1.1 Background

The contractile vacuole (CV) is an osmoregulatory organelle found only in protists and algae. Its main function is simple: the expulsion of excessive water from the cell. Despite being known since the late 18th century (Spallanzani, 1799), the CV remains a relatively obscure organelle. The total number of articles discussing the CV—less than 300—speaks for itself. Subtracting from this number all the articles discussing the CV from an anatomical, structural, biophysical, biochemical, or taxonomic angle, we are left with a handful of works that provide molecular-biological insights as to the function of the CV.

Why is the CV interesting at all? As it turns out, there is much more to it than merely being a rather rare and exotic organelle that occurs in but a handful of genera. First, as the mechanisms underlying the CV's function increasingly become elucidated, it appears more and more clearly that very basic cellular processes and phenomena, such as vesicle formation, budding and fusion, endo- and exocytosis, membrane dynamics, and ion transport across membranes, all play a major role. Learning more about the CV contributes to a body of knowledge that goes well beyond the organelle itself.

Second, while higher organisms have no CV, they seem to have retained several functions that resemble that of the CV to a great extent (Allen et al., 2008). The fashion in which the nephrons in the mammalian kidney filter toxic waste out of the blood; the way neurotransmitters diffuse from one neuron into its neighbor in the synapse; and the way hydrochloric acid is secreted in the stomach; all these processes are linked in one way or the other to the function of the CV, and are conceivably a remnant from the olden days of unicellularity (Allen et al., 2008). Allen and his colleagues articulately opine: "Thus, further study of how primitive cells solved problems they faced in their environments can continue to shed light on how the essential properties of these systems changed and evolved in higher organisms".

Third, several pathogens, most notably *Trypanosoma*, the causing agent of sleeping sickness and Chagas disease, possess CVs (Rohloff et al., 2004). The parasite, residing within different organisms (mosquitos and humans), and while in humans travelling in different compartments (blood, lymph), needs the CV to handle these diverse osmotic environments. The CV can thus serve as a target for novel therapeutic agents.

1.1.2 Features

The CV is a circular organelle, surrounded by a membrane. In addition to its main part, the vacuole itself, it also consists of a network of water-carrying ducts (also called arms, tubules, ampullae, or spongiome). The vacuole and the ducts combined are sometimes called "the contractile-vacuole complex" (CVC). The CV works in a simple, straightforward way: when the cell fills with excessive water, usually water that diffuses from the extracellular environment into the cell, the CV absorbs some of this water and swells. After swelling to its maximum volume it collapses and expels the water out of the cell. The water-collecting stage is called diastole, the expulsion—systole. The former lasts from 10 seconds to several minutes, depending in which organism, while the systole lasts a fraction of a second.

1.1.3 Current research and open questions

Four organisms star in, tentatively, 99 % of CV publications. In *Amoeba* and *Paramecium*, harboring the largest and second-largest CVs, respectively, pioneer biophysical work has been performed, often involving micromanipulation and CV isolation, and discussing the osmoregulatory aspect of the CV as well as membrane dynamics. *Dictyostelium* entered the scene in 1978 (Chastellier et al.) and has since then been dominating the field, appearing in around half of all CV-related articles. Its sequenced genome (Eichinger et al., 2005) and easy genetics (Kuwayama et al., 2002) make it an ideal candidate for finding and characterizing novel CV-related proteins, indeed the dominant subject of CV articles in this organism. Last but not least, *Trypanosoma* occupies the niche of CV-containing pathogens. The remaining 1 % are articles characterizing new species of algae and protists that, incidentally, contain CVs. Despite a surge in CV-related publications in the last decade, much remains unknown.

1.1.3.1 Membrane composition and dynamics

The CV is a membrane-bound organelle. Is this membrane identical to the plasma membrane? What are its lipid composition and biophysical properties? What happens to the membrane after the CV contracts? Does a new CV form *de novo* or does the old CV refill with water? And mainly: is the pumping an active process of contraction or rather a passive collapse? Work in *Paramecium*, *Amoeba* and *Dictyostelium* has supplied some answers—and controversy. While Wigg and colleagues (1967) determined that the CV passively collapses rather than actively contracts, to the extent of suggesting to rename it "water expulsion vesicle", almost three decades later both motor proteins myosin (Doberstein et al., 1993) and α-actinin (Furukawa and Fechheimer, 1994) were found to localize to the CV, and, in the former case, to be essential to its function (indeed, those three articles discuss different organisms—*Amoeba*, *Acanthamoeba* and *Dictyostelium*, respectively—but this does not diminish the controversy). In *Paramecium*, eight articles published between 1997 and 2002 (summarized in Tani et al., 2002), all from the same group at the University of Hawaii, provided a detailed biophysical analysis of the CV contraction in this organism, and concluded that periodic changes in the spontaneous curvature of the CV's lipid bilayer membrane, combined with pressure from the cytosol, are responsible for water expulsion. In *Dictyostelium* a similar conclusion was reached: the CV contracts of its own accord, with no involvement of any motor proteins (Heuser, 2006). Concise experimental evidence to support any of the hypotheses is still lacking.

1.1.3.2 Water dynamics

How does water enter the CV? Does diffusion take place, or rather active transport? How is water kept segregated within the CV, although its lipid membrane is essentially water-permeable? Is water the only thing expelled by the CV? This much is known: aquaporins, a class of water channels, are present in the CV membrane (Montalvetti et al., 2004; Nishihara et al., 2008), in addition to vacuolar proton pumps (V-H^+ATPases; Heuser et al., 1993; Fok et al., 1995). The fluid inside the CV was found to be very rich in potassium and chloride ions (Stock et al., 2002). The CV was shown to function in the regulation of calcium-ion concentrations in the cell, with the aid of a Ca^{2+}-ATPase located in the CV membrane (Moniakis et al., 1999). In fact, high extracellular calcium concentrations induce the formation of extra CVs in *Paramecium* (Iwamoto et al., 2003). In *Trypanosoma*, inorganic phosphate was shown to play a major role: acidocalcisomes, small organelles rich in phosphate, were shown to fuse with the CV, presumably in order to increase the latter's ionic strength (Rohloff et al., 2004). Combining all these observations, it seems that the CV constantly works to increase its own osmotic strength

in order to create a gradient that will cause water to migrate, facilitated by aquaporins, from the cytosol to the CV. This is achieved by means of ion transfer across the CV membrane. In addition, the cell uses the CV as a tool for ionic homeostasis. Still, many gaps exist in this model: for instance, only a single ion transporter, aside from the proton pumps, has thus far been found in the CV membrane (Moniakis et al., 1999).

1.1.3.3 Organellar interactions

There is much evidence pointing toward intracellular interactions between the CV and other organelles and structures in the cell. As described above, acidocalcisomes were shown to fuse with the CV in *Trypanosoma* (Rohloff et al., 2004). The cytoskeleton, despite the uncertainty revolving around myosin's and actin's involvement in contraction (see above), was unequivocally shown to interact with the CV: Jung and colleagues (2009) showed that a myosin protein is responsible for the recycling of CV membranes after contraction, for anchoring the CV to the plasma membrane, and for movement of CV components along actin filaments and microtubules. In flagellated species, such as *T. cruzi* and *C. reinhardtii*, the CV is located near the flagellar pit. The two organelles are apparently not indifferent to each other: upon inactivation of a single protein in *C. reinhardtii*, Komsic-Buchmann and colleagues (2012) observed both aberrant CVs and overlong flagella. The water expelled from the CV pours into the flagellar pocket in *T. cruzi* (Rohloff et al., 2004). Lastly, the CV was shown to be responsible for transporting a certain cell-membrane protein to its destination, thereby replacing the classical ER and Golgi vesicles normally used for this purpose, and adding yet another role to the CV (Sesaki et al., 1997).

1.1.3.4 Proteins

As of March 2011, a total of 23 CV-related proteins have been reported in all organisms. The work of Ulrich and colleagues (2011), in which the *Trypanosoma* CV was subjected to mass-spectrometry-aided proteomic analysis, more than tripled this number. Alkaline phosphatase was the first protein to be found in the CV (Quiviger et al., 1978). The proteins that followed represent a wide variety of families and functions: motor proteins (Jung et al., 2009), regulators of cytoskeletal reorganization (Heath et al., 2008), ion transporters (Moniakis et al., 1999), messenger proteins (Zhu and Clarke, 1992), proton pumps (Heuser et al., 1993; Fok et al., 1995), water channels (Montalvetti et al., 2004; Nishihara et al., 2008), a caspase (Saheb et al., 2013), a cell-adhesion protein (Sesaki et al., 1997), various calcium regulators (Damer et al., 2005; Ladenburger et al., 2006), and,

prominently, several proteins involved in traffic, secretion and vesicle physiology (Gerald et al., 2002; Du et al., 2008; Komsic-Buchmann et al., 2012).

Should the incentives listed above (**Section 1.1.1**) for researching the CV not suffice, several CV-related proteins are associated with human diseases: MEGAP (mental retardation GTPase-activating protein; Heath et al., 2008) proteins are implicated in 3p⁻ syndrome; BEACH (beige and Chediak-Higashi; Gerald et al., 2002) proteins—in Chediak-Higashi syndrome; VwkA (von Willebrand kinase A; Betapudi et al., 2005)—in von Willebrand disease; and last but not least, VMP1, the main subject of our study, has a proven role in cancer (Sauermann et al., 2008; Ying et al., 2011; Guo et al., 2012), in diabetes (Grasso et al., 2009), and in pancreatitis (Dusetti et al., 2002; Vaccaro et al., 2003).

In the majority of the studies disruption of the genes encoding these proteins was attempted. This produced a wide spectrum of phenotypes, only a fraction of which manifested in the CV itself. Focusing for the moment on the CV, we are met with CV-less cells (Calvo-Garrido et al., 2008); cells with abnormally enlarged CVs (Damer et al., 2007); cells with morphologically and functionally defective CVs (Betapudi et al., 2009); cells with overnumbered CVs (Heath et al., 2008); and cells that encompass, in separate individuals, all of the above (Komsic-Buchmann et al., 2012). Osmoregulation was defective in practically all of these CV mutants. As for other phenomena, silencing of CV-related genes has resulted in defects in protein secretion and targeting (Calvo-Garrido et al., 2008); in multinucleated cells (Damer et al., 2007); in defective calcium regulation (Moniakis et al., 1999); in abnormal cell morphology (Heath et al., 2008); to name but a few. **Figure 1** provides a visual sample of aberrant CVs in some of the examples listed above.

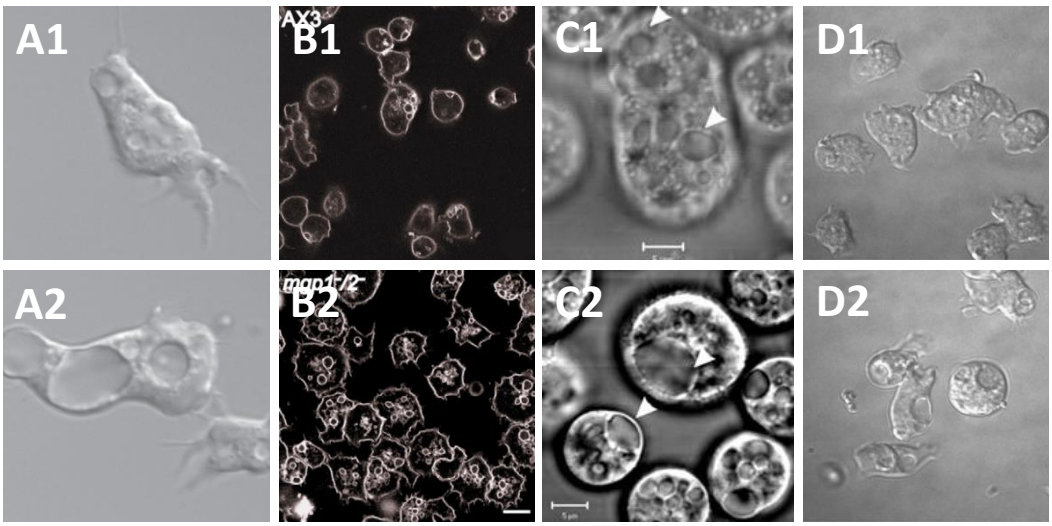

Figure 1 (previous page)**. Disruption of certain genes in *D. discoideum* results in aberrant CVs.** Top-panel images show WT cells, bottom-panel images their corresponding mutants. (A) Taken from Damer et al. (2007). (B) Taken from Heath et al. (2008). (C) Taken from Betapudi et al. (2009). (D) Taken from Du et al. (2008).

The link that those studies create between the CV and crucial cellular processes is unmistakable and underscores the importance of this organelle. The study by Ulrich and colleagues (2011), revealing 220 proteins associated with the *Trypanosoma* CV, points at the incompleteness of our current documented repertoire of CV proteins.

1.1.4 The *Chlamydomonas* CV

As of 2013, only three articles have been published that directly discuss the CV in *C. reinhardtii*. Another handful of articles mentions the *C. reinhardtii* CV in passing. Considering the model-organism status of this species, the thousands of articles discussing it, its sequenced genome (Merchant et al., 2007), and its ever-growing toolbox, this paucity of articles discussing its CV is perplexing.

The CV in different species comes in a wide array of sizes, numbers and physiological characteristics. Some species of *Amoeba* have CVs that span 300 µm in diameter. Such large CVs can be easily isolated and micromanipulated; microscopic electrodes can be inserted into them and their biophysical properties measured (Schmidt-Nielsen and Schrauger, 1963). *C. reinhardtii* sports, with a diameter of 1–2 µm, the smallest known CV. Its small size all but precludes applying those methods. In addition, common tools regularly used in CV research, such as gene silencing and protein localization by means of fluorescence, are more challenging in *C. reinhardtii*, with its high-GC-content genome, its reluctance to express foreign genes, and its intractability in terms of homologous recombination as a means for gene silencing. All of this may serve to explain the meagre attention that the *Chlamydomonas* CV has received.

C. reinhardtii has two CVs, while other *Chlamydomonas* species have one, or four, or more. This has occasionally been used in the past—not only in *Chlamydomonas*—as a species-defining feature in cases of ambiguous taxonomic identification (Harris, 2009). The CV cycle in *C. reinhardtii* takes 10–20 seconds; the two CVs usually contract alternately, not together. Luykx and colleagues (1997a) assayed the *C. reinhardtii* CV extensively in terms of function and ultrastructure, and observed that the CV lacks the distinction between bladder and collection ducts (spongiome), which is a hallmark of the CV in *Paramecium* and *Dictyostelium*. Instead, at the water-filling stage

of the CV cycle in *C. reinhardtii*, the CV appears to be composed of several small vacuoles that eventually fuse to form one large vacuole (a total of two in each cell). Whether the *Chlamydomonas* CV is indeed fundamentally different from the one in other organisms, or whether the former's structure is similar but perhaps less visible, remains to be clarified. The same group also generated mutants that showed various defects in the CV cycle (Luykx et al., 1997b). However, the underlying genes were never identified.

1.2 Our approach

Focusing our efforts on the "proteins" category of unresolved questions, we wondered how many of the CV-related proteins already reported in the literature had homologues in *C. reinhardtii*; and what was known about them. The answers we found were: many; and not much. Indeed, almost every CV-related protein in *D. discoideum* has a *C. reinhardtii* homologue, and in almost every case these are novel, non-annotated, non-reported proteins of unknown function.

We embarked on a simple reverse-genetics endeavor which consisted of silencing as many genes as we could handle and watching what happened to the CV. It had been clear even before we started that the task would soon outgrow our capabilities: gene silencing in *Chlamydomonas* is still in its infancy and is by no means problem-free; the number of genes in our list was overwhelming; and we assumed, even hoped, that the CV would not be the end of the story and that our silenced strains might honor our efforts with a motley palette of phenotypes that would threaten to cause our original quest to fade into distant memory. Indeed, these considerations forced us to gradually narrow the scope of our work, focusing on an ever-diminishing number of genes, trading amount for depth.

1.3 Aim of the thesis

The initial aim of the thesis had been the characterization of novel, putative, CV-related proteins in *C. reinhardtii*. As our focus gradually narrowed on one such protein, namely VMP1, we aimed to characterize it in terms of its role in the various processes to which it appeared to be linked—cell division and autophagy—but also on a broader scale, by analyzing its effects on global metabolism. We aimed to compare our observations regarding this protein with reports from other organisms, and to offer explanations for the differences and similarities, especially in light of the structural features and the phylogenetic lineage of the proteins in questions.

2. Materials and Methods

2.1 Materials

2.1.1 Chemicals

Chemicals and reagents were purchased from Sigma-Aldrich (München, Germany) and Carl Roth (Karlsruhe, Germany), with the following exceptions: the fluorescent styryl dye FM4-64 was purchased from Molecular Probes, now Life Technologies (Darmstadt, Germany); paromomycin was purchased from VWR (Darmstadt, Germany); ATP was purchased from Roche (Mannheim, Germany). Vectashield was purchased from Vector Labs (Burlingame, California, USA).

2.1.2 Media

For *Chlamydomonas* cultivation, tris-acetate-phosphate (TAP) medium (Gorman and Levine, 1965) was almost always used. This medium provides acetate as carbon source; cells growing in it, when combined with light, grow mixotrophically. For several experiments we used high-salt medium (HSM; Sueoka, 1960), which contains no carbon source, and in which cells grow autotrophically. Both TAP and HSM contain a mixture of trace elements developed by Hutner et al. (1950).

Hutner's trace elements:

50 g EDTA in 250 ml water

11.4 g boric acid in 200 ml water

22 g zinc sulfate heptahydrate in 100 ml water

5.06 g manganese chloride tetrahydrate in 50 ml water

5 g iron (II) sulfate heptahydrate in 50 ml water

1.6 g cobalt (II) chloride hexahydrate in 50 ml water

1.57 g copper (II) sulfate pentahydrate in 50 ml water

1.1 g ammonium heptamolybdate tetrahydrate in 50 ml water

► Mix and allow two weeks to precipitate. Remove pellet by filtration.

Salt solution:

15 g ammonium chloride

4 g magnesium sulfate heptahydrate

2 g calcium chloride

► Add water to 1,000 ml.

Phosphate solution:

28 g dipotassium hydrogen phosphate

14.4 g potassium dihydrogen phosphate

► Add water to 100 ml.

Beijernick's solution:

100 g ammonium chloride

4 g magnesium sulfate heptahydrate

2 g calcium chloride

► Add water to 1,000 ml.

TAP medium:

1 ml Hutner's trace elements

1 ml acetic acid

2.42 g tris

25 ml salt solution

375 µl phosphate solution

► Add water to 1,000 ml.

HS medium:

5 ml phosphate solution

5 ml Beijernick's solution

1 ml Hutner's trace elements

► Add water to 1,000 ml.

Solid medium:

15 g agar

2 g tryptone or peptone

2 g yeast extract

► Add to 1,000 ml TAP or HSM.

For *Escherichia coli* cultivation, lysogeny broth (LB; Bertani, 1951) medium was used:

10 g tryptone or peptone

5 g yeast extract

10 g sodium chloride

► Add water to 1,000 ml.

Solid medium:

15 g agar

► Add to 1,000 ml LB medium.

2.1.3 Kits, plasmids and enzymes

Enzymes were, unless stated otherwise, purchased from New England Biolabs (Frankfurt am Main, Germany). **Table 1** provides an overview of the kits and enzymes used in this work, excluding enzymes purchased from New England Biolabs.

Table 1. Kits, plasmids and enzymes used in this work

Purpose	Product's name	Manufacturer
RNA isolation	Universal RNA Purification Kit	Roboklon (Berlin, Germany)
cDNA synthesis	First Strand cDNA Synthesis Kit	Thermo Scientific (Schwerte, Germany)
DNA extraction from PCR and gels	Wizard SV Gel and PCR Clean-Up System	Promega (Mannheim, Germany)
Plasmid extraction from bacterial cultures	QIAprep Spin Miniprep Kit	Qiagen (Hilden, Germany)
qRT-PCR	Power SYBR Green PCR Master Mix	Life Technologies (Darmstadt, Germany)
PCR	DreamTaq	Thermo Scientific (Schwerte, Germany)
High-fidelity PCR	Q5 High-Fidelity DNA Polymerase	New England Biolabs (Frankfurt am Main, Germany)
Cloning	pGEM-T	Promega (Mannheim, Germany)

2.1.4 Primers and oligonucleotides

Primers and other oligonucleotides (**Table 2**) were ordered from Sigma-Aldrich (Taufkirchen, Germany). Primers were always synthesized on a 0.025 µmol scale and purified by desalting. The indication -F and -R in a primer's name stand for "forward" and "reverse", respectively. Most qRT-PCR primers were a gift from Jessica Jueppner, MPIMP. qRT-PCR primers that were not a gift were designed using the online service QuantPrime (Arvidsson et al., 2008).

Table 2. Primers and oligonucleotides used in this work

Name	Sequence
Purpose: cloning of amiRNA construct for silencing *VMP1*. The sequence targeting the gene's mRNA is underlined.	
amiRNA-vmp1-F	CTAGTTTGAGGTAGAGGATCTTTCAATCTCGCTGATCGGCACCATGGGGGT GGTGGTGATCAGCGCTATTGAGGGATCCTCTACCTCAAG
amiRNA-vmp1-R	CTAGCTTGAGGTAGAGGATCCCTCAATAGCGCTGATCACCACCACCCCCAT GGTGCCGATCAGCGAGATTGAAAGATCCTCTACCTCAAA
Purpose: screening for bacteria carrying the cloned amiRNA construct using colony PCR, and sequencing positive clones to confirm the integrity of the construct.	
amiRNA-F/R	GGTGTTGGGTCGGTGTTTTTG and TAGCGCTGATCACCACCACCC
Purpose: quantification of mRNA levels by qRT-PCR. Nomenclature: qPCR-gene-F/R.	
qPCR-vmp1-F/R	TGACGGACTGAGTTGGAAAGGC and GAGCTAGAGGCTTCTTGCGTTG
qPCR-ubiquitin-F/R	TTACCTGCCTTCCGATTGCGTAGC and TTACTATGCCTGAGCACGCAGCAC
qPCR-RACK1-F/R	CTTCTCGCCCATGACCAC and CCCACCAGGTTGTTCTTCAG
qPCR-RCC1-F/R	AGGTATGGAAGCCGGAGTCACT and CCGCACACCAGCTTCTTGA
qPCR-RCCD1-F/R	GTGTGAGAACACGGCAATTGC and TCCGCATCGCGTACTGATG
qPCR-CYN20-2-F/R	GACGCATGCCCCATAATGC and CCACCAGGAGGAGGTAGAAAGC
qPCR-CY28-F/R	GCTTGGCTTGCAGCTCGTAGT and TCCACCCCTGCCACTCAAC
qPCR-CYN20-1-F/R	GGACGTTGAATGCCCTAGTAAGC and CGTTCCGCTCGCACATG
qPCR-PIN4-F/R	GGGCATAGCGTGTGATGCAT and TTGCAACTATTTGCGCAGTTATGA
qPCR-CYN19-2-F/R	GAGGGCCTGACATCGGAGTT and TGCCAAATTGCTCCATGCA
qPCR-CYN20-3-F/R	CTTCCACCGCGTCATCAAG and TTGCCGGCAGTGAAGTCA
qPCR-FKB15-1-F/R	CAGCAGGGCCGAGTTTCAC and AGGTATCATAGCCGGGCGTTAC
qPCR-FKB12-F/R	CGTGTTCTTGATTTGATGGTAGTGTAAC and CCGTCCTTCGCAGTGCAA
qPCR-CYN40-F/R	CCACGTACGCACGCATGTT and CAACGGATCGCCGACTCA
qPCR-CYCA1-F/R	TTCCGTCGGCGATTAACTACTCC and TACTCCCTTGCTCACATCCTGGTG
qPCR-CYCB1-F/R	AATGGAAGAGGAGTCGCTGTTCGG and TCCAACATCACTGCAAGTCTCTGG
qPCR-CYCC1-F/R	AGAACTCGCATGCAGAAGACAGG and AAGCTCCGCGATACTTGTGC
qPCR-CYCD1-F/R	ACAAAGGACTGGGCAATGGCATC and TGGAGGTGCGAGAAAGAGTCTG
qPCR-CYCD2-F/R	GCAACAAGAAGCCACTGTATCAGC and AGCAGTGCGTTGTGGTACTGAC
qPCR-CYCD3-F/R	ACAGCGGCGAGATGGTTATTGC and ACGCCCTCAGAATGCATGTTCC
qPCR-CYCL1-F/R	GTGTTTGACCGGATCAACAAGCG and TACTCCTTGGTCTCGGGTATCAGC
qPCR-CYCM1-F/R	AGAAGGTTCTGGCGCTTGCTAAC and GGCATAGAGCTCGTTGATTTGCG
qPCR-CYCU1-F/R	CAAGCTCACAGACGACCACTAC and GTTGATCTCCTGGACACTGACG
qPCR-E2FR1-F/R	AAAGCTCATCGTGTGGCAAGGC and TGCCGTTTCTGTGCGGTATCTG
qPCR-CDC48-F/R	GGCGGATGTCGCCTTGA and CCCTAAGCATGCAACAATGCA
qPCR-ACY1-F/R	TTCCTTGTGTTTGCGTTGTGG and TCAAAACAGGTCCCCCAACAG
qPCR-Asp-Prot-F/R	GCATTGACCCTACCCACTTCAC and TGAACTGCCAGTAGCCCTGG
qPCR-ATG3-F/R	GGTGCTGTTTCTCAAGTTCATCGC and ACAGACATGGTGTAGTCGTACTGG
qPCR-ATG12-F/R	CAGCAAAGCAAGGTCAAGGTCTC and CAGAGTCCGTCTTTAGCTGCTTTC
qPCR-ATG6-F/R	TTTGACAACGCGAGCGTGGATG and TGTGACCCAACAGAAGCACCTTG
qPCR-ATG10-F/R	GGATCCTCTTGAGGGAGATACAGC and TCTCGCCTACACCTTTCCTCAG
qPCR-ATG4-F/R	TCGCACTAGGCACCTACTTCTGTG and ACGAAGCCAATCGCTAGAGACG
qPCR-ATG8-F/R	CGACATTCAAGCAGGAGCATTCC and TCTGCCTTCTCGACAATGACTGG
qPCR-ATG13-F/R	TGACAAGAGAGCTGGAAGATGGC and ACGTCCTTCAAGTCCACCTCATC
qPCR-UBC4-F/R	TTCCATGCTCGACCAGAAACCG and TGTGGCACTTCCACTTCATCAGG
qPCR-RPT4-F/R	AGAGCGTGGGACAGATTATTGGC and TCAGCTTGGTCTTGTCCACCTTTG
qPCR-PBE1-F/R	CGAATGACACGAATGACCTGCAC and GGCACTTAATCCATCGCAACGC
qPCR-UBP19-F/R	AGTTGACGGCCACGCATAGAAG and GTCCGCACACAACACAATGCAC

Name	Sequence
qPCR-SUMO-F/R	TGCCTCTTTACACGCCTTGCAC and AACACCTTCTCAAGGCGGGTCTTC
qPCR-sporangin-F/R	GTCCGTGCTTCAAATCGTGCTC and ACCACGAACTCCACATCTGTCC
Purpose: PCR amplification of *VMP1* from *C. reinhardtii* cDNA for the sake of generating YFP constructs.	
VMP1-F/R	AGCCATATGGCGGAGGTGGAGGTAG and ATACCATTGCTGCTGCTTGCGCTCG

2.1.5 Antibodies

The only specific antibody used in this work was a polyclonal antibody raised in mouse against TMEM49, the human homologue of VMP1. It was purchased from Novus Biologicals (Cambridge, UK), catalogue number H00081671-B01P.

Two secondary antibodies were used as well. For the purpose of immuno-fluorescence of VMP1, a goat anti-mouse IgG (H+L) CF 488A antibody was used. For Western blot, a goat anti-mouse IgG alkaline-phosphatase was used. Both antibodies were purchased from Sigma-Aldrich (München, Germany).

2.1.6 Strains

2.1.6.1 *Chlamydomonas reinhardtii* strains

Two strains were used in this work. The first, CC-4350, better known as cw15-302, is cell-wall-deficient, is known for its high transformation efficiency, and carries three mutations: *arg*$^-$, *nit1*$^-$ and *nit2*$^-$. The former inactivates the argininosuccinate lyase (ASL; argininosuccinase) gene, whose product enables the cell to synthesize arginine (the enzyme cleaves argininosuccinate into fumarate and arginine). Therefore, *arg*$^-$ strains are arginine auxotrophs, unable to survive without an external supply of arginine. This quality can be, and frequently is, utilized for the selection of successfully transformed cells. *nit1*$^-$ and *nit2*$^-$ indicate the disruption of the genes that encode for nitrate reductase, an enzyme (Fernandez et al., 1989), and NIT2, a transcription factor (Camargo et al., 2007), respectively. These inactive genes deem the cells unable to grow on media that contain nitrate as nitrogen source; they can grow only on ammonium.

The second strain used in this work is UVM11 (Neupert et al., 2009). These cells are in fact CC-4350 cells that underwent UV mutagenesis with the purpose of enhancing their capacity for expressing foreign genes (Neupert et al., 2009). This was indeed achieved, and these cells, while looking and behaving normally, tend to express foreign genes to a much higher extent than is normally observed in CC-4350 cells, or indeed in cells of any tested *C. reinhardtii* strain.

2.1.6.2 *Escherichia coli* strains

For the propagation of plasmids for cloning, *E. coli* DH5α competent cells (Bethesda Research Laboratories, 1986) were used.

2.1.7 Internet websites

BLAST (Basic Local Alignment Search Tool): used for aligning sequences and for searching for similar sequences. http://blast.ncbi.nlm.nih.gov (Altschul et al., 1990).

WMD3 (Web MicroRNA Designer): used for designing artificial microRNAs for gene silencing in plants. http://wmd3.weigelworld.org (Ossowski et al., 2008).

QuantPrime: used for designing primers for mRNA quantification by qRT-PCR. http://www.quantprime.de (Arvidsson et al., 2008).

Phytozome: a comprehensive database of plant genomes. Used in this work for obtaining *C. reinhardtii* gene and protein sequences. http://www.phytozome.net.

PANTHER (Protein Analysis Through Evolutionary Relationships): a database of protein families. http://www.pantherdb.org (Thomas et al., 2003).

KEGG (Kyoto Encyclopedia of Genes and Genomes): a database for the integration of sequence information, specializing on assigning functions. http://www.kegg.jp (Ogata et al., 1999).

Pfam (Protein Families): a database of protein families. http://pfam.sanger.ac.uk/ (Punta et al., 2012).

TMHMM (TransMembrane Hidden Markov Model): used for the prediction of transmembrane helices in proteins. http://www.cbs.dtu.dk/services/TMHMM (Krogh et al., 2001).

TMPRED (TransMembrane Prediction): used for the prediction of transmembrane helices in proteins. http://www.ch.embnet.org/software/TMPRED_form.html (Hofmann and Stoffel, 1993).

MINNOU (**M**embrane protein **I**de**N**tificatio**N** with**OU**t explicit use of hydropathy profiles and alignments): used for the prediction of transmembrane helices in proteins. http://minnou.cchmc.org (Cao et al., 2006).

Phobius: used for the prediction of transmembrane helices in proteins. http://phobius.sbc.su.se/index.html (Käll et al., 2007).

COILS: used for the prediction of coiled-coil regions in proteins. http://www.ch.embnet.org/software/COILS_form.html (Lupas et al., 1991).

MyHits Motif Scan: used for finding motifs in protein sequences. http://myhits.isb-sib.ch/cgi-bin/motif_scan (Pagni et al., 2007).

PredAlgo: used for the prediction of subcellular protein localization. Designed especially for algal proteins. https://giavap-genomes.ibpc.fr/cgi-bin/predalgodb.perl?page=main (Tardif et al., 2012).

TargetP: used for the prediction of subcellular protein localization. http://www.cbs.dtu.dk/services/TargetP (Emanuelsson et al., 2007).

SherLoc2: used for the prediction of subcellular protein localization. http://abi.inf.uni-tuebingen.de/Services/SherLoc2 (Briesemeister et al., 2009).

Cello: used for the prediction of subcellular protein localization. http://cello.life.nctu.edu.tw (Yu et al., 2006).

YLoc: used for the prediction of subcellular protein localization. http://abi.inf.uni-tuebingen.de/Services/YLoc/webloc.cgi (Briesemeister et al., 2010).

SignalP: used for the prediction of signal peptides and their location. http://www.cbs.dtu.dk/services/SignalP (Petersen et al., 2011).

Predator: used for the prediction of signal peptides and their location. http://urgi.versailles.inra.fr/predotar/predotar.html (Small et al., 2004).

2.1.8 Software

MapMan: used for displaying metabolomics data in a biological context. http://mapman.gabipd.org/web/guest/mapman (Thimm et al., 2004).

R: used for statistical analysis. http://www.r-project.org.

DNASTAR Lasergene MegAlign: used for sequence analysis and alignment. http://www.dnastar.com/t-megalign.aspx.

SDS Plate Utility: used for obtaining qRT-PCR data. http://www.appliedbiosystems.com/absite/us/en/home/support/software/real-time-pcr/ab-7900ht.html.

BioRad Quantity One: used for visualizing electrophoresis gels. http://www.bio-rad.com/en-us/product/quantity-one-1-d-analysis-software.

2.2 Methods

2.2.1 Cultivation of *Chlamydomonas*

Unless otherwise stated, *Chlamydomonas* cells were grown in TAP medium, at 25 °C, under continuous light at an intensity of 85 µmol m^{-2} s^{-1}, and while shaking at 100 rpm. To control bacterial and fungal contaminations on agar plates, the latter were supplemented with 500 µg/ml ampicillin, 100 µg/ml cefotaxime, and 40 µg/ml carbendazim, according to Kan and Pan (2010).

2.2.2 Nuclear transformation of *Chlamydomonas*

Nuclear transformation of *Chlamydomonas* was performed, with slight modification, using glass beads as described in Kindle (1990). In brief: the plasmid to be transformed was linearized using restriction digest (HindIII for the amiRNA constructs). Linearization greatly increases transformation efficiency. 10 µl of the digest reaction, containing 1 µg vector DNA (no purification is needed after digestion) were added to a 2-ml tube containing ~50 µl glass beads (425–600 µm in diameter). In parallel, cells were cultivated to a density of 5–10 million cells/ml, then harvested by a 3-min centrifugation at 1,000 *g*. The medium was removed and pellet resuspended in 400 µl TAP medium. The cells were then added to the tube containing beads and DNA. The tube was vortexed vigorously for 15 sec, the cells were then plated onto a TAP-agar plate (without any prior incubation, as recommended by several protocols). Small colonies were usually seen after a week and streaked onto a new plate a fortnight after transformation.

2.2.3 Cell counting

Chlamydomonas cells were counted using a Multisizer Z2 Coulter Counter (Beckman Coulter, Krefeld, Germany). The cells were measured while immersed in 10 ml of the manufacturer's Isoton II electrolyte. The electrode used had a capillary with a diameter of 100 µm. Two consecutive measurements were always performed and then averaged.

2.2.4 Staining and indirect immunofluorescence

To stain *Chlamydomonas* contractile vacuoles with the fluorescent dyes FM 4-64 and DAPI, 1 µl of undiluted dye was added to 1 ml of cell culture, then immediately analyzed with a microscope (both confocal and epifluorescence).

For subcellular localization of VMP1 by means of indirect immunofluorescence, the method described in Cole et al. (1998), with slight modifications, was used. In brief: *Chlamydomonas* cells in liquid culture were centrifuged (500 *g*, 5 min), the pellet then resuspended in 3 % (v/v) paraformaldehyde dissolved in 0.1 M dipotassium hydrogen phosphate. The cells were fixed in this manner for 30 min at RT, then washed three times in PBS. The last pellet was resuspended in 0.5 ml water and the cells then spread on a polylysine microscope slide, to which the cells adhere. The cells were allowed to air-dry, then permeabilized by immersing them in 0.5 % (v/v) NP-40 in PBS for two min. The slide was washed thrice with water, then with cold acetone, in order to remove the cells' chlorophyll, whose fluorescence may interfere with that of our secondary antibody. The slide was then washed thrice with water, then blocked in blocking buffer (5 % (w/v) BSA in PBS) for 30 min, incubated with the primary antibody (diluted 1:50 in blocking buffer) for 2 h, then with the secondary (diluted 1:400 in blocking buffer) for 1 h. Incubations were done at 37 °C, and the slides were washed with PBS between incubations. After the final wash, the slide was allowed to air-dry; a drop of Vectashield was laid on the cells, followed by a cover slip. The cells were analyzed on a confocal microscope.

2.2.5 Starch quantification (performed by Julia Smirnova, MPIMP)

Starch content in *Chlamydomonas* cells was measured as described in Garz et al. (2012). In brief: 2 ml of *Chlamydomonas* cells in liquid culture were centrifuged (5,000 *g*, 5 min), immediately flash-frozen in liquid nitrogen and stored at –80 °C until use. The pellet was resuspended in 1 ml 80 % (v/v) ethanol and sonicated 4 times, 8 sec each, at 25 % maximum power) with a Sonoplus sonicator (Bandelin Electronics, Berlin, Germany). The homogenate was then heated for 1 h at 95 °C, then centrifuged (20,000 *g*, 4 °C, 10 min), the pellet then lyophilized with a vacuum centrifuge. The pellet was washed with 1 ml water, then resuspended in 200 µl 0.2 N KOH and heated for 1 h at 95 °C. 35.2 µl 1 N acetic acid was added and the sample centrifuged (10,000 *g*, 10 min). 200 µl of the supernatant were mixed with 30 µl amyloglucosidase (Starch Assay Kit), then incubated overnight at 55 °C. The enzyme splits the starch into its glucose subunits; those in turn were quantified as described in Kunst et al. (1988). In brief: a mixture of NAD^+, ATP,

HEPES and $MgCl_2$ was added to the glucose samples, whereupon their optical density (OD) at a wavelength of 340 nm was measured using a microplate reader (GENios, Tecan; Crailsheim, Germany). Then, 1 unit each of hexokinase and glucose 6-phosphate dehydrogenase was added to the samples. Glucose is converted to 6-phosphogluconate, NAD^+ is concomitantly converted to NADH. The latter is then measured with the microplate reader. The change in OD divided by 6.22 $\mu mol^{-1}\ cm^{-1}$, NADH's extinction coefficient, equals the amount of glucose in µmol.

2.2.6 Microscopy

2.2.6.1 Light microscopy

Light and fluorescence microscopy were performed on an Olympus BX51 microscope (Olympus Optical Co., Hamburg, Gemany). 5 µl of *Chlamydomonas* culture were dropped onto a microscope slide and covered with a 22-mm^2 slip. As described by Luykx et al. (1997a), "such preparations have a thin layer of fluid thin enough to hold most cells stationary between the slide and coverslip and, with a substage heat filter, last about 15 min without any significant change in CV activity". We used, unless stated otherwise, a 100× oil-immersion objective and differential interference contrast (DIC; also called Nomarski) optics. Images were captured using a digital camera and CellPrism software.

2.2.6.2 Confocal microscopy (performed by Eugenia Maximova, MPIMP)

Confocal microscopy was performed on a Leica TCS SP5 II microscope (Leica Microsystems, Wetzlar, Germany) equipped with a Leica DM6000 confocal fixed stage.

2.2.6.3 Electron microscopy (performed by Eugenia Maximova, MPIMP)

Chlamydomonas cells were fixed for 3 h at 4 °C with 2 % (v/v) glutaraldehyde in 0.1 M sodium cacodilate buffer (pH 7.4). Samples were then fixed and osmicated for 1 h in 1 % OsO_4. They were then stained for 2 h in 2 % (w/v) uranyl acetate and dehydrated progressively in 50, 75, 95, and 100 % ethanol, followed by two washes in 100 % propylene oxide. The samples were embedded in Spurr's low-melting epoxy resin. Samples were degassed and cured at 60 °C for 24 h. Sections (50 nm) were obtained with a Leica UC 6 ultramicrotome (Leica Microsystems, Wetzlar, Germany), mounted on 200-mesh nickel grids, counterstained with uranyl acetate followed by lead citrate, and examined with an energy-filter transmission electron microscope (EFTEM) at 80 kV (Zeiss, Oberkochen, Germany).

2.2.7 Artificial microRNA constructs

Silencing by means of artificial microRNA (amiRNA) was performed as described in Molnar et al. (2009). In brief: we commenced by designing long oligonucleotides that contained a silencing sequence specific to the gene to be silenced (the target gene). This was done *in silico* using a dedicated website, WMD3 (Web MicroRNA Designer; Ossowski et al., 2008). The identifier or sequence of the target gene was submitted, and a list of candidate silencing sequences was obtained. Upon deciding on a silencing sequence (based on the location of its binding site on the mRNA, and on the thermodynamic binding stability between amiRNA and mRNA; both mediated by the website), the sequences of the oligonucleotides to be used was provided. Next, the 90-nt long single-stranded oligonucleotides were annealed to each other: this was achieved by heating a mixture of the oligonucleotides in annealing buffer (20 mM tris pH 8.0, 2 mM EDTA, 100 mM NaCl) to 98 °C for 5 min, followed by slow cooling for several hours. The resulting double-stranded DNA was purified with a PCR cleanup kit and then phosphorylated using T4 polynucleotide kinase (PNK) to facilitate ligation into the amiRNA vector. In parallel, the amiRNA vector (pChlamiRNA2 or pChlamiRNA3-int) was linearized using the restriction enzyme SpeI, then dephosphorylated using calf intestine alkaline phosphatase (CIAP). The insert was diluted 1:10, then ligated into the vector. The ligation reaction was transformed into competent *E. coli* cells, plated onto agar plates containing 50 µg/µl ampicillin, and incubated at 37 °C overnight. Colonies were tested by colony PCR with primers amiRNA-F and amiRNA-R (annealing temperature 65 °C, elongation time 30 sec), then run on a 2.5-% (w/v) agarose gel. Positive clones, showing a 182-bp band, were sequenced. Clones that showed even a single mismatch were rejected and redone, since this could greatly diminish their silencing capability. Positive clones were transformed into *Chlamydomonas* cells.

2.2.8 Molecular cloning

Molecular cloning was used in this study for the generation of amiRNA constructs (see above; Section 2.2.7) and fluorescent-protein constructs for subcellular localization (Section 3.10). Procedures and reactions were performed as follows:

2.2.8.1 PCR

The polymerase chain reaction (PCR) serves to amplify—create many copies of—DNA fragments, either for downstream applications, such as ligation, or, when used in conjunction with gel electrophoresis, for the purpose of confirmation, detection or validation of certain sequences. For the cloning of *Chlamydomonas* genes, a high-fidelity DNA polymerase was used, as well as a "GC enhancer", a proprietary mixture that increases amplification of GC-rich sequences. The reaction contained, unless stated otherwise:

2.5 µl each of 10 µM forward and reverse primer
10 µl DNA polymerase buffer
10 µl GC enhancer
0.5 µl DNA polymerase
1 µl of 10 mM dNTPs
Template DNA
Water to 50 µl

The reactions were performed in a thermocycler with the following settings:

98 °C	2 min	
98 °C	30 sec	┐
52–72 °C	30 sec	├ 25–35 cycles
72 °C	30–200 sec	┘
72 °C	3 min	

Colony PCR was used for the confirmation of successful bacterial transformation (see below; Section 2.2.8.8). The reaction was similar to the one written above, with the following differences: an ordinary DNA polymerase was used; the final volume was 20 µl; no GC enhancer was used; and a picked colony from an LB plate served as template DNA.

2.2.8.2 Sequencing

DNA fragments were sequenced by LGC Genomics (Berlin, Germany).

2.2.8.3 Restriction digest

DNA was cut (digested) using restriction enzymes for the purpose of ligation of inserts into plasmids (vectors), as well as for, when used in conjunction with gel electrophoresis, confirming the integrity or identity of various DNA fragments and constructs. All the double digests in this work were performed in single reactions, using two enzymes simultaneously. The reaction:

1–2 µg DNA

2 µl 10× Thermo FastDigest buffer

1 µl Thermo FastDigest restriction enzyme

1 µl Thermo FastDigest restriction enzyme (optional)

Water to 20 µl

The reaction was incubated at the temperature and for the duration recommended for each enzyme, then heat-deactivated, again using the recommended temperature and duration recommended for each enzyme.

2.2.8.4 Phosphorylation

DNA was phosphorylated for the purpose of inserting it into a dephosphorylated vector, as in the case of amiRNA constructs. The reaction:

1 µl purified dsDNA oligo (~0.7 µg/µl; adjust volume accordingly)

1 µl 10× T4 DNA ligase buffer

1 µl T4 polynucleotide kinase (PNK, 10 u/µl)

7 µl water

The reaction was incubated for 30 min at 37 °C , then heat-deactivated for 20 min at 65 °C.

2.2.8.5 Dephosphorylation

DNA (usually plasmids, but sometimes inserts as well) was dephosphorylated in order to increase the efficiency of ligation reactions. Plasmids cut with a single restriction enzyme favor religation (recircularization). In ligation reactions with such plasmids most inserts, if not all, remain uninserted. In the case of plasmids digested with two enzymes, these may form concatamers (chains) among themselves, which again excludes ligation with the correct insert. Dephosphorylation removes the phosphate groups from the free DNA ends, thereby greatly reducing the chance of plasmids interacting with themselves and increasing the chance of correct insertion. The reaction:

0.5 µl calf-intestine alkaline phosphatase (CIP or CIAP) added directly to a restriction-digest reaction after deactivation.

The reaction was then incubated for 1 h at 37 °C. CIP cannot be heat-deactivated; but it must be eliminated, since it may interfere with the subsequent ligation reaction. Therefore, the dephosphorylation reaction was gel-purified.

2.2.8.6 Polyadenylation

Polyadenylation (or "A-tailing") is the addition of adenyl residues at the ends of blunt DNA fragments. The purpose of this is to facilitate ligation of the adenylated fragments into linearized vectors that have thymidine residues in their ends. The adenyl residues attach to their thymidine counterparts, and the fragments are thus ligated. PCR reactions result in either blunt or adenylated fragments, depending on the polymerase used. In the former case, the fragments then need to be polyadenylated. In this work we used polyadenylation to insert PCR-amplified genes into the plasmid pGEM-T. Keeping the genes inside the plasmid enables easy and reliable future amplification, and negates the need for amplification from the genome, which is more challenging and less reliable. The reaction:

1 µl Taq DNA polymerase

1 µl Taq buffer (without $MgCl_2$)

0.3 µl of 50 mM $MgCl_2$

1 µl of 2 mM dATP

6.7 µl PCR product

The reaction was incubated at 70 °C for 30 min.

2.2.8.7 Ligation

Ligations serve to connect DNA fragments. In this work ligations were used exclusively to insert DNA fragments into plasmids (vectors). The reaction:

Insert DNA and plasmid DNA at a molar ratio of 3:1

1 µl DNA ligase buffer

1 µl T4 DNA ligase

Water to 10 µl

The reaction was incubated at 16 °C overnight. In addition to the reaction written above, a negative-control reaction, one lacking the insert DNA, was performed in parallel. This helped estimate the ratio of unwanted self-ligation events, and thereby assess the success of the insertion.

2.2.8.8 Transformation into bacteria

Plasmids ligated with inserts are transformed into bacteria (typically *E. coli*) for the purpose of propagation and proliferation, so that substantial amounts of the plasmid can be obtained for downstream applications. Despite the existence of more modern techniques for creating many copies of DNA fragments, bacteria remain the most efficient and economic propagators of vectors. Untreated bacteria do not readily absorb

foreign DNA; they therefore need to be made "competent" in a process that weakens their cellular envelope and membrane. In brief: the cells underwent a series of cold washes in buffers that contained cations (rubidium, manganese, potassium and calcium). The cations interact with the negatively charged phospholipids and lipopolysaccharides in the bacteria's membrane and weaken it, a process promoted by the cold temperature. Subsequently the cells were frozen in liquid nitrogen and kept at –80 °C.

Upon transformation, 50 µl of competent cells were thawed on ice. 2 µl of the DNA to be transformed were added to the bacteria, which were then kept for further 20 min on ice. The bacteria were then subjected to a 1-minute heat shock using a thermoblock or a water bath at 42 °C. The cells were the moved immediately back on ice; after 5 min 1 ml LB medium was added to the bacteria. The bacteria were then incubated for 1 h at 37 °C with shaking. 200 µl bacteria were plated on an LB-agar plate which was then incubated at 37 °C overnight.

2.2.8.9 Glycerol stocks

Liquid cultures of bacterial strains harboring various vectors were mixed with glycerol (1:3 glycerol:culture), then frozen at –80 °C and kept for future usage.

2.2.9 qRT-PCR

Quantitative real-time reverse-transcription PCR was used for the quantification of the mRNA levels of specific genes. The process included the following steps.

2.2.9.1 RNA extraction

RNA was extracted from *Chlamydomonas* cells using kits purchased from Roboklon (Berlin, Germany). The starting material was 2 ml of culture. Cell were harvested by centrifugation (4,000 *g*, 4 °C, 3 min). In the last step RNA was eluted with 40 µl water. Contrary to common practice, we found it unnecessary to remove genomic DNA by means of precipitation or with a kit. The amount of residual genomic DNA in our RNA samples proved, when using the Roboklon kit, negligible for our purpose. RNA concentration was measured using a NanoDrop spectrophotometer from Life Technologies (Darmstadt, Germany).

2.2.9.2 Reverse transcription

1 µg of RNA was used as template for cDNA synthesis by reverse transcription using kits purchased from New England Biolabs (Frankfurt am Main, Germany). We used 10-µl reactions, half the volume recommended by the manufacturer. First, the following components were mixed:

1 µg RNA

0.5 µl oligo $d(T)_{18}$

Water to 5 µl

The mixture was incubated at 65 °C for 5 min. The following components were then added:

0.5 µl RiboLock RNAse inhibitor

0.5 µl reverse transcriptase

1 µl dNTPs

2 µl reaction buffer

The reaction was incubated at 45 °C for 1 h, then deactivated at 70 °C for 5 min.

2.2.9.3 qRT-PCR

qRT-PCR was performed on an 7900HT Fast Real-Time PCR System from Applied Biosystems, now Life Technologies (Darmstadt, Germany). The reaction:

5 µl Power SYBR Green Master Mix

1.5 µl each of 0.5 µM forward and reverse primer

2 µl of diluted (1:3 to 1:10) cDNA

For normalization we used the common reference genes ubiquitin and RACK1. For result analysis we used the SDS 2.3 software from Applied Biosystems. For calculation of the results we used the $2^{-\Delta\Delta Ct}$ method (Livak and Schmittgen, 2001).

2.2.10 Western blot

Western blot (immunoblotting) was used for the detection of VMP1 protein levels in *Chlamydomonas* cells that had undergone amiRNA silencing. The process included the following steps.

2.2.10.1 Protein extraction

10 ml of *C. reinhardtii* cells in liquid culture, with a density of ~10^6 cells/ml, were harvested by centrifugation (4,000 *g*, 4 °C, 10 min). The pellet was immediately flash-frozen in liquid nitrogen and stored at –80 °C. Frozen samples were resuspended in 0.5 ml breakage buffer (100 mM tricine, 5 mM $MgCl_2$, 1 mM EDTA, 10 mM DTE, 0.5 mM PMSF, 2 mM benzamidine, 2 mM aminocaproic acid; adjusted to pH 7.8 with NaOH) and proteins were extracted by sonication (10 %, 5 sec, cycle 6). After centrifugation (20,000 *g*, 4 °C, 10 min) the supernatant, containing the buffer-soluble proteins, was withdrawn and the pellet (insoluble, membrane proteins) was resuspended in 0.5 ml breakage buffer containing 1 % (v/v) Triton X-100. After a 30-min incubation on ice samples were centrifuged as above. Proteins in both fractions were quantified according to Bradford (1976) using the micro-version of the Bio-Rad Protein Assay Kit (Bio-Rad, München, Germany). The protein concentration was calculated using bovine serum albumin (BSA) as standard.

2.2.10.2 SDS-PAGE

The samples were mixed with SDS-sample buffer (62.5 mM tris-HCl, pH 6.8, 10 % (v/v) glycerol, 2 % (w/v) SDS, 0.007 % (w/v) bromophenol blue; 20 mM DTE) and boiled for 10 min at 95 °C. Subsequently, samples were loaded onto a tricine SDS-PAGE (Schägger, 2006) using a 9-% (w/v) separation gel.

2.2.10.3 Western blot and immunodetection

Following electrophoresis, proteins were electroblotted for 16 h at 16 V to a Protran Nitrocellulose membrane (Whatman, GE Healthcare, München, Germany) in blotting buffer (50 mM Tris, 150 mM glycine, 20 % (v/v) methanol, 0.02 % (w/v) SDS). Following transfer, the membranes were blocked with 3 % (w/v) milk powder.

For immunochemical detection of VMP1 protein, membranes were probed with an α-TMEM49 polyclonal antibody raised in mouse (see above; Section 2.1.5), diluted 1:500, followed by an alkaline-phosphatase conjugated secondary antibody, diluted 1:20,000. The signal was detected using NBT/BCIP ready-to-use tablets (Roche, Mannheim, Germany).

2.2.11 Lipidomic profiling

2.2.11.1 Lipid extraction

Lipids were extracted according to a protocol modified from Roessner et al. (2001). In brief: ~20 million *Chlamydomonas* cells were pelleted, then flash-frozen in liquid nitrogen and, optionally, kept at –80 °C. 1 ml of methyl-*tert*-butyl ether (MTBE):methanol (3:1) was added to the pellet, then vigorously mixed and sonicated. 500 µl water:methanol (3:1) were added. Upon vortexing and centrifugation the homogenate separated into an upper organic phase (contains mainly lipids) and a lower polar/semi-polar phase. The phases were collected, then dried with a vacuum centrifuge and stored at –20 °C.

For the later standardization of technical measurement errors, internal standards, contained in the MTBE:methanol buffer, were used: the carbohydrate ^{13}C-sorbitol (polar standard) and the lipid phosphatidylcholine 34:0 (non-polar standard).

2.2.11.2 Lipid profiling using UPLC-FT/MS

Lipids and secondary metabolites were separated using ultra-performance liquid chromatography (UPLC) and measured using mass spectrometry (MS). The procedure was based on the one described in Hummel et al. (2011). In brief: lyophilized pellets were resuspended in buffer B (see below), centrifuged and separated on a reversed-phase C8 column, installed in a Waters Acquity UPLC system (column and UPLC: Waters). Separation was performed at a flow rate of 400 µl/min; total running time per sample equaled 22 min. Buffer A (1 % (w/v) 1 M ammonium acetate, 0.1 % (v/v) acetic acid, dissolved in water) and buffer B (the same, dissolved in acetonitrile:isopropanol (7:3)) served as mobile phases.

After separation, the analytes moved onto a coupled Fourier transformation (FT) MS (Exactive, Thermo-Fisher, Bremen, Germany), where they ionized by electrospray. Obtained raw-chromatograms were further processed using the software Xcalibur (Thermo-Fisher) and Refiner MS (GeneData, Basel, Switzerland). Peaks from raw chromatograms were aligned by their parent masses; chemical noise was subtracted; and an output file, containing the peaks' m/z-ratio and retention times was produced. For peak annotation, the locally developed GoBioSpace database was used (Hummel et al., 2011). Peak intensities were normalized to the total ion count (TIC).

3. Results

3.1 Searching for CV-related proteins in *C. reinhardtii*

We commenced our search for *Chlamydomonas reinhardtii* proteins related to the contractile vacuole (CV) in the literature. Virtually all articles reporting novel CV-related proteins describe work done in slime mold (*Dictyostelium discoideum*). One recent exception is a study reporting the proteome of the CV in *Trypanosoma cruzi* (Ulrich et al., 2009). Since we wished to focus on proteins with reported, proven function and/or localization to the CV, and not merely proteins detected in a proteomic analysis, we excluded the proteins reported in this article from our list. We listed the *D. discoideum* proteins and searched, using Basic Local Alignment Search Tool (BLAST; Altschul et al., 1990) for homologues in *C. reinhardtii*. Out of 17 novel proteins reported in *D. discoideum*, 11 were found to have homologues in *C. reinhardtii*. The total number of proteins found in *C. reinhardtii*, considering that several *D. discoideum* proteins had more than one homologue in *C. reinhardtii*, was forty. **Table 3** summarizes the *C. reinhardtii* homologues that we found. Only homologues with the arbitrary Expect score of e–10 or less, which indicates strong homology (see also **Table 8**), were included.

Table 3. *C. reinhardtii* homologues of CV-related genes from *D. discoideum*

Family	Identifier in *C. reinhardtii*	Homologues in *D. discoideum*	Reference
Clathrin assembly factor	**g9746**	AP180 (*clmA*)	Stavrou et al., 2006
Adaptin	**Cre12.g488850**	AP2 (*ap2a1-1*)	Wen et al., 2009
RabGAP	**Cre10.g461400**	Disgorgin and drainin (*phgA*)	Du et al., 2008
	Cre17.g727450		
	Cre02.g077700		
	Cre17.g737050		
	Cre07.g315350		
	Cre12.g486400		
	Cre12.g537750		
	Cre10.g459800		
	Cre12.g541350		
Calcium ATPase	**Cre12.g505350** and 18 others	Calcium ATPase (*patA*)	Moniakis et al., 1999
VMP1	**Cre06.g272000**	VMP1 (*vmp1*)	Calvo-Garrido et al., 2008
BEACH	**Cre06.g274950**	LvsA and LvsD (*lvsA*, *lvsD*)	Gerald et al., 2002
	Cre17.g732650		

Family	Identifier in *C. reinhardtii*	Homologues in *D. discoideum*	Reference
Copine	**Cre03.g170150**	Copine A (*cpnA*)	Damer et al., 2007
	Cre03.g170200		
	Cre09.g399550		
Dynamin	**Cre17.g724150**	Dynamin B (*dymB*)	Rai et al., 2010
	Cre05.g245950		
VwkA	**Cre02.g095250**	VwkA (*vwkA*)	Betapudi et al., 2009
	Cre02.g095550		

Gene identifiers in bold represent genes that we attempted to silence in this study. For D. discoideum homologues, protein names are written in normal text, the encoding genes are in parenthesized and in (*italics*).

3.2 Silencing attempts

We narrowed the list of proteins to eleven (bold text in **Table 3**), aiming to represent the major families while still keeping the endeavor manageable. We attempted to silence these eleven genes by means of artificial microRNA (amiRNA; Molnar et al., 2009; Zhou et al., 2009). Indeed, complete knockout is currently hardly possible in *Chlamydomonas* (Schroda, 2006), and the best that can be achieved is partial silencing, or knockdown. To this end we used an online service, WMD (Ossowski et al., 2008), to design oligonucleotides that have complementary sequences in the target genes; we ligated the oligonucleotides into the expression vectors described in Molnar et al. (2009); transformed the vectors into *C. reinhardtii* cells; and selected and screened for silencing.

Our *C. reinhardtii* strain of choice was CC-4350, also called cw15-302. These cells are relatively small, are largely cell-wall-deficient, have very short flagella, and are known to exhibit high transformation efficiency. In addition, the cells are arginine auxotrophs: they cannot synthesize arginine and must have it provided externally in order to survive. This latter quality facilitates selection after transformation. The amiRNA vector used, pChlamiRNA2 (Molnar et al., 2009), harbors the argininosuccinate lyase gene, which is mutated (inactivated) in the cells. Cells that were successfully transformed and that deigned to express the foreign genes were now able to synthesize arginine and thus grow on arginine-deficient media plates.

We initially plated our cells following transformation on TAP-agar plates supplemented by sucrose. The aim was to increase the medium's osmolarity, thus providing the cells with an iso-osmotic environment that would exert no osmotic stress upon them. We reasoned that since our silenced genes were putatively related to the CV and thus to osmoregulation, exposing the mutant cells to hypo-osmotic stress might undermine their capacity to survive if indeed the silencing caused defective

osmoregulation. In such a case we would lose our best knockdown lines, the ones in which silencing was superior, leaving only weak lines and false positives on the plate. TAP medium alone was apparently hypo-osmotic for our cells, since we consistently observed prominent CV activity in cells grown in TAP. A similar observation was reported by Komsic-Buchmann and colleagues (2012). We assessed, in the same manner described in the cited study, using various sucrose concentrations, the intracellular osmolarity of our cells, then chose a sucrose concentration of 90 mM, in which CV activity was minimal, to go in our TAP-agar plates. At a later stage we determined that this measure had not been necessary, that no difference was observed between mutants grown in TAP and in TAP-sucrose, and that our mutants were probably not osmosensitive (see below).

In addition to strain CC-4350, we attempted silencing in another strain, UVM11. These cells are in fact CC-4350 cells that underwent UV mutagenesis with the purpose of enhancing their capacity for expressing foreign genes (Neupert et al., 2009). This was indeed achieved, and these cells, while looking and behaving normally, tend to express foreign genes to a much higher extent than is normally observed in CC-4350 cells, or indeed in cells of any tested *C. reinhardtii* strain. We were curious to see whether UVM11 cells would express the amiRNA construct more than in CC-4350, and thus, perhaps, bring about increased silencing. UVM11 is not an arginine auxotroph, and therefore requires selection by means of antibiotics. To this end we used a modified amiRNA vector, namely pChlamiRNA3int (Molnar et al., 2009). This vector harbors the *aphVIII* gene from the bacterium *Streptomyces rimosus*, which confers resistance against paromomycin (Sizova et al., 2001); amiRNA expression is controlled by the strong *PsaD* promotor (Fischer and Rochaix, 2001), with help from the first intron of *RBCS2*, a known transcriptional enhancer in *Chlamydomonas* (Lumbreras et al., 1998).

3.3 Screening for silenced genes

3.3.1 qRT-PCR

Once we obtained positive colonies of *Chlamydomonas* cells transformed with our amiRNA constructs, we embarked on screening for silenced genes. To detect colonies with silenced genes, we extracted RNA from the cells, synthesized cDNA from it using reverse transcriptase (RT), and subjected the cDNA to quantitative real-time reverse-transcription polymerase chain reaction (qRT-PCR), a method for the accurate quantification of specific mRNA transcripts. Although equal amounts of RNA were used

in each RT reaction, small, inevitable errors could have vast influence on the results. To normalize the amounts of material across the samples we assayed in parallel for the transcript abundance of two housekeeping, or reference, genes: ubiquitin and RACK1. These genes are believed to exhibit constitutive, stable expression under various conditions, and can thereby serve as a measure of the total amount of mRNA in the sample. Though ubiquitously used, the reliability of this method is a matter of debate, having been shown to not always reflect reality (Gutierrez et al., 2008). In our case, however, great accuracy was not required: we simply wished to identify the clones with the least amount of residual transcript.

Our silencing endeavor in six out of the eleven genes met with various technical hurdles—obstinately persistent sequence mismatches in the cloned amiRNA construct, failed transformations, insignificant or unstable silencing—that led us to discard the effort. Five genes, in contrast, registered strong silencing, as measured by qRT-PCR, with residual mRNA levels smaller than 30 % of WT (data not shown). As control we transformed cells with the empty expression vector used for the amiRNA constructs. To confirm the reproducibility of our observations, we performed several silencing rounds for each target gene.

As the project progressed we chose to focus our efforts on one gene: *VMP1*. Other genes in our list proved inferior candidates for in-depth analysis: many were family members with high sequence similarities, which necessitated the silencing of all members, alone and in different combinations, in order to dissect the role and contribution of each member and to avoid situations in which non-silenced members compensated for the absence of one silenced member; also, silencing specificity would always be an issue when there are several homologues. Other genes in the list were excessively long, perhaps wrongly annotated, which would have deemed molecular techniques nearly impossible. *VMP1* (henceforth named *CrVMP1* whenever the need arises to stress that specifically the *C. reinhardtii* protein is discussed) appeared to be an ideal candidate: modestly long, unique in the genome, and, judging from its reported homologues, of potentially great interest.

As described above (**Section 3.2**), we attempted silencing in two *C. reinhardtii* strains, one of which, UVM11, is an artificially generated "overexpressor" strain, showing remarkable capacity to express foreign genes (Neupert et al., 2009). We envisioned that this strain might show increased expression of the amiRNA, leading to improved silencing. Our results, however, showed no coherent difference between the UVM11 and its parental strain, CC-4530. Both strains boasted the entire spectrum of residual target-gene mRNA levels, from a minimum of 5 % to no silencing at all (100 %

mRNA still present), at equal rates. Still, we have not attempted silencing enough times to make this observation statistically significant. Especially, the number of genes we tried to silence was low (only seven in UVM11). Since anecdotal reports point towards strong dependency of silencing success on the individual gene in question (Stefan Schmollinger, UCLA; personal communication), it may still be that the silencing of certain genes would be more successful in UVM11 than in a WT strain. Since we did not measure the expression of the amiRNA construct in our clones, we could not deduce whether the equal silencing capacities observed in the two strains were the result of equal expression levels of the amiRNA, or rather that UVM11 indeed expressed the amiRNA more than its WT counterpart did, but came short in other, unknown, respects.

3.3.2 Western blot

In addition to screening for silencing by measuring mRNA levels, we attempted to assay for residual protein levels using Western blot. We did not intend for this to serve as a screening method: the high price of the antibodies used in Western blots, combined with the high number of clones to test, precluded this. Instead, we wished to use Western blot to confirm silencing in clones already identified by qRT-PCR. Our attempts concentrated on one protein: VMP1, the focus of this work. CrVMP1, together with nearly all the other proteins that we tried to abolish, was novel and unreported; commercial antibodies against it were therefore not available. The generation of antibodies on our own, or using the services of a company, proved beyond the scope of our resources. The six transmembrane domains that VMP1 is predicted to harbor (see below, **Section 3.4.2**) added complexity: membrane proteins are notoriously challenging to express and to purify (Carpenter et al., 2008). Before nearly deserting the effort, we came across a commercial antibody raised against the complete human homologue of VMP1 (also called TMEM49). We used it to perform Western blots and obtained ambiguous results: while a band did appear at the expected CrVMP1 size of 50 kDa, it was faint, it was not the most prominent band on the blot, and, most importantly, it appeared in both WT and mutant (**Figure 2**).

Presumably overloading the gel with protein caused saturation, whereby the ability to distinguish between different amounts of protein on the blot was lost. Another issue was the appearance of the band in both soluble and insoluble fractions. VMP1, strongly predicted to be a membrane protein (**Section 3.4**), hence insoluble in the water-based extraction buffer, would be expected to appear only in the insoluble fraction; at any rate, not in both fractions. Optimization of the extraction protocol (adjusting detergent type and concentration, for instance) may help prevent such leakiness between the fractions. Time constraints, however, did not allow us to perform this and other optimizations (titering the amount of loaded protein; titering antibody concentration; using alternative visualization methods to increase sensitivity). We later used the same antibody in an attempt to find VMP1's subcellular localization (**Section 3.10**). Western blots were performed by Julia Smirnova, MPIMP.

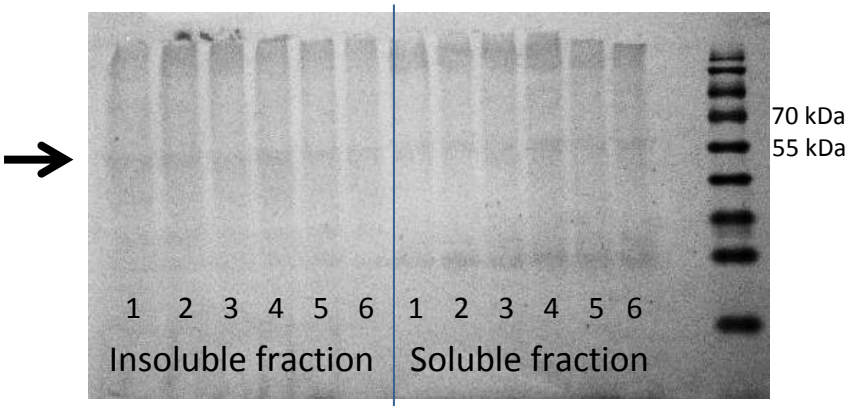

Figure 2. Western blot for the detection of VMP1. Protein extracts from six *C. reinhardtii* clones, all in strain UVM11, were immunoblotted with anti-TMEM49 antibody. Both soluble and insoluble fractions were blotted. The samples: (1) vmp-i (2) vmp-iv (3) vmp-vii (4) ev-1 (5) ev-2 (6) UVM11. Samples 1–3 are *VMP1* knockdown strains, as mediated by qRT-PCR, samples 4–5 are empty-vector controls, and UVM11 is WT. The black arrow points to the putative VMP1 band. The ladder: Thermo Scientific PageRuler Prestained Protein Ladder.

3.4 Bioinformatic analysis of VMP1

3.4.1 General

Before we discuss our experimental results, we present a brief bioinformatic analysis of our major target gene. **Table 4** provides an overview of several basic parameters.

Table 4. Basic sequence details of CrVMP1

Parameter	Value
Name	VMP1, vacuole membrane protein 1
Identifier	Cre06.g272000; also: g6103
Genomic location	Chromosome 6, 2,870,722–2,875,466
Gene size	4,745 nt
GC content	63.92 %
Transcript size	2,163 nt
Coding-sequence size	1,344 nt
GC content	66.29 %
Exons/introns	9/8
Protein size	477 aa

VMP1 is unique in the *C. reinhardtii* genome: there are no other genes similar to it in sequence, and it belongs to no family. We submitted the CrVMP1 sequence to various Internet databases to obtain a notion of the way it is annotated using different algorithms and classification methods. The only database that provided an annotation of any sort was PANTHER (Thomas et al., 2003), which assigned CrVMP1 to the large family of "membrane-associated progesterone receptor component-related" proteins.

3.4.2 Structure and domains

We next analyzed CreVMP1 for predicted domains, motifs, and binding sites. Two independent databases, KEGG (Ogata et al., 1999) and Pfam (Punta et al., 2012), predicted a 111-aa "SNARE-associated Golgi domain" in the CrVMP1 protein sequence, spanning aa 170–281. The E-value of this match numbered at around 10^{-6}, indicating a very high probability for this prediction.

We used four different algorithms for the prediction of transmembrane domains: MINNOU (Cao et al., 2006), TMPred (Hofmann and Stoffel, 1993), TMHMM (Krogh et al., 2001), and Phobius (Käll et al., 2007). All four algorithms seemed to agree that CrVMP1 boasts at least four transmembrane domains. The domains that were commonly

predicted by the latter three algorithms were located in almost precisely the same places along the protein's sequence. MINNOU, in contrast, delivered a structure that was in part significantly different. **Figure 3** summarizes the results.

N–1	2	3	4	5	6	7	8	9	10	11	12	13–C
1–51	**52–71**	72–91	**92–114**	115–169	**170–192**	193–233	**234–256**	257–275	**276–298**	299–398	**399–421**	422–447
1–51	**52–73**	74–93	**94–120**	121–168	**169–189**	190–232	**233–256**	257–272	**273–297**	298–398	**399–420**	421–447
1–51	**52–73**	74–92	**93–119**	120–231			**232–251**	252–398			**399–420**	421–447
(1–56)	**57–78**	(74–79)	**80–107**	(108–113)	**114–128**	(129–161)	**162–182**	(183–393)			**394–418**	(419–447)

Figure 3. Schematic representation of transmembrane-domain predictions for CrVMP1. The protein's sequence was divided into 13 ranges, with the N-terminus on the left and C-terminus on the right. Each row represents one prediction algorithm; from top to bottom: TMHMM, TMPred, Phobius, MINNOU. The small numbers represent residues; **bold red** residues are transmembrane domains; underlined residues are domains outside the cell; normal-text residues are cytoplasmic domains; residues in (parentheses) are undetermined in that respect.

The four algorithms all provided graphic representations of their predictions. These graphs, which add information regarding the calculated probability for the prediction of each amino acid along CrVMP1's sequence, can be seen in **Figure 4**.

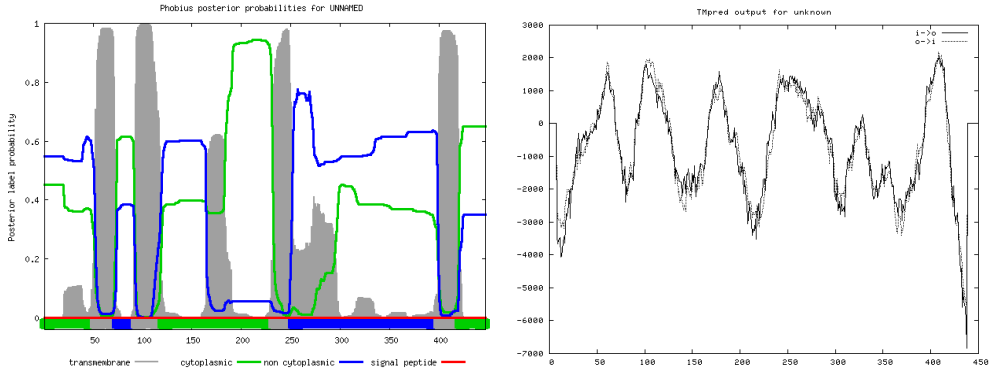

Figure 4 (previous page)**. Graphic transmembrane predictions** delivered by Phobius (top left), TMPred (top right), and TMHMM (bottom). The x-axes represent the protein's residues from 1 to 447, the y-axes show probability values. The colored curves distinguish between transmembrane, cytoplasmic ("inside") and extracellular ("outside") domains, according to the respective legends. The graphs were copied unchanged from the respective websites.

The prediction algorithm MINNOU delivered a sketch of a different kind (**Figure 5**). Information regarding the directionality of the domains is absent; instead, the protein's secondary structure is predicted, as well as the solvent accessibility—the degree of exposure to the surrounding environment—of each residue.

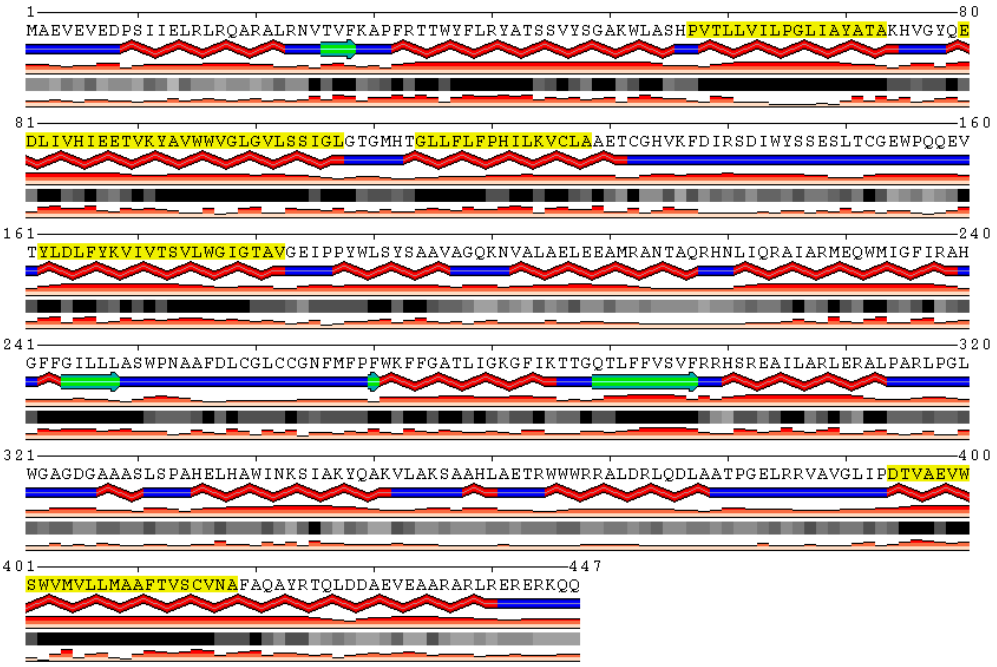

Figure 5. CrVMP1's protein sequence, analyzed by MINNOU. Secondary structures appear immediately below the letters representing the amino acids. Zigzag red lines are α-helices; green arrows are β-sheets; straight blue lines are coils. The red bars below that represent the prediction's confidence level, or probability—the higher the bar, the more probable the prediction is. The grey and black squares represent the residue's solvent accessibility. Black squares are residues completely buried inside the protein or a membrane, and therefore show the poorest solvent accessibility; bright-grey squares are fully exposed to the solvent. The red bars below that represent, again, the probability of the solvent-accessibility prediction. Transmembrane domains are marked residues shaded yellow. The graphic was copied unchanged from the MINNOU website.

Proceeding with CrVMP1's secondary-structure analysis, we used the COILS algorithm (Lupas et al., 1991) to predict coiled-coil domains in our protein. Such domains are known for their likelihood of taking part in protein-protein interactions (Burkhard et al., 2001). As can be seen in **Figure 6**, two domains—one of them comprising the last ~25 aa of the proteins—were predicted to assume the form of a coiled coil.

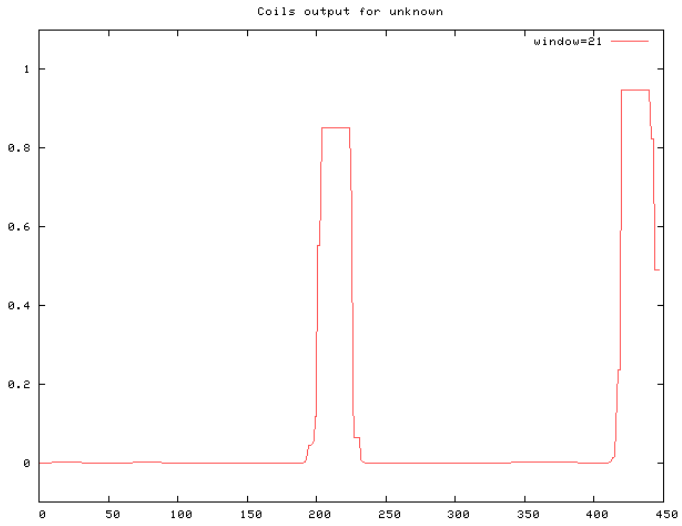

Figure 6. Graphic coiled-coils prediction of CrVMP1's protein sequence, delivered by COILS. The x-axis shows the protein's residues from 1 to 447, the y-axis shows the prediction's probability score. The graphic was copied unchanged from the COILS website.

Figure 7 provides a graphic overview of the most important domains predicted for CrVMP1.

Figure 7. Schematic representation of CrVMP's primary structure. Red areas represent transmembrane domains predicted by TMPred and TMHMM. One circle represents a domain absent from the Phobius prediction, two circles—absent from both the Phobius and the MINNOU predictions. The yellow area shows the predicted SNARE domain.

We next submitted our protein to a prediction of binding sites. The algorithm MotifScan (Pagni et al., 2007) predicts binding sites for sugars, lipids, phosphate groups, and many other moieties. The algorithm found 17 potential binding sites in CrVMP1 (**Table 5**); however, all sites were assigned the lowest probability score, indicating that the veracity of the predicted sites is questionable.

Table 5. Binding sites in CrVMP1 as predicted by MotifScan

First residue	Last residue	Type of modification
10	13	Casein kinase II phosphorylation
24	27	*N*-glycosylation
72	74	Protein kinase C phosphorylation
89	91	Protein kinase C phosphorylation
100	105	N-myristoylation
106	111	N-myristoylation
151	154	Casein kinase II phosphorylation
161	164	Casein kinase II phosphorylation
177	182	N-myristoylation
260	265	N-myristoylation
298	301	cAMP- and cGMP-dependent protein kinase phosphorylation
319	324	N-myristoylation
326	331	N-myristoylation
342	345	*N*-glycosylation
380	383	Casein kinase II phosphorylation
395	398	Casein kinase II phosphorylation
425	428	Casein kinase II phosphorylation

3.4.3 Subcellular localization

We next subjected our protein to analysis of its predicted subcellular localization. To this end we used six different localization prediction tools: SherLoc2 (Breisemeister et al., 2009), YLoc (Breisemeister et al., 2010), TargetP (Emanuelsson et al., 2007), Cello (Yu et al., 2006), Predator (Small et al., 2004), and PredAlgo (Tardif et al., 2012); as well as SignalP (Petersen et al., 2011), an algorithm that predicts whether—and where—a protein has a signal peptide, this by scanning for potential signal-peptide cleavage sites. Starting with the latter, SignalP predicted an N-terminus signal peptide in CrVMP1, spanning residues 1–73 (**Figure 8**). It should be noted that SignalP only predicts signal peptide in the narrow sense of the term: N-terminus endoplasmic-reticulum (ER) signal peptides, also known as secretory signal peptides. C-terminus or internal signal peptides (such as those that direct toward nuclear localization) are not processed. It should also be noted that although SignalP's final verdict proclaims the signal peptide mentioned above, the graphic representation of the results shows another cleavage site, almost 60 aa away from the first site, and with almost the same high probability.

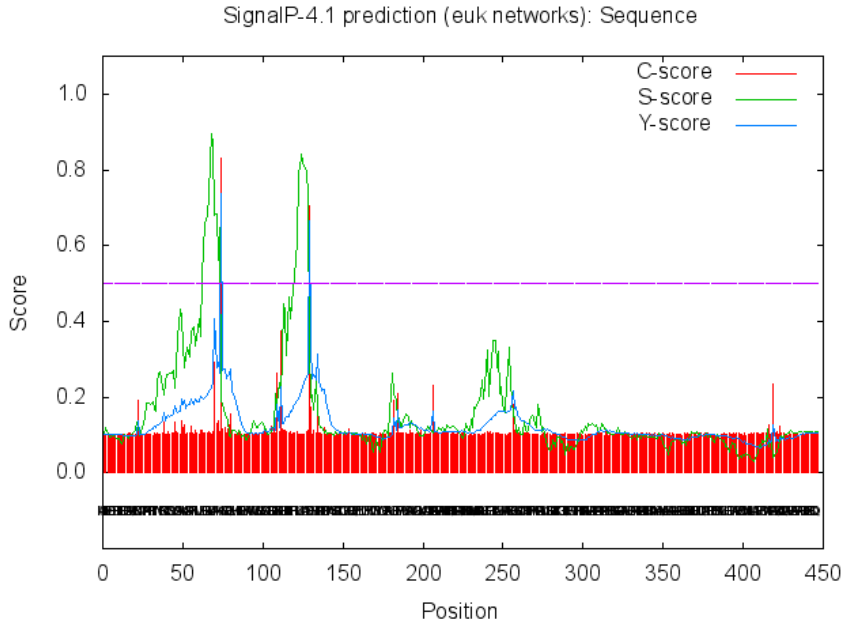

Figure 8. Graphic representation of signal-peptide cleavage-site prediction for CrVMP1 as mediated by SignalP. The x-axis represents the protein's residues from 1 to 447, the y-axis shows the prediction's probability score. The algorithm calculates three scores, represented by the colored curves. The C-score focuses on distinguishing cleavage-site sequences from other sequences; the S-score distinguishes between typical signal-peptide sequences and those that are not; the Y-score integrates the two other scores to produce the most meaningful prediction. The graphic was copied unchanged from the SignalP website.

We proceeded with the bona fide prediction of CrVMP1's subcellular localization. Confusingly, no two algorithms seemed to reach agreement over CrVMP1's location. The analysis resulted in highly ambiguous and at times contradictory results (**Table 6**), which even at their best could not contribute much to predicting our protein's location.

Table 6. Prediction results of CrVMP1's subcellular localization

Algorithm ▶ Localization ▼	TargetP	PredAlgo	Cello	YLoc	Predator	Sherloc2
Chloroplast	8 %	**38 %**	0.41		4 %	0.01
Mitochondria	21 %	2 %	0.50	16 %	1 %	0.03
Vacuole			0.00			0.22
Cytoplasm			0.08	**63 %**		0.08
Nucleus			0.04	21 %		0.07
Golgi						**0.27**
ER			0.01			0.2
Peroxisome			0.42			0.01
Plasma membrane			**3.48**			0.06
Secretory pathway	3 %	4 %		0.3 %		0.05
Other	**77 %**				**96 %**	

Table 6 (previous page): cells with **bold, shaded text** mark the best prediction of each algorithm. Note that SherLoc2 and Cello do not use percentage as output, like the other four services, rather use arbitrary units. Also, note that percentage outputs do not always add up to 100 %, for calculatory reasons.

Interestingly, the CrVMP1 sequence ends with the amino acids RKQQ, which is reported (as RKXX) to be one of four signals for ER retention (Shin et al., 1991). It is not clear why our prediction algorithms failed to recognize this sequence, and why the ER was not favored by any of them.

Table 7 summarizes the results we obtained for CrVMP1 from the various bioinformatic algorithms that we employed.

Table 7. Summary of bioinformatic analysis of CrVMP1

Property	Result	Algorithms used
Functional domains	SNARE-associated Golgi domain	Pfam, KEGG
Transmembrane domains	4 TM domains almost certain, 2 domains questionable	TMHMM, TMPred, Phobius, MINNOU
Coiled-coil domains	Two coiled-coil domains	COILS
Modification sites	17 sites with very low probability	MotifScan
(ER) signal peptides	N-terminus signal peptide	SignalP
Subcellular localization	Ambiguous	PredAlgo, TargetP, SherLoc2, YLoc, Predator, Cello

3.4.4 Homology

BLAST (Altschul et al., 1990) analysis showed that VMP1 has homologues in hundreds of organisms. Most of these organisms have only one *VMP1*-like gene in their genomes. *Arabidopsis thaliana*, with its two KMS genes (Wang et al., 2011), is a notable exception.

The homologue most similar to CrVMP1 comes from *Chlamydomonas*'s close relative, *Volvox carteri*. The similarity between the different VMP1 homologues is at its highest around the conserved SNARE-associated Golgi domain in the middle of the protein. VMP1 homologues have been researched in detail in six different organisms. **Figure 9** provides a sequence alignment of those six proteins, along with CrVMP1. Such alignments are useful in gaining insight regarding conserved regions in proteins. **Table 8** provides basic information about these homologues. **Figure 10** shows a phylogenetic tree of CrVMP1 and its six reported homologues. The tree, created computationally with the different sequences as input, shows to what extent the seven proteins are related to and

diverged from each other. Interestingly, the *Chlamydomonas* protein can immediately be seen in its isolated position, on a branch of its own, indicating that the other six homologues are closer to each other than to CrVMP1.

Table 8. CrVMP1 homologues reported in the literature

Organism	Protein's name	Length	Expect value	Identity	Similarity	Reference
Dictyostelium discoideum (slime mold)	VMP1	403	4e–56	29	46	Clavo-Garrido et al., 2008
Homo sapiens (human)	VMP1, TMEM49 (Transmembrane protein)	406	5e–46	36	55	Ropolo et al., 2007
Rattus norvegicus (rat)	VMP1	406	3e–49	36	54	Dusetti et al., 2002
Caenorhabditis elegans (nematode)	EGP-3 (Ectopic PGL granules)	458	4e–47	40	54	Tian et al., 2010
Drosophila melanogaster (fruit fly)	TANGO-5 (Transport and Golgi Organiszation)	428	3e–44	34	48	Bard et al., 2006
Arabidopsis thaliana (thale cress)	KMS1 (Killing Me Slowly)	416	2e–49	32	50	Wang et al., 2011

Figure 9 (next page)**. Sequence alignment (ClustalW) of CrVMP1 and its six reported homologues** from *Dictyostelium discoideum* (Dd), *Homo sapiens* (Hsa), *Arabidopsis thaliana* (Ath), *Drosophila melanogaster* (Dme), *Caenorhabditis elegans* (Cel), and *Rattus norvegicus* (Rno). Black shading denotes identical residues, grey shading—similar residues. Most of the homologue residues aligned before CrVMP1's first residue were omitted. Empty arrowheads point to the first and last residues of CrVMP1's SNARE domain.

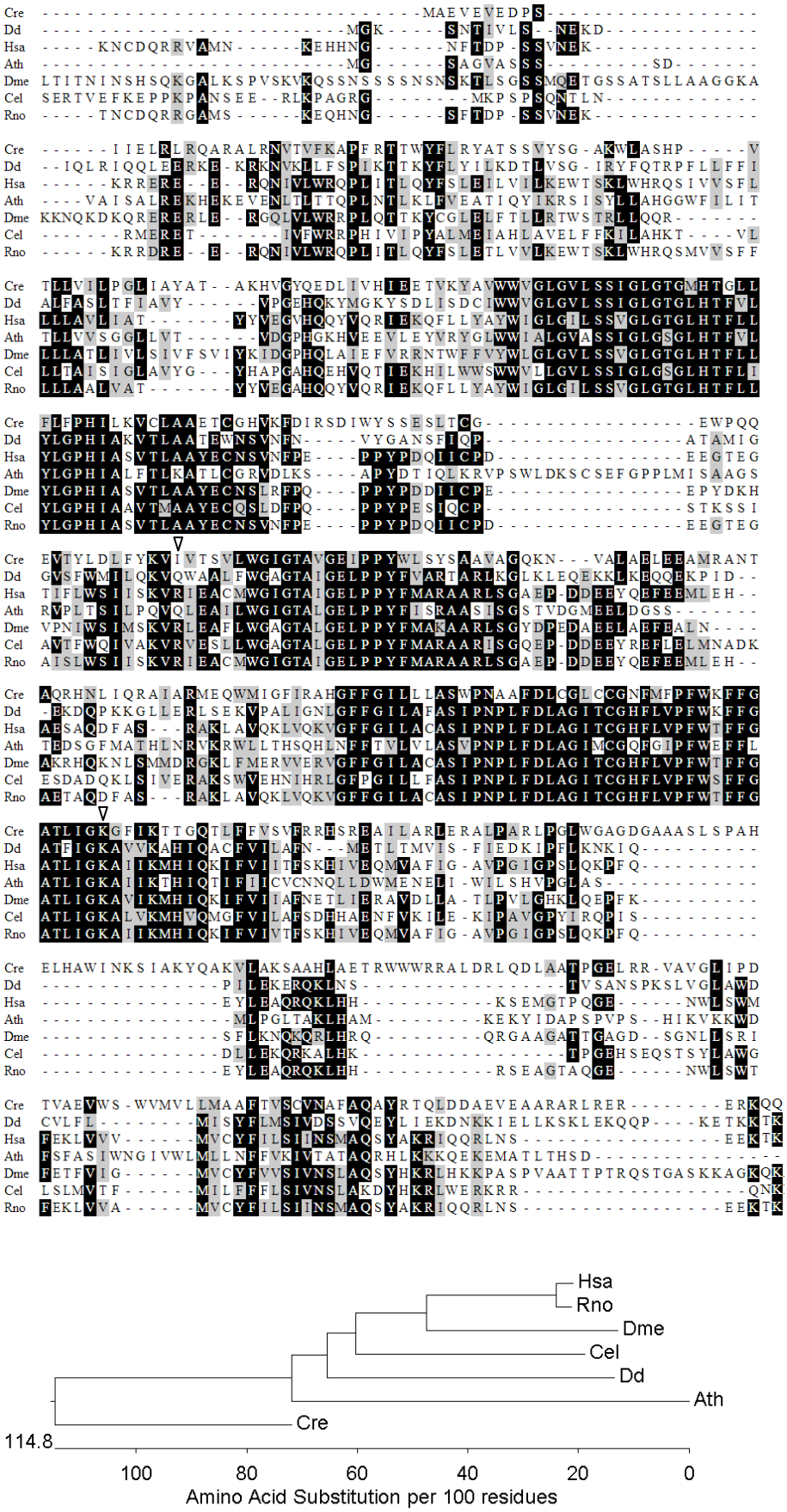

Figure 10. Phylogenetic tree, prepared in MegAlign, of the seven VMP1 homologues depicted in **Figure 9**.

3.5 VMP1-deficient cells display pleiotropic phenotypes

Next we submitted our mutant to light-microscopic analysis. All our knockdown lines exhibited striking, strong phenotypes (**Figures 11–13**). The phenotypes were highly pleiotropic: they were not restricted to one organelle, compartment, structure or process.

The hallmark of the mutant phenotype in all our knockdown lines was defective cytokinesis. In these cells division was initiated but did not reach completion. Daughter cells that were abnormally attached to each other, often with visible division furrows, were frequently observed. We could not determine whether the initial stages of cell division were progressing in a normal fashion, but we observed clearly that the later stages, mainly the detachment of daughter cells from one another, were defective.

Additionally, and often concomitantly, cells exhibited aberrant organelle numbers. The organelles in question were pyrenoids (**Figures 12B, D, J**) and eyespots (**Figures 11D, E, H, L, M; 12B, F, K, M**), of which many of our cells had two or more (compared with one pyrenoid and one eyespot in WT cells), CVs (**Figures 11C, F; 12B, C, E, J, M**; two or more pairs in mutants, one pair in WT), and nuclei (**Figure 13**; two or more in mutants, one in WT). The latter were detected by staining the cells with the fluorescent DNA dye 4',6-diamidino-2-phenylindole (DAPI), followed by epifluorescent microscopy. The binucleated cells could hardly be mistaken for WT cells undergoing normal mitosis: the nuclei were abnormally positioned, the cells were perfectly round and devoid of cleavage furrows, and lastly, the images were taken at a time point in which almost no cell underwent mitosis, indicating that the binucleated cells were a several-hour-old remnant from the previous round of division (**Figures 13B, D, E**).

Multiple pyrenoids per cell were frequently easily discernible in brightfield microscopy (**Figures 12B, D, J**), but in epifluorescence microscopy many cells that looked normal in brightfield and whose pyrenoid number was hard to determine visually would often reveal, by means of the characteristic cavity in the center of the red-autofluorescing chloroplast, that they indeed harbored two pyrenoids (**Figures 13C, F**). The aberrant numbers of nuclei, pyrenoids, eyespots and CVs point again toward defective cytokinesis.

Figure 11 (next page)**. VMP1-deficient CC-4350 cells display pleiotropic phenotypes.** (A) WT cell. (B–M) VMP1-deficient cells. Images labeled with the same letter show the same cell, using different focus, done in order to reveal more details. White arrows point at CVs; black arrows point at flagella. All images were taken using Nomarski (DIC) optics. Scale bars = 5 μm.

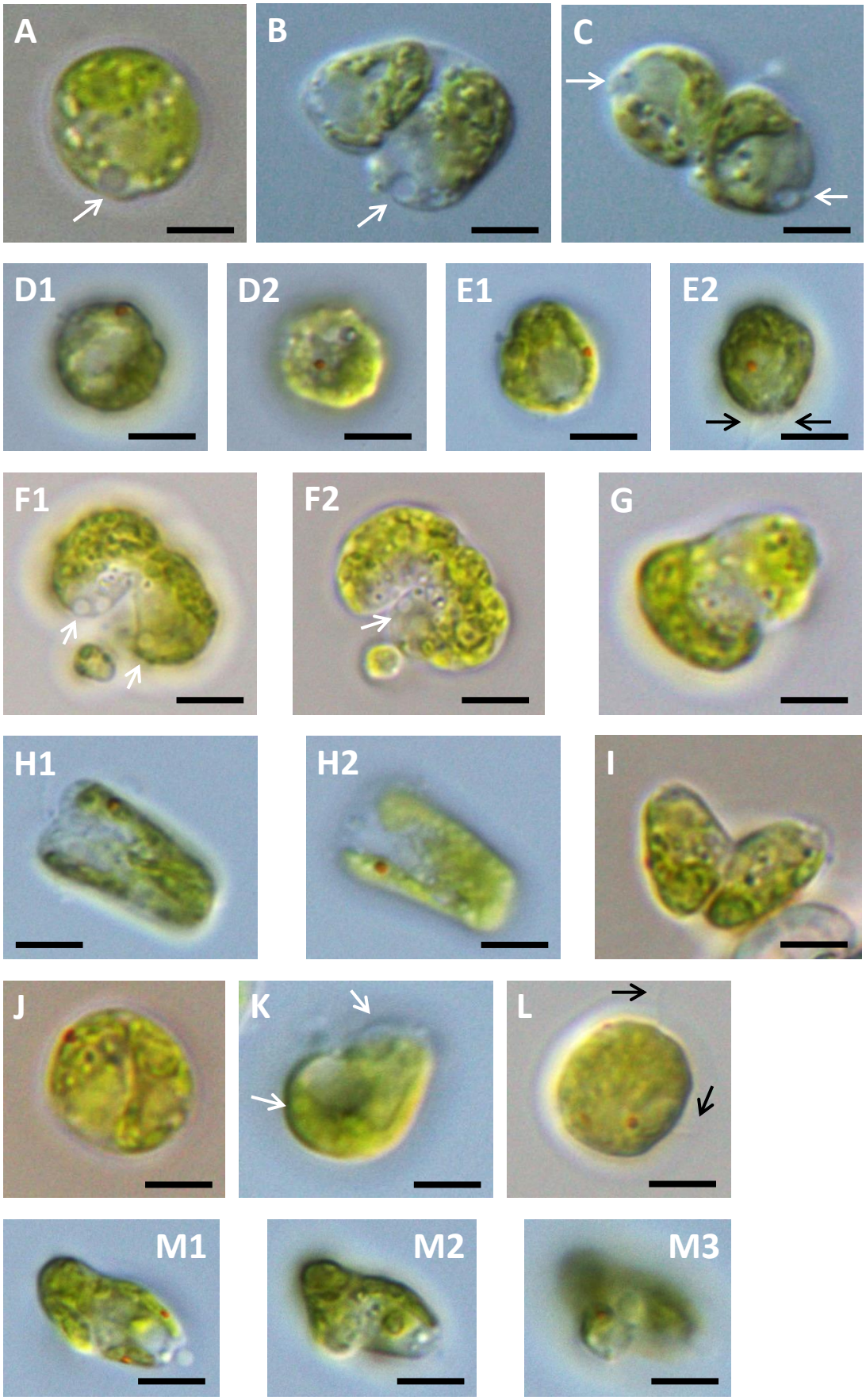
A
B
C
D1
D2
E1
E2
F1
F2
G
H1
H2
I
J
K
L
M1
M2
M3

Many of our mutant cells displayed aberrant cell shapes and internal structures. Cells of the former category failed to maintain the usual round or oval external shape of WT *C. reinhardtii*, but rather appeared in an impressive variety of irregular shapes. Notable examples can be seen in **Figures 11B, C, F, G, H, I, K, M**; and **Figures 12G, H**. In cells with aberrant internal features, the usual structures and organelles that are the trademark of WT *C. reinhardtii*, especially the cup-shaped chloroplast, appeared deformed and misshapen. Such specimens can be seen in **Figures 11B, C, F, G, H, M**; and **Figures 12B–M**. We hypothesize that defective cytokinesis again was the culprit, as organelles misdeveloped and undetached daughter cells pressed against each other to cause deformities. This, however, bears further investigation.

Lastly, two additional phenotypes appeared on occasion: a small fraction of the cells were highly vacuolated, presumably an indication of undergoing cell death (**Figures 11B, K**). More rarely, cells were brimming with numerous globules, deeming any organelle unrecognizable (**Figure 12I**). Such cells lost any distinguishable internal structure (chloroplasts and other organelles could not be observed) and showed instead a dense cluster of globules, each around 1 μm in diameter. This latter phenotype appeared also in WT cells, though much more rarely than in the mutant.

3.6 Osmoregulation and growth in the mutants

Since the visual phenotypes (**Figures 11–13**) indicated defects in cell division, we sought to assay the growth capacity of our mutants. The cytokinetic defects notwithstanding, our mutants were not notably growth-deficient. Mutant liquid-cultures grew slightly, but not significantly, more slowly, and after a while always reached WT cell-densities, indicating that most mutant cells eventually underwent successful cytokinesis.

Our target genes had been selected by virtue of their homology to *D. discoideum* genes implicated in the CV. In the case of VMP1, the absence of this protein in slime mold caused severe defects in the CV and in osmoregulation (Calvo-Garrido et al., 2008). This notwithstanding, the CV did not seem to be affected in our mutants, with the exception of the multiple CVs mentioned above, which were presumably the result of defective cytokinesis. The CVs in our mutants appeared ordinary in shape as well as in function. To confirm that the CV indeed functioned normally in our mutants, we performed a simple osmosensitivity assay: we incubated cells in water (hypo-osmotic environment) for various periods of time, then measured the percentage of surviving cells using a Coulter counter. The results (not shown) showed no significant difference between mutant, WT and empty-vector control.

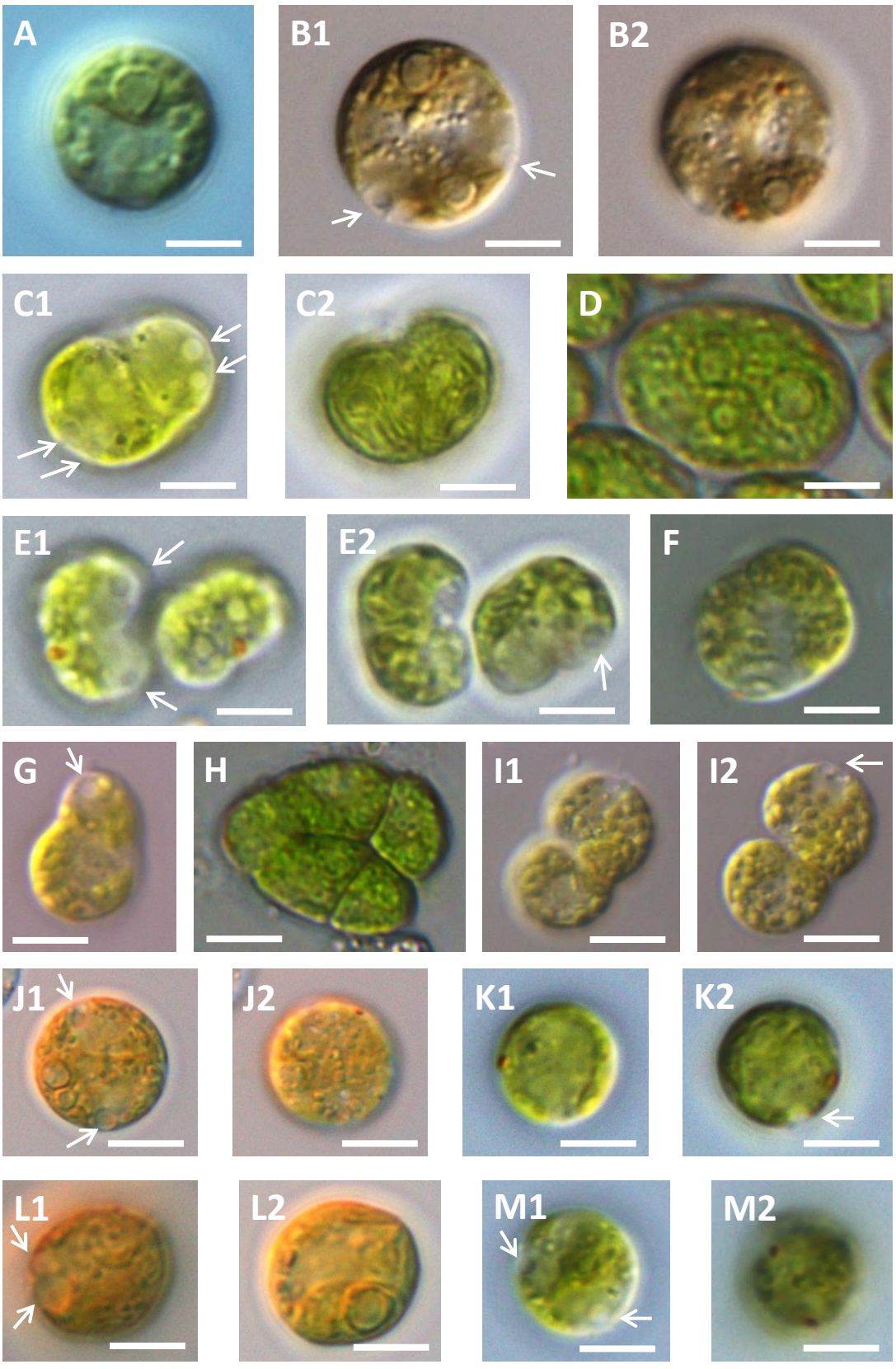
A
B1
B2
C1
C2
D
E1
E2
F
G
H
I1
I2
J1
J2
K1
K2
L1
L2
M1
M2

Figure 12 (previous page)**. VMP1-deficient UVM11 cells display pleiotropic phenotypes.** (A) WT cell. (B–M) VMP1-deficient cells. Images labeled with the same letter show the same cell, using different focus, done in order to reveal more details. White arrows point at CVs. All images were taken using Nomarski (DIC) optics. Scale bars = 5 μm.

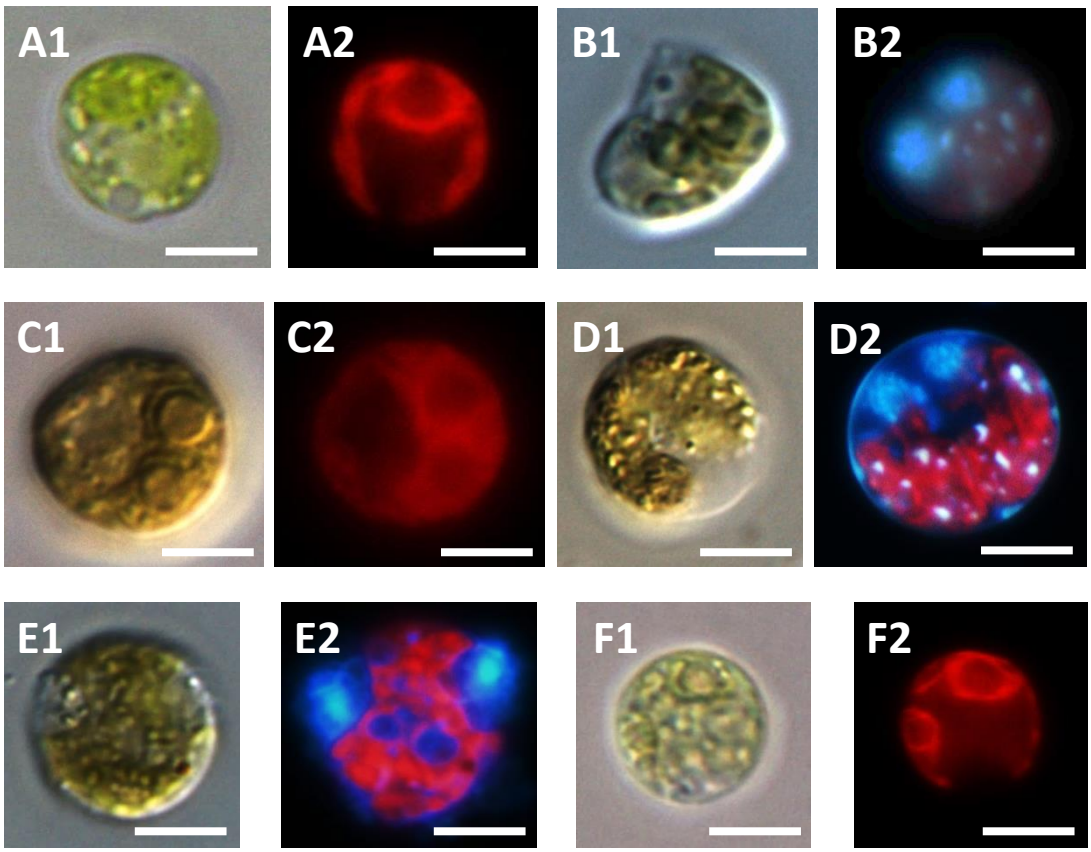

Figure 13. VMP1-deficient UVM11 cells readily display double nuclei and double pyrenoids under an epifluorescent microscope. (A) WT cell. (B–F) VMP1-deficient cells. Images labeled with the same letter show the same cell; images numbered 1 are Nomarski (DIC) images; images numbered 2 are their corresponding epifluorescence images. Blue areas in epifluorescence images display DAPI-stained DNA; red areas show chlorophyll autofluorescence.

3.7 Quantification of the phenotypes

All the mentioned phenotypes appeared both in strain CC-4350 and UVM11, with a tendency of the former toward gross deformities and the latter toward milder, WT-like cell forms with double pyrenoids and nuclei. Quantification of the various phenotypes in different cultures proved a major challenge: the penetrance and distribution were erratic and irreproducible. Our efforts to elucidate the underlying factors that influenced the appearance or lack thereof of this phenotype or the other, or to indeed increase the total penetrance of all aberrant phenotypes, came to no avail. Obvious factors such as mode of

growth (heterotrophic versus photoautotrophic), temperature, light intensity and regime, shaking speed, and the culture's age, did not seem to influence the phenotypes in a coherent fashion. Although CrVMP1 may be potentially involved in the cell cycle and thus be differently expressed in different stages of the cycle, we saw no difference in phenotypic strength or in *CrVMP1* mRNA levels when assayed periodically in an attempt to capture representative stages (data not shown). It should be noted that no synchronized cultures were used in this study.

Our initial estimation was that the penetrance of the aberrant phenotypes was rather low: in each particular culture only a minority of the cells, between 10 and 40 %, displayed a phenotype; the rest assumed WT appearance. As the project progressed we started to suspect that poor visibility or detectability of some phenotypes was leading us to underestimate the penetrance. Many cells revealed their aberrance only following lengthy scrutiny or a serendipitous event (for instance, a normal-looking cell suddenly turning on its side, revealing an additional eyespot), while others exhibited marginal phenotypes: mildly irregular shapes, vague internal structures that while seeming aberrant, were hard to define. Later on, DAPI staining revealed, on occasion, double and multiple nuclei (**Figures 13B, D, E**) in a majority of the cells, a feature that could not have been observed with brightfield microscopy. The milder phenotypes, such as double pyrenoids and nuclei, appeared at times in up to 90 % of the cells, whereas extreme deformities showed a penetrance of around 20 %. The evidence detailed here, in combination with significantly reduced—indeed, at times nearing zero—target-gene mRNA levels as observed with qRT-PCR, which presumably could not result from the gene being silenced in only a minority of the cells, leads us to believe that silencing was successful in most of our cells. We hypothesize that the lower penetrances were a combined result of low visibility of some of the phenotypes, the influence of the cell-cycle stage of individual cells, as well as stochastic effects.

3.8 Electron microscopy reveals internal cellular defects

To expand our understanding of the phenotypes observed with light microscopy, we analyzed our cells—only the UVM11 mutants—using transmission electron microscopy (TEM). This work was performed by Eugenia Maximova, MPIMP. Our findings (**Figures 14–15**) concurred with our light-microscopic observations and added details to them, but also provided novel aspects and phenotypes.

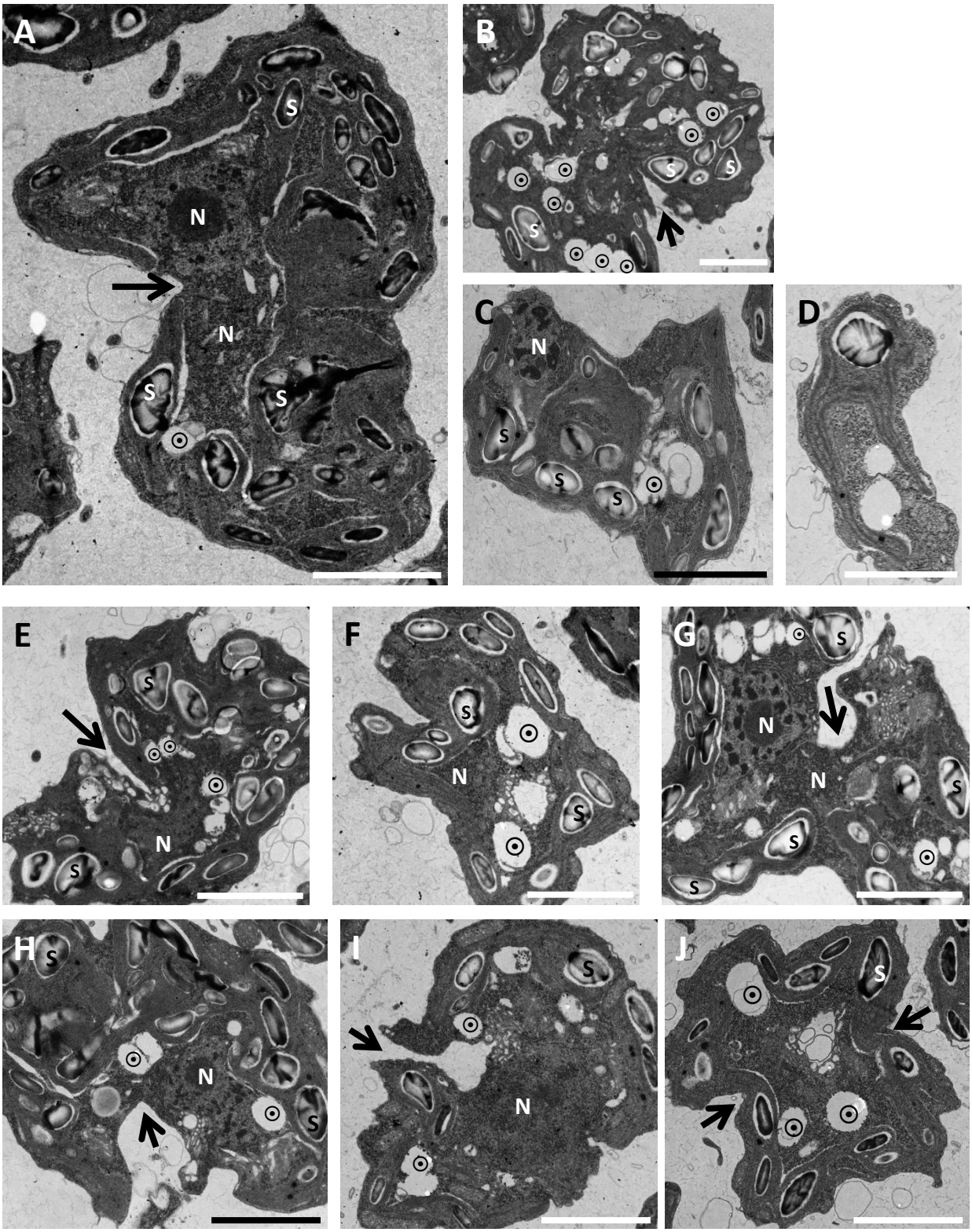
A
S
N
N
S
S
B
S
S
S
C
N
S
S
S
D
E
S
N
S
F
S
N
S
G
S
N
N
S
S
S
H
S
N
S
I
S
N
J
S

Figure 14 (previous page)**. Transmission electron microscope analysis of VMP1-deficient cells.** All panels show abnormally shaped knockdown cells (for an example of a WT cell, see **Figure 15A**). Panels A–B and E–J show cells at various stages of cytokinesis, with visible division furrows (black arrows). Note the mostly clear vacuoles (⊙), the often numerous and abnormally large starch granules (S; not all labeled), and the oddly placed and often deformed nuclei (N). Scale bars = 2 μm.

Our primary light-microscopy observations were reiterated: many cells displayed defective cytokinesis and grotesque cell morphologies (**Figure 14**). Many internal defects, mostly inevident in light microscopy, came to light in TEM. Mutant cells often had deformed and misplaced nuclei (**Figure 14**). Golgi apparatuses were abnormally numerous: 3–4 per cell (**Figure 15E**), compared to almost always one in WT (although many *C. reinhardtii* strains often exhibit two aparatuses, our UVM11 cells seldom did). In many cases the Golgi seemed deformed (**Figure 15E**, lowest aparatus). The mitochondria in the mutant were excessively large, sporting areas up to threefold greater than WT mitochondria, and featuring markedly dilated cristae (**Figure 15D**). Many vacuoles were visible in both WT and mutant, but whereas in the mutant they were almost always vacant (**Figures 14–15**), WT vacuoles often contained what appeared like membranous and cytoplasmic particles (**Figure 15A**). These matter-containing vacuoles are most likely autolysosomes, and their absence in the mutant may indicate a defect in autophagy. The chloroplast in the mutant appeared disorganized and misshapen, with numerous protrusions (**Figure 14**); the stacked thylakoid membranes, always visible in WT as dark lines within the chloroplast (**Figure 15A**), were often absent or much weaker in the mutant (**Figures 14–15**). Lastly, mutants seemed to accumulate more starch granules than WT, with some granules being excessively large (**Figures 14–15**). To test whether starch content indeed differed between WT and mutant, we performed enzymatic starch quantification, both in the end of a 12-hour light period, when starch levels peak, and in the end of the dark period, when most starch is degraded. We observed no significant difference between WT and mutant with regard to starch content (data not shown). Starch quantification was performed by Julia Smirnova, MPIMP.

Figure 15 (next page)**. Transmission electron microscope analysis of WT (UVM11) and VMP1-deficient cells.** (A) WT cell. Note the matter-filled vacuoles, presumably autolysosomes (⊙), the modestly-sized starch granules and mitochondria (S and M, respectively; not all labeled), the well-defined and properly located nucleus (N), and the stacked thylakoid membranes (black arrows). (B) Golgi aparatus from a WT cell. (C–D) Two mutant cells. Note the mostly clear vacuoles (⊙), the often numerous and abnormally large starch granules, the enlarged mitochondria, and the Golgi aparatuses (G), at times only visible through their transport vesicles. (E) Close-up of Golgi aparatuses from a third mutant cell. Scale bars = 1 μm.

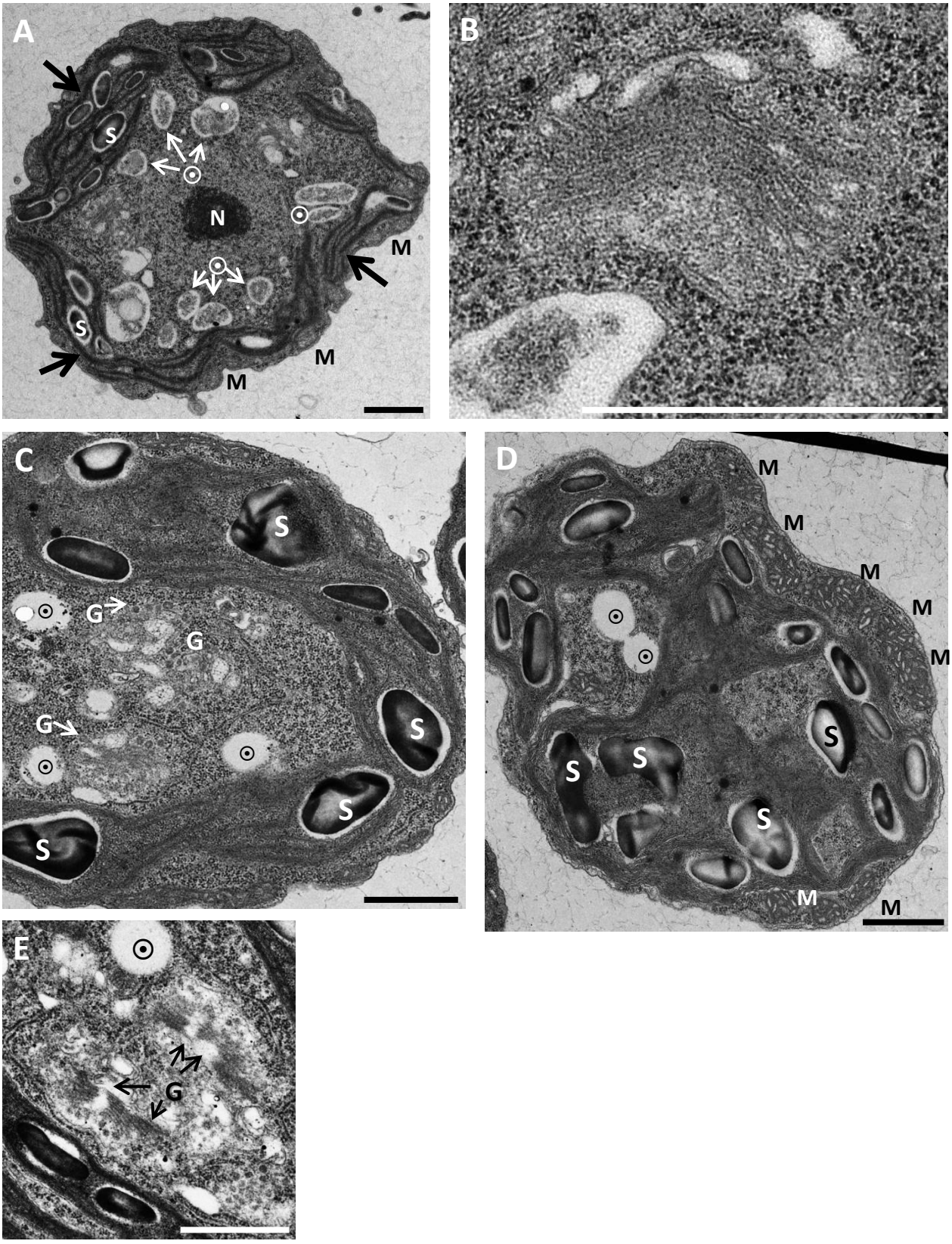
A
S
N
M
S
M
M
B
C
S
G
G
G
S
S
S
D
M
M
M
M
M
S
S
S
S
S
M
M
E
G

3.9 Expression analysis of key cell-cycle and autophagy genes

Given that the microscopic phenotypes pointed toward defective cell division, we sought to assay for the expression in the mutant of several key regulators of the cell cycle. In addition, VMP1's strong involvement in apoptosis (Dusetti et al., 2002) and autophagy in humans (Ropolo et al., 2007) and slime mold (Calvo-Garrido et al., 2010) led us to assay for the expression of several autophagy markers, as well as genes participating in protein degradation. Transcript levels were heterogeneous, with several genes retaining WT-like expression levels, and others exhibiting significant, at times extreme, downregulation in the knockdown (**Figure 16**). mRNA levels of three cell-cycle regulators were, in VMP1-deficient cells, less than 15 % of WT: *RCC1* (Regulator of Chromosome Condensation), *CYN20-3* (of the cyclophilin family), and *CYCA1* (cyclin-dependent protein kinase regulator) (**Figure 16C**). Two genes whose products participate in protein degradation, the AMP-forming ubiquitin ligase *UBC4* and the aspartyl protease *ASP1*, expressed in the mutant at less than 20 % of WT (**Figure 16A**). Notably, two crucial autophagy genes were downregulated in the mutant: *ATG8* (called *LC3* in mammals), whose product is an established marker of autophagy in *C. reinhardtii* (Pérez-Pérez et al., 2010), and *ATG6*, whose human homologue encodes a protein, beclin-1, that interacts with human VMP1 (Ropolo et al., 2007) (**Figure 16B**). Lastly, we assayed for the expression of sporangin, the vegetative cell-wall lytic enzyme that facilitates daughter-cell hatching following cytokinesis (Kubo et al., 2009). The sporangin gene was consistently expressed in the knockdown at 40–50 % of WT (**Figure 16B**). Combined, these results indicate that reduced VMP1 levels result in underexpression of several key regulators of the cell cycle and of autophagy, which in turn results in defective cytokinesis and, tentatively, reduced ability to undergo autophagy.

Figure 16 (next page). Expression levels of selected cell-cycle, autophagy and protein-degradation genes. Values are shown as fold expression; expression levels in empty-vector control (white columns) is always 1. (A) Expression of genes involved in protein degradation. (B) Expression of autophagy regulators and markers and of sporangin. (C) Expression of selected regulators of the cell cycle. Expression levels were measured by qRT-PCR. Error bars represent standard deviations from three technical replicates.

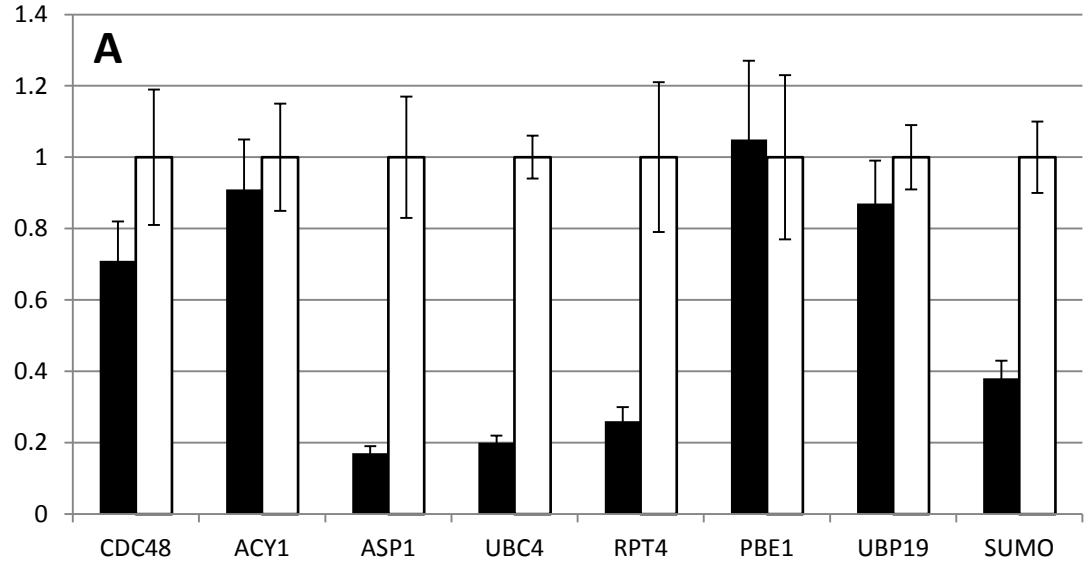
A
1.4
1.2
1
0.8
0.6
0.4
0.2
0
CDC48
ACY1
ASP1
UBC4
RPT4
PBE1
UBP19
SUMO

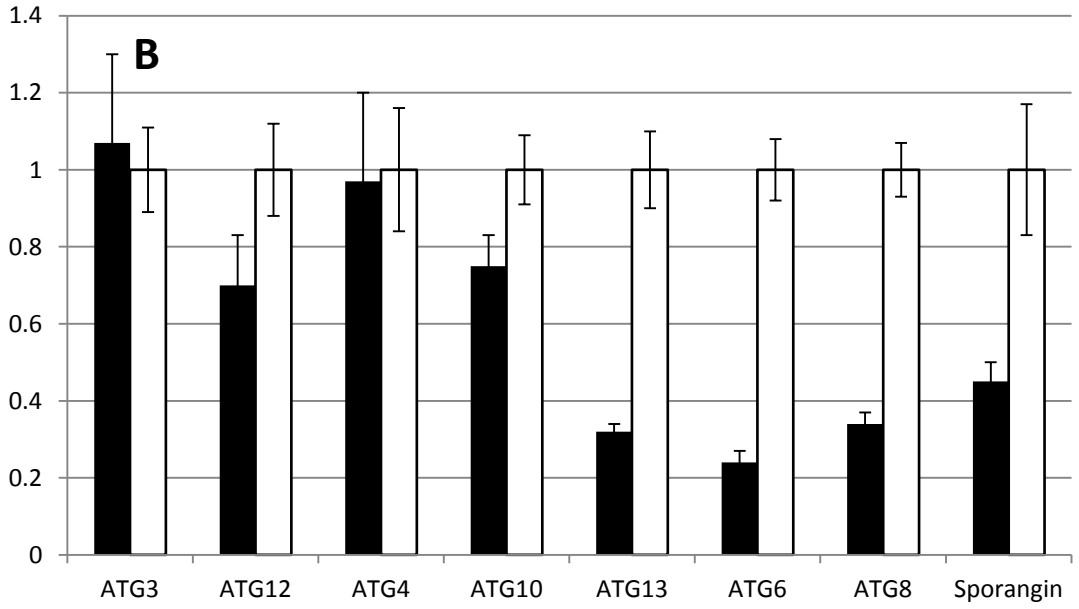
B
1.4
1.2
1
0.8
0.6
0.4
0.2
0
ATG3
ATG12
ATG4
ATG10
ATG13
ATG6
ATG8
Sporangin

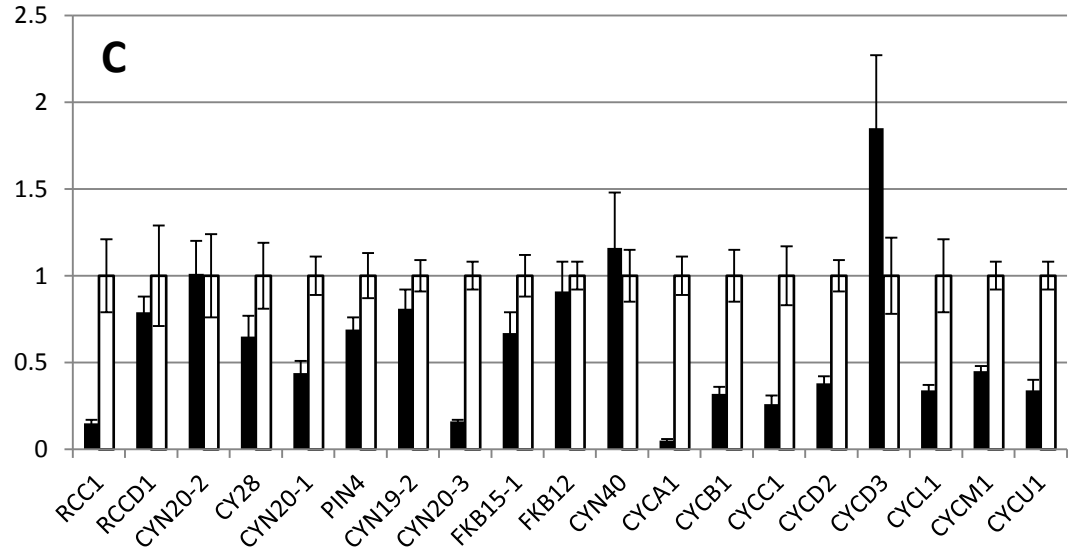
C
2.5
2
1.5
1
0.5
0
RCC1
RCCD1
CYN20-2
CY28
CYN20-1
PIN4
CYN19-2
CYN20-3
FKB15-1
FKB12
CYN40
CYCA1
CYCB1
CYCC1
CYCD2
CYCD3
CYCL1
CYCM1
CYCU1

3.10 Lipidomic profiling

To obtain a more comprehensive picture of the changes that occur in our mutant, and to enhance our understanding of the mechanisms that underlie the observed mutant phenotypes, we subjected our cells to lipiomic profiling. This was achieved by means of long-established bioanalytical methods: liquid chromatography (LC) for analyte separation, and mass spectrometry (MS) for identification. Metabolomic profiling was greatly assisted by Gudrun Wolter, Änne Eckardt, and Antje Bolze, MPIMP.

The results showed numerous differences between mutant and WT. In several cases, whole classes lipids were commonly affected. Some of the observed changes could be correlated with and attributed to our phenotypes. More on this: below. Included in the analysis shown here were three strains: UVM11 (WT), empty-vector control (EVC), and a UVM11 amiRNA transformant with reduced *VMP1* levels, as mediated by qRT-PCR. Six biological replicates were used for each strain to obtain a total of 18 samples; however, two mutant samples were destroyed in preparation. MS analysis produced chromatograms with thousands of peaks. After using several public databases to query these, most notably GoBioSpace (Hummel et al., 2011), we remained with around 120 lipids.

Before we discuss the observed changes, we present an analysis of the variance between our samples. The principal component analysis (PCA) shown in **Figure 17** demonstrates the reliability of our results: the replicates for each strain tend to concentrate together; and the replicates of WT and EVC localize in each other's vicinity and distantly from those of the mutant strain. This arrangement indicates that the replicates of each strain delivered, to a certain extent, similar values; that the values for WT and EVC are similar; and that the values for WT and EVC are significantly different from those of the mutant strain. Indeed, all this can be understood upon looking at the actual values for each specific lipid: the MS intensities, the difference between WT and mutant, and the standard deviations. This notwithstanding, the PCA allows for a brisk overview, with the entire 120 lipids averaged in, an overview that is otherwise hardly possible.

Figure 18 shows a schematic, prepared using the software MapMan (Thimm et al., 2004), of the major classes of lipids detected in our analysis. The schematic serves as a heat map of our results. The most striking trend we observed was the vast accumulation in the mutant of triacylglycerides (TAGs), a class of lipids commonly used as storage molecules. In addition, most detected diacylglyceroltrimethylhomoserine (DGTS) lipids, which replace phosphatidylcholines (PC) in *C. reinhardtii*, accumulated in

knockdown cells, whereas most digalactosyldiacylglycerols (DGDG), phosphatidyl-ethanolamine (PE), and phosphatidylglycerols (PG) showed higher levels in WT than in the mutant.

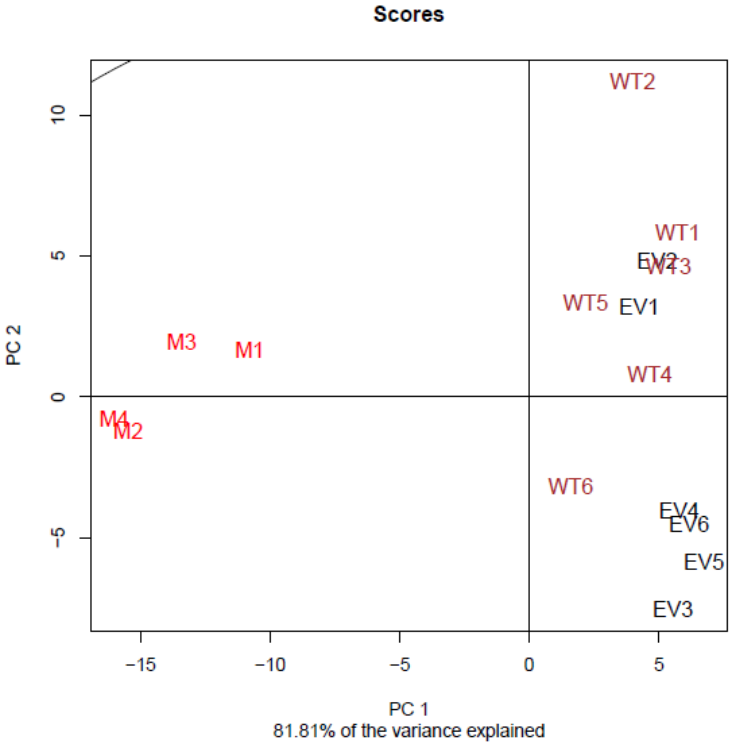

Figure 17. Principal component analysis of our lipidomic profiling results. Six replicates of WT (brown), six of empty-vector control (black) and four of the mutant are shown (red). These are the very samples whose results are shown in **Figure 18**.

Figure 18 (next page)**. Lipidomic profiling of mutant, WT and empty-vector control.** Heat map of the lipids measured, sorted according to lipid class, carbon-chain length (numbers from 30 to 60) and number of double bonds (numbers from 0 to 9). The schematic, produced by MapMan (Thimm et al., 2004), shows the lipids' $\log_2$ fold-change in the mutant compared to empty-vector control: red circles denote lipid accumulation in the mutant, blue circles denote accumulation in empty-vector control, white and pale circles denote nearly no change. Note that the scale margins, 1 and –1, are "at least" values. Values greater than 1 or smaller than –1 have the same color as 1 and –1, respectively.

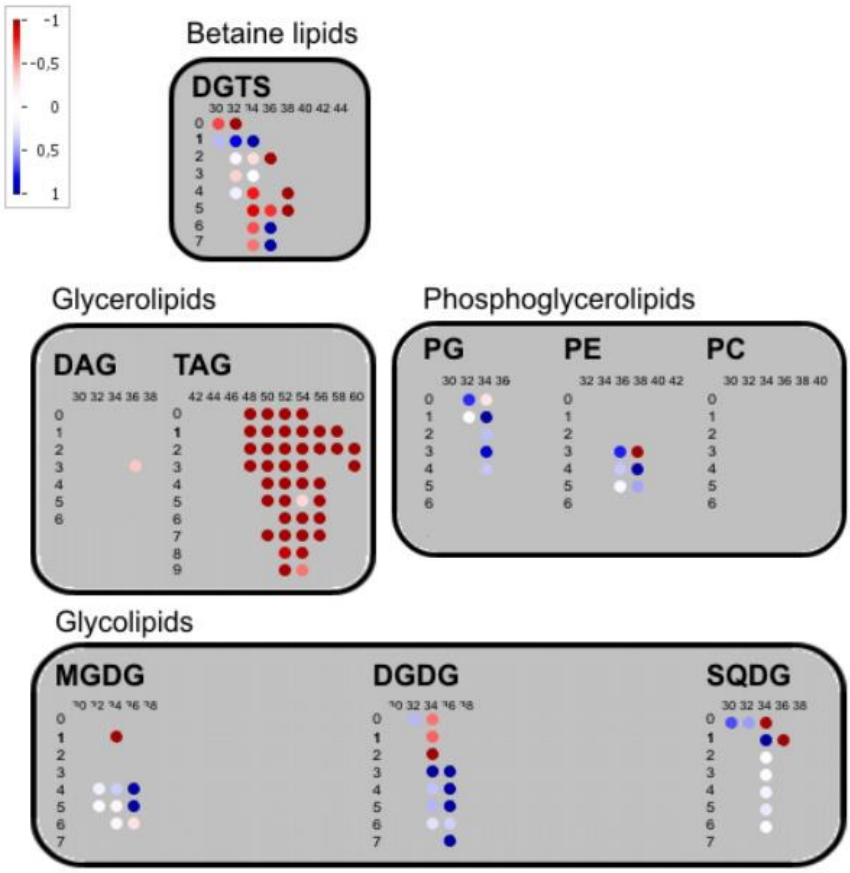

3.11 Subcellular localization

To determine the intracellular location of VMP1, we attempted to employ two common strategies: fluorescent protein constructs; and indirect immunofluorescence. The former can be performed on live cells, which enables kinetic studies and the visualization of proteins as they move within the cell; but it may require complex molecular cloning, and the fused fluorescent protein may interfere with the correct localization or folding of the main protein. Immunofluorescence can only be performed on dead, fixed cells; it requires antibodies against the target protein, whereby antibodies that worked in Western blot may not necessarily work in immunofluorescence; and it prerequisites the penetration of the antibody into the cell (except for the detection of external membrane proteins) and the accessibility of the protein's epitope (antibody recognition site). *Indirect* immunofluorescence means that the fluorescent dye does not bind directly to the target protein, but indirectly, through a primary and then a secondary antibody.

For the purpose of immunofluorescence we utilized an antibody raised against the human homologue of VMP1 (TMEM49), the same that we had used for Western blot (see above; **Section 3.3**). The results can be seen in **Figure 19**. Although considerable staining can be seen, it is impossible to draw any conclusions with regard to CrVMP1's subcellular localization. The staining appears to be quite specific in that not the entire cell is evenly stained. On the other hand, the intense staining is rather counter-intuitive, considering the primary antibody's poor performance in Western blot, as well as the protein's supposedly low abundance, as judged by its mRNA levels in qRT-PCR. At any rate, two additional measures are essential: control stainings need to be performed, once omitting the primary antibody, once the secondary, to confirm that the staining in our images is specific and derives from our protein. Next, co-stainings need to be performed, whereby established markers for various cellular compartments would be used for staining alongside our primary antibody, in order to be able to identify the areas, compartments, organelles or structures that are stained by said primary antibody. Unfortunately, time constraints did not allow us to perform any of this.

Our attempt at utilizing fluorescent protein constructs achieved even less. To this end, we tried to clone our gene into a plasmid containing yellow fluorescent protein (YFP), as described in Neupert et al. (2009), and to express it in the high-expression strain UVM11, also described in this article, and, incidentally, also used in our work as one of the background strains for amiRNA silencing. We were able, after many a trial, to PCR-amplify the *VMP1* gene from cDNA, upon which we cloned it into the generic vector pGEM-T to facilitate easy amplification in the future. Next, we eliminated, using site-directed mutagenesis, a BsmI restriction site in the gene, so that we could later use the same enzyme, in combination with EcoRI, to facilitate the gene's insertion into the plasmid. Unfortunately, the persistent failure of subsequent steps, combined with the time constrained discussed above, led us to discard the effort.

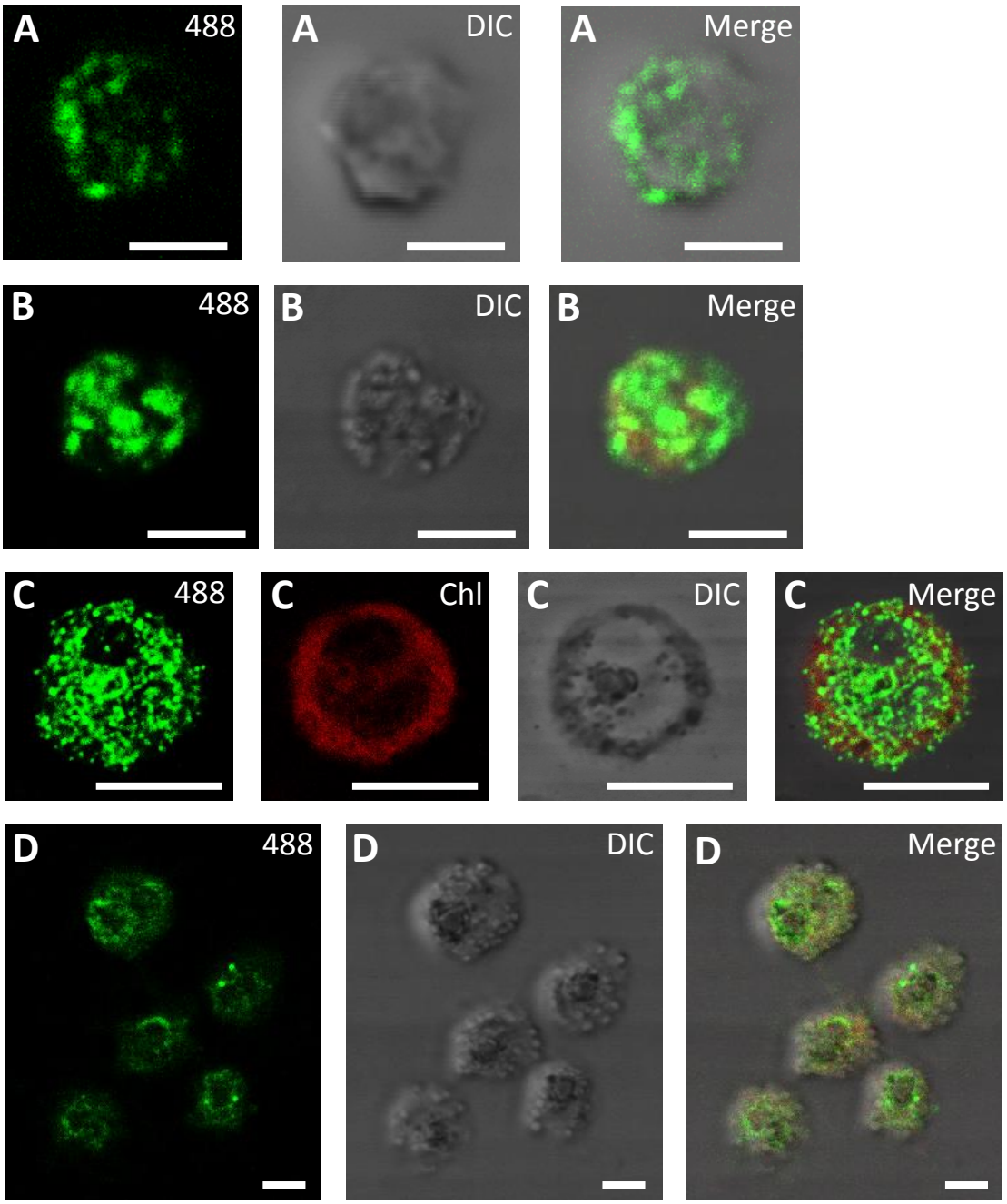

Figure 19. Indirect immunofluorescence for CrVMP1. *C. reinhardtii* cells (strain UVM11) were fixed, permeabilized, stained with a primary α-TMEM49 antibody, then with a secondary antibody conjugated to the fluorescent dye CF 488A. Images labeled "488" show areas stained by the secondary antibody; images labeled "DIC" show the DIC-acquired view of the respective fluorescence images. The image labeled "Chl" shows chlorophyll-derived autofluorescence. Although chlorophyll was removed during sample preparation, residual, and at times more than that, autofluorescence can be seen in image C-Chl and in some of the Merge images. Scale bars = 7 μm.

3.11.1 The *Chlamydomonas* CV can be chemically stained

Several specific markers for the staining of the CV have been developed over the years. These markers proved useful for localization studies. Whereas the *Chlamydomonas* CV is quite conspicuous and easy to identify, the CV in *Dictyostelium*, for instance, is less so: it is not localized next to cellular hallmarks, such as the flagella in *Chlamydomonas*; and the phagocytic *Dictyostelium* cell abounds with various kinds of similar-looking vacuoles. The localization of a novel protein to a vacuole in *Dictyostelium*, using one of the methods described above, is often ambiguous. Using specific markers can clarify in such cases what kind of vacuole is in question (for an example see Betapudi et al., 2005). Some CV markers are fusions of fluorescent proteins, typically GFP, and a protein that is known to specifically localize to the CV, for example dajumin (Gabriel et al., 1999). Other investigators have used antibodies against specific CV proteins, such as calmodulin (Heuser et al., 1993) and subunits of the vacuolar proton pumps that attire the CV's membrane (Fok et al., 1993). Other CV markers are fluorescent dyes, such as FM4-64, that stain specific lipids (Heuser et al., 1993).

Due to the paucity of research articles discussing the *Chlamydomonas* CV (discussed in **Section 1.1.4**), it is scarcely a surprise that almost no markers have been reported for the *Chlamydomonas* CV. Only two articles report progress in this matter: Ruiz and colleagues (2001) used antibodies against the vacuolar proton pump as a marker, whereas Komsic-Buchmann and colleagues (2012) used a GFP-aquaporin construct.

Predicting the need for such a marker, we had tested, during the initial stages of this work, the capacity of the styryl dye FM4-64 to stain the *Chlamydomonas* CV. The results were positive (**Figure 20**), constituting the first staining of the *Chlamydomonas* CV that does not require antibodies or GFP fusions. In addition to still images from a laser-scanning confocal microscope, we were able to record a short video, using a light microscope, of the *Chlamydomonas* CV cycle (**Figure 21**), demonstrating the usability of this fluorescent dye in kinetic studies of the CV. Staining of the *Chlamydomonas* CV was performed in collaboration with Carsten Hille, UPPC.

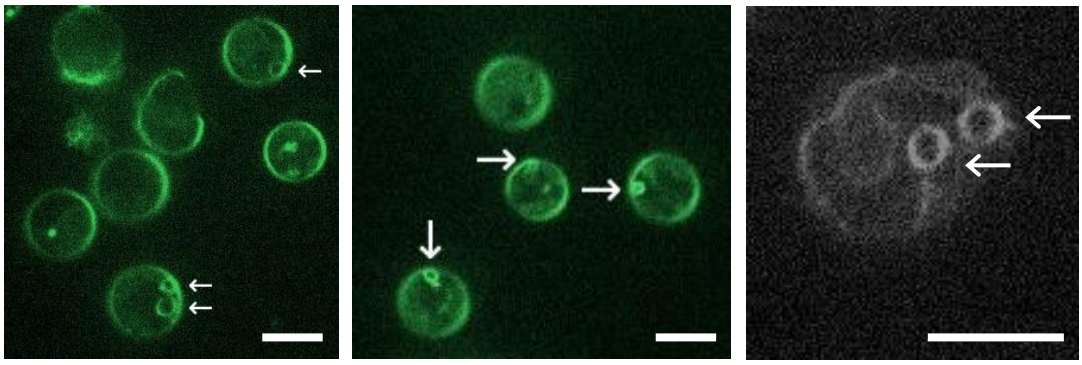

Figure 20. *C. reinhardtii* CVs stained with FM 4-64: confocal-microscope images. White arrows point at CVs. Scale bars = 10 μm.

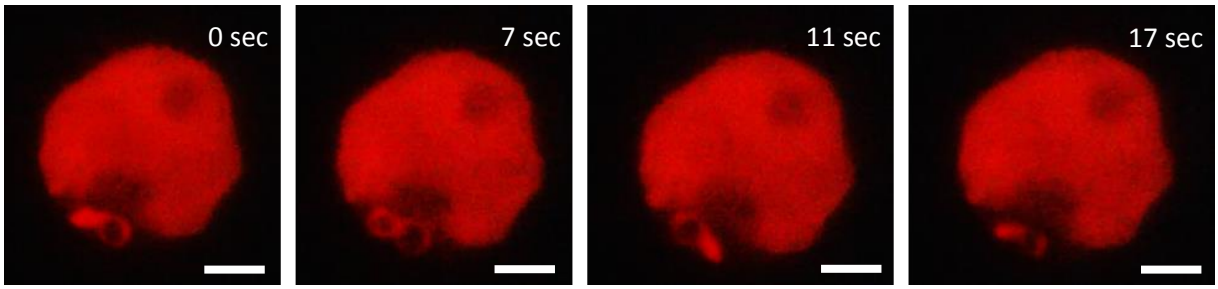

Figure 21. *C. reinhardtii* CVs stained with FM 4-64: still images from a video taken on an epifluorescence microscope. CVs are at the bottom of the cell; the dark area at the top of the red chloroplast is the pyrenoid. Scale bars = 3 μm.

4. Discussion

4.1 Overview

This work, like many scientific endeavors before it, produced results greatly diverging from its initial aim. We had set out to turn some of the stones in the towering pile of contractile-vacuole (CV) unknowns, and ended up with a protein of vast interest but apparently little relation to the CV in *Chlamydomonas*. Likewise, our study had weaknesses and strengths: while technical hurdles and other circumstances prevented us from addressing many of our questions, we were able to utilize a rather uncommon combination of techniques, which added to the work's validity. The protein that became the focus of our work, VMP1, has attracted much interest, to the tune of around 35 articles, since its first characterization (Dusetti et al., 2002), and we were glad to contribute to the growing body of knowledge surrounding it.

4.2 Using amiRNA for gene silencing in *Chlamydomonas*

We attempted to silence our genes using artificial microRNA (amiRNA), a novel method in general (Schwab et al., 2006) and a true yearling in *Chlamydomonas* (Molnar et al., 2009; Zhao et al., 2009). Its novelty, along with the subsequent paucity of articles attesting to its usage, warrant a short discussion here.

AmiRNA has been superseding the older and inferior RNAi, inverted repeats and antisense methods since its, the former's, inception. The latter three methods (reviewed in Schroda, 2006) have been plagued by imperfect specificity, whereby off-target genes become inadvertently and unpredictably silenced (Xu et al., 2006), and by silencing of the silencing-agent itself, such as frequently occurs with inverted repeats (Yamasaki et al., 2008). AmiRNA silencing is posttranscriptional: the gene to be silenced gets to be transcribed, but the mRNA then degrades. Since mRNA degradation is imperfect, certain levels of mRNA, and hence protein, remain in the cell. Though this is not ideal, the achieved downregulation is in many cases sufficient and manifests itself phenotypically.

The stability of the different silencing methods is another issue. Cells are in general not fond of having parts of their genomes silenced; they also dislike expressing foreign genes, which is a requirement in amiRNA silencing. Unless offered adequate

incentives, or, more biologically put, subjected to selective pressure, they would often silence the silencing construct, refuse to express it, or even, when relevant, eject it from the cell. Reports about the stability of amiRNA in *Chlamydomonas* are sporadic, since not much time has passed since the introduction of the method. Molnar et al. (2009) and Zhao et al. (2009) attested to silencing stability of at least 500 generations, or six months, respectively. Burgess and colleagues (2012) report a decrease in silencing capacity following an 18-month period. In our hands, silenced clones remained unchanged for at least three months, whereupon slight, inconsistent increases in target mRNA levels were observed. Silencing constructs would normally show greater stability if the gene at question were not essential—in other terms, if the absence of the protein were not detrimental for the cell. In our case, VMP1 deficiency definitely resulted in detrimental abnormalities, but on the other hand the cells were not growth-deficient. Given these circumstances, it is hard to define to what extent our mutant cells found it essential to resist silencing.

Section 3.3 describes the screening process for finding silenced clones. Why would cells grow at all on a selective plate if their target gene were not silenced? It often occurs that only a portion of a transformed construct is incorporated into the recipient *Chlamydomonas* genome. The mechanisms controlling this are unknown, but presumably go hand-in-hand with *Chlamydomonas*'s inherent disinclination to express foreign genes. In this fashion, many of the cells in our transformations seemed to have absorbed the resistance (in the case of paromomycin selection) or the argininosuccinate lyase gene (in the case of arginine selection), but discarded or degraded the actual amiRNA part. Such cells gave rise to colonies on the selective plates but showed no silencing of the target genes. Anecdotal reports (Stefan Schmollinger, UCLA; personal communication) attest to silencing rates of around 50 % using this method: in other words, half of the colonies on each plate are expected to show some degree of silencing. This observation was confirmed in our experiments.

4.3 Penetrance

The issue of phenotypic penetrance preoccupied us to a great extent throughout the study. What portion of our cells was affected by the mutations? Should we not expect the answer to be "one-hundred percent", and if not, why? We cannot offer conclusive answers to these questions, but here are some thoughts.

As described above, (**Section 3.7**), we had initially been baffled to see phenotypes appearing in but a trifling minority of the cells in each particular culture. Did this observation mean that silencing worked only in the phenotypic cells? we wondered. This did not reconcile with the excellent silencing that we saw at the mRNA level, as assayed by qRT-PCR; if the majority of the cells produced normal amounts of our gene's mRNA, this would surely mask the lower levels in the few mutant cells, and the qRT-PCR results would read: no silencing. This, indeed, was not the case.

As our phenotyping skills and methods improved, penetrance started to soar. We reckoned that our phenotypes were oftentimes marginal, difficult to detect and define, and that the vast majority of our cells exhibited at least some degree of aberrance. Still, visible penetrance never rose above 90 %.

Several possible explanations can be attributed to so-called "stochastic effects". *Chlamydomonas* cells are notoriously sensitive to growth conditions. It is safe to assume that, vigorous shaking notwithstanding, no two cells in a *Chlamydomonas* culture share an identical growth experience, as cells incessantly mask the light from and collide with each other. Such stochastic—that is, random, unpredictable—events, may cause one or more of the following: amiRNA could be produced in different amounts in each cell; amiRNA could show variability in its capacity to track partner mRNA and to bind to it; the subsequent mRNA degradation mechanism could function with differing efficacy in each cell; and the downstream effects of the silencing could be manifested to a different degree in each cells.

Another important factor is the cell cycle. Our protein, CrVMP1, as immediately evident from the visual phenotypes, is involved in cell division, indeed the climax of the cell cycle, a tightly regulated and timed process. If our protein acts, in WT cells, only in conjunction with cell division, it is to be expected that its absence will affect only cells undergoing division or preparing for it. This may serve as the main explanation to our penetrance issue: only cells undergoing division display aberrant phenotypes; in other stages of the cell cycle the cells have no need for our target protein and the absence of the latter does not play a role.

How can this theory be tested? The most promising way would be to use synchronized (or synchronous) cultures. In such cultures almost all the cells grow in synchrony: at any given moment they all share the same cell-cycle stage. Synchronized cultures can be obtained by several methods: size filtration (small daughter cells pass through a filter while bigger cells are retained; Maruyama and Yanagita, 1956), centrifugation (heavy, aged cells precipitate at the bottom, light daughter cells remain in the supernatant; Hartwell, 1970), chemical growth arrest (a growth inhibitor, often

nocodazole, is introduced into the culture, then removed; Nüsse and Egner, 1984), and the membrane-elution method, whereby cells are passed through a filter, whereupon some cells are retained on it; it is then immersed in fresh medium; daughter cells grow, all simultaneously, from the retained cells, detach and collect below (Helmstetter and Cummings, 1963). The main method used in *Chlamydomonas*, though, is growing the cells in minimal medium, alternating between light and dark, and repetitively diluting the culture (Bernstein, 1960). It should be noted that the entire concept of synchronization and its feasibility is a matter of heated debate (Cooper, 2004). Due to technical hurdles and time constraints we were not able to obtain synchronized cultures in this study. Another way to exercise control over the cell cycle, and thereby to test whether our phenotypes were more manifested in certain stages, would have been to induce, and, alternatively, inhibit, cell division. Division can easily be induced in *Chlamydomonas* by resuspension in new medium. Division can be inhibited by treatment with, amongst others, microtubule-polymerization inhibitors such as trifluralin (Hess and Bayer, 1977) and oryzalin (Strachan and Hess, 1983). When division is induced, we would expect almost all cells to show a phenotype if indeed VMP1 were essential for cell division. Conversely, we would expect almost no aberrant cells in a division-arrested culture. This, unfortunately, was another endeavor that we were not able to undertake.

To conclude, stochastic factors that influence individual cells in a culture, as well as the cell-cycle stage in which a particular cell is found, presumably work in concert to bring about the phenotypic heterogeneity, in terms of penetrance, that we observe in our mutant cells. Further investigation is required to determine the exact factors and mechanisms that play a role.

4.4 VMP1: eleven years of research

VMP1 (Vacuole Membrane Protein 1), the focus of our study, is a transmembrane protein with homologues in all eukaryotic kingdoms, with fungi being a notable exception. It has been shown in separate studies to be localized to several cellular compartments: the Golgi apparatus (Dusetti et al., 2002), the endoplasmic reticulum (Calvo-Garrido et al., 2008), autophagosomes (Ropolo et al., 2007), and the plasma membrane (Sauermann et al., 2008). It has been implicated in an array of cellular processes: organellar biogenesis, endo-, exo- and phagocytosis, and protein secretion (Calvo-Garrido et al., 2008); apoptosis (Dusetti et al., 2002); adhesion (Sauermann et al., 2008); and, perhaps most notably, autophagy (Ropolo et al., 2007), as well as a

specialized type of autophagy, namely zymophagy, in which zymogen granules—subcellular structures that contain inactive digestive enzyme—are selectively degraded (Grasso et al., 2011). Last but not least, it is known to play a key role in certain human diseases, namely diabetes (Grasso et al., 2009), pancreatitis (Dusetti et al., 2002; Vaccaro et al., 2003) and several types of cancer (Sauermann et al., 2008; Ying et al., 2011; Guo et al., 2012). It has recently been shown *in vitro* that when human VMP1 is silenced, human immunodeficiency virus (HIV), the causative agent of AIDS, achieves much lower replication rates (Dziuba et al., 2012) The link between this fascinating protein's molecular characteristics and the phenotypes and processes in which it is involved are gradually being elucidated:, its cell-membrane localization and cell-adhesion capacity, for instance, account for its reduced expression in metastasized cancer cells (Sauermann et al., 2008), since loss of adhesion is essential for metastasis (Benoliel et al., 2003); and its role in zymophagy helps to protect pancreas cells from digesting themselves during pancreatitis. VMP1 had first been characterized in rat (*Rattus norvegicus*), eleven years before the writing of these lines (Dusetti et al., 2002). It has since been reported in five additional organisms—not including *Chlamydomonas* (see **Table 8**). Incidentally, its name points rather toward its induction of cytoplasmic vacuolization when overexpressed in rat cells, rather than toward a vacuole-membrane localization—rat VMP1 indeed localized to the membranes of the vacuoles whose formation it induced, but it also localized to the Golgi aparatus and to the ER (Dusetti et al., 2002).

4.5 VMP1 and cell division: analysis of our results

In this work we were able to assign a novel role to the already versatile VMP1. VMP1 has thus far not been implicated in relation to defective cell division. At the same time, a rather modest number of cytokinesis mutants has been reported in *Chlamydomonas* (Harper, 1999). Some were natural isolates (Harper et al., 1995), others generated by and identified following nonspecific mutagenesis (Hirono and Yoda, 1997), while others yet were the result of targeted silencing (Koblenz et al., 2003; Pfannenschmid et al., 2003; Qin et al., 2007). In the three latter examples, proteins of the basal bodies, cytoskeleton, and flagella, respectively, were silenced. Indeed, these three structures are tightly related to cell division; processes such as flagellation and cleavage-furrow formation, formerly thought to be completely distinct, are gradually losing the borders between them, and proteins that are associated to these structures often exhibit multiple roles. Not much can be deduced though with regard to the cytoskeleton, basal bodies and flagella in our mutant. As for the latter, our *Chlamydomonas* strains harbor very short

flagella; often no flagella were observed under the microscope, anecdotally more so in the mutant than in WT, but it was impossible for us to determine whether this should be ascribed to the VMP1 deficiency or rather to limited visibility.

Another organelle starring in our knockdown cells was the eyespot (**Figure 2, Figure 3**). It has been reported that a few cells with two eyespots can frequently be seen in WT cultures. True mutants that harbor multiple eyespots (as well as mutants that have unusually small eyespots and ones that have no eyespots at all) have also been reported (Lamb et al., 1999). Our mutant cells were markedly different: they almost always showed cell-division defects (cleavage furrows, deformed chloroplasts) in addition to harboring multiple eyespots; and they lacked the *mlt1*$^-$ characteristic of usually having one correctly placed eyespot and an additional, aberrantly placed eyespot near the base of the flagella (Lamb et al., 1999).

Electron microscopy revealed in the mutant enlarged mitochondria, disorganized chloroplasts, autophagosomes in WT but not in the mutant, overnumbered and perhaps misshapen Golgi apparatuses, and, excessively large starch granules (**Figures 4–5**). The latter two phenomena are known to be linked: plants tend to accumulate starch when their Golgi system is inhibited or disrupted (Hummel et al., 2009). However, claiming that such is the case in our mutant would be unsubstantiated: our EM images do not allow for a clear-cut definition of the Golgi's well-being or lack thereof in our cells, and we cannot exclude that the Golgi is normal in our mutant. The same applies for starch: enzymatic quantification showed no difference in starch content between WT and mutant, and our EM images allow no statistical analysis of the amount or size of starch granules. This aspect of our phenotype therefore remains anecdotal and bears further investigation. A connection between VMP1 and Golgi in *Chlamydomonas* would correspond to observations in the former's homologues: VMP1 was shown to be localized to the Golgi apparatus in the first VMP1 study (Dusetti et el., 2002), and VMP1-deficient slime mold showed morphological and functional Golgi defects (Calvo-Garrido et al., 2008).

4.6 VMP1 and autophagy: analysis of our results

VMP1 has been shown several times to be an inducer of autophagy, and the molecular mechanisms by which it so acts are gradually being elucidated (Molejón et al., 2013a). Autophagy, despite being a topic of extensive research and discussion, still bears many unknowns; doubly so in *Chlamydomonas*, in which the subject is in its infancy (Pérez-Pérez et al., 2010).

Autophagy is a catabolic process in which cellular organelles and other components are degraded in lysosomes. Initially thought esoteric, it is now known to be a basic and essential process that has implications in a legion of other processes. Correct growth and development, the maintenance of cellular health, and the ability to react to conditions of stress are impossible without autophagy. The cell uses autophagy to gain precious building blocks at times of scarcity: unnecessary proteins and lipids are degraded and the resulting free amino and fatty acids are utilized for survival (reviewed in Mizushima et al., 2011). In addition, autophagy serves to rid the cell of damaged organelles, such as mitochondria. It is now believed that age-dependent reduction in autophagic capacity, and the subsequent accumulation of damaged organelles, is a major factor for the deleterious effects that are the hallmark of aging (Cuervo et al., 2005). One more notable and relatively novel role of autophagy is in immunity: the autophagy apparatus is apparently also capable of digesting intracellular pathogens (Levine, 2005). Autophagy can be induced by a multitude of treatments, conditions and signals, converging into several signaling pathways. We will avoid a general review of autophagy, by all means beyond the scope of this work, and discuss only the issues relevant to our protein of interest, VMP1.

How does the cell degrade its own components in autophagy? Upon induction, membranes that probably derive from the ER (Tooze and Yoshimori, 2010) start curving and engulfing the component to be degraded. The membranes close up and an autophagosome is born: a double-membrane vacuole that contains cellular components. The autophagosome migrates within the cytoplasm until it meets a lysosome—a vacuole containing digestive enzymes. Autophagosome and lysosome fuse and unite to obtain an autolysosome. The digestive enzymes degrade the engulfed component and the inner membrane; the products—amino acids, lipids, and other building blocks—are eventually released into the cytoplasm (Mizushima et al., 2011). It should be importantly noted that the process described here refers to macroautophagy, one of three known types of autophagy. In the other two types, microautophagy and chaperone-mediated autophagy, lysosomes interact directly with the components to be degraded and there is no autophagosome. Macroautophagy is the most common and researched type of autophagy, and is frequently meant when "autophagy" is discussed. Such shall be the case here as well.

A staggering number of proteins and other molecules participate in autophagy. Some are signaling molecules that contribute to the induction of autophagy. Most of the others are involved in autophagosome formation, indeed the hallmark of autophagy (**Figures 22–23**). Our protein of interest, VMP1, has been shown, as much as its

involvement in autophagy is concerned, to participate in autophagosome formation (Molejón et al., 2013a and 2013b). Its location and interaction with other autophagosome proteins are shown in **Figures 22–23**.

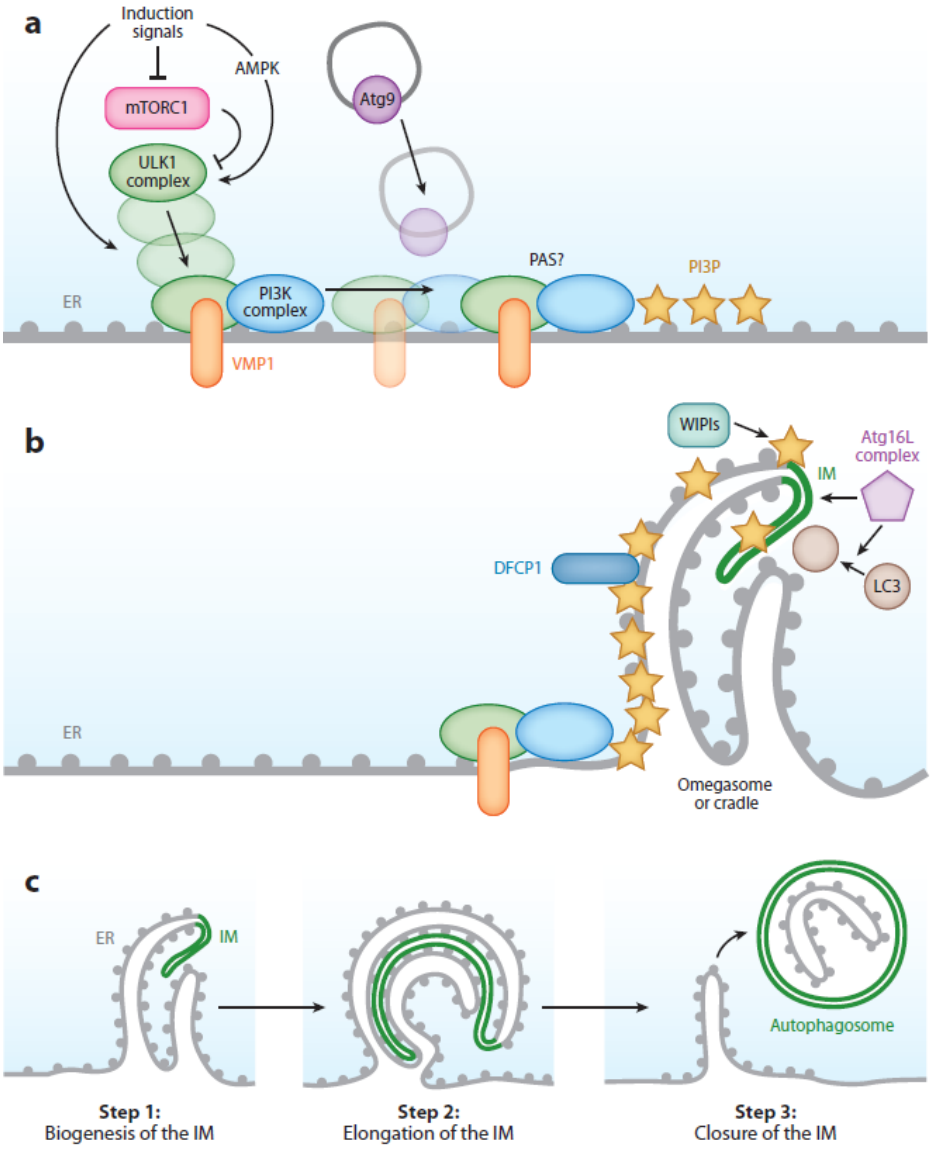

Figure 22. A proposed model of autophagosome formation. (A) The first molecules that gather at the site of autophagosome formation upon induction of autophagy. Note that the depicted induction pathway, involving mTOR (mammalian target of rapamycin), is by no means the only one known. (B) The molecular basis of the initial curving of the ER membrane, later to become an autophagosome. (C) Membrane dynamics of autophagosome formation, from the initial curving of the ER membrane, via cradle formation (also called omegasome, for its shape resembling the Greek letter omega), to closure and detachment. AMPK: adenosine monophosphate-activated protein kinase; PAS: preautophagosomal structure; WIPI: WD-repeat protein interacting with phosphoinositides; PI3K: phosphatidylinositol 3-kinase; PI3P: phosphatidylinositol 3-phosphate; IM: isolation membrane; LC3: microtubule-associated protein 1 light chain 3; ULK1: Unc-51-like kinase; DFCP1: double FYVE-containing protein 1. Taken from Mizushima et al. (2011). Original figure was cropped.

A large group of proteins called ATG (autophagy-related proteins) are the key players in autophagosome formation. They were first characterized in yeast, but since then highly conserved homologues were found in numerous eukaryotic species (Khalfan and Klionsky, 2002). To better tackle the complexity of the process, we provide two different schematics of the molecular events that lead to autophagosome formation (**Figures 22–23**). The sole role of many ATG proteins is to recruit other proteins and molecules to the preautophagosomal structure (PAS)—the site in the ER in which a new autophagosome is born. The most notable non-protein molecules that are essential for autophagosome formation are the lipids phosphatidylinositol 3-phosphate (PI3P) and phosphatidylethanolamine (PE). The former is a known recruiter of proteins to membranes, and the latter a major component of cellular membranes, amongst them the autophagosome's (Mizushima et al., 2011). VMP1, it is thought, is part of the complex that recruits the enzyme phosphtidylinositol 3-kinase (PI3K) to the PAS. This enzyme synthesizes PI3P, which in turn attracts other proteins to the PAS. Many of those are functional proteins that are able to bend and curve membranes—the nascent autophagosome is thereby starting to gain shape (Mizushima et al., 2011). As for PE, it is recruited to the membrane of the new autophagosome by ATG8 (named LC3 in mammals), the most widely used marker for measuring and tracing autophagy in research (Geng and Klionsky, 2008). ATG8 is responsible for the membrane tethering and fusion which are required for autophagosome formation (Nakatogawa et al., 2007). We so far named two roles for ATG proteins: recruitment of components, and membrane dynamics. A third role is protein processing: ATG4, for instance, is a cysteine protease that modifies the C-terminus of ATG8; the latter is not functional without this modification (Kirisako et al., 2000).

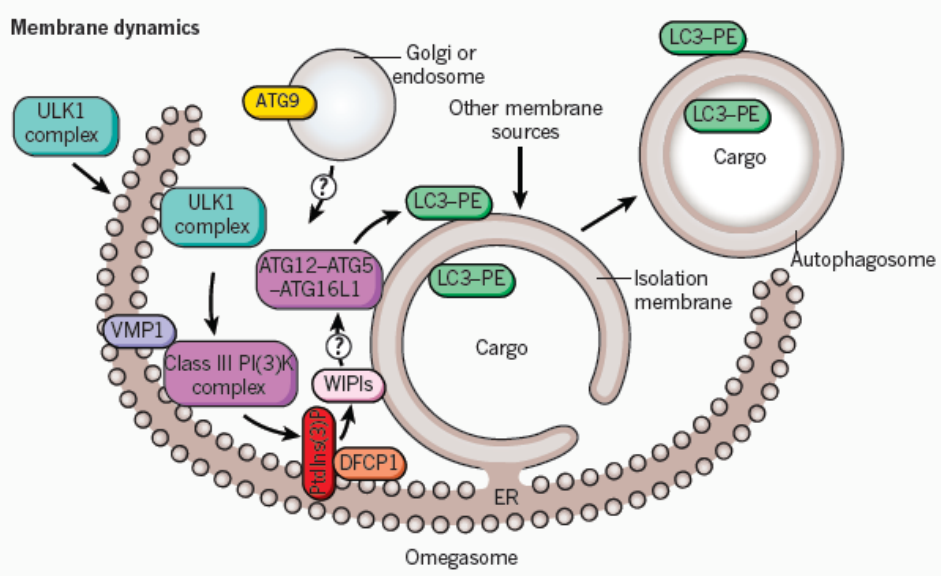

Figure 23 (previous page)**. Another depiction of the canonical autophagosome-formation model.** Abbreviations are the same as in **Figure 22**, plus: PtdIns(3)P: phosphatidylinositol 3-phosphate; PE: phosphatidylethanolamine; Taken from Levine et al. (2011). Original figure was cropped.

Can VMP1 be considered an ATG protein? This much is not yet clear. Aside from its localization to autophagy-related compartments, VMP1 was, in different reports, also localized in the Golgi apparatus (Dusetti et al., 2002) and the plasma membrane (Sauermann et al., 2008); and aside from its autophagy-related roles, it was assigned different functions as well—cell adhesion, for instance (Sauermann et al., 2008). This in itself is not reason enough to discredit VMP1 as an ATG protein: several canonical ATG proteins have been assigned additional, non-autophagy-related roles (Radoshevich et al., 2010). But, importantly, VMP1 has no homologue in yeast, whereas the greater part of the autophagy aparatus is conserved between yeast and mammals. VMP1 is not the only autophagy-related protein to not have a yeast counterpart (FIP200 is another example; Hara et al., 2008), but this fact certainly adds to its interest, since any divergence from the otherwise universally, highly conserved autophagy poses curious questions. Another interesting fact worth mentioning is that all ATG proteins, with ATG9 being the sole exception (Noda et al., 2000), are not transmembrane proteins. Whether VMP1 is the second one may be a matter of semantics, but the interest that this protein evokes is irrefutable.

In our study we show, albeit tentatively, that autophagy may be downregulated in *Chlamydomonas* VMP1 knockdown cells (it should be noted that autophagy was never actively induced in our experiments. The observed autophagic phenomena in our WT cells represent basal autophagy, possibly in combination with slight, unintentional nutrient deprivation as a function of the culture's age). With regard to the observed underexpression of autophagy markers (**Figure 16B**), we identified with interest VMP1's interaction partner in humans, beclin-1 (named ATG6 in yeast), as one of the genes downregulated in our knockdown. The VMP1-beclin-1 interaction in human was shown to be essential for the induction of autophagy (Ropolo et al., 2007). It would be of interest to test whether a regulatory adaptation of beclin-1 levels to VMP1 levels in the cell accounts for the former's decreased levels in our mutant. Further evidence for compromised autophagy was delivered by TEM in the form of autolysosomes that were present in WT but nearly absent in the mutant (**Figures 14–15**), and of grossly enlarged mitochondria in the mutant (**Figure 15D**). It has been shown that inhibited autophagy results in the accumulation of enlarged mitochondria in rat myoblast cells (Terman et al., 2003). Mitochondria frequently undergo fission in healthy cells, but a fraction fail to

do so, for unknown reasons. These larger, non-fissioned mitochondria are presumably discriminated against by the autophagic (more precisely: mitophagic) machinery, since the engulfment of large organelles by autophagosomes requires more energy than that of smaller organelles. This is exacerbated by compromised autophagy, such as occurs in senescent cells or in experimental inhibition of autophagy: clearance of larger mitochondria by means of autophagy is reduced even more, and soon enough they become a majority (Cuervo et al., 2005). The increased levels of reactive oxygen species that enlarged, damaged mitochondria produce (Sohal and Sohal, 1991) in turn damage the autophagic machinery even more.

The accumulation of starch, as seen in our TEM images, may also be a sign of disrupted autophagy: the aberrant accumulation of glycogen, starch's animal counterpart, in three genetic human diseases—Lafora disease (Aguado et al., 2010), Pompe disease (Fukuda et al., 2007), and Danon disease (Nishino et al., 2000)—with detrimental pathophysiologies, has been shown in the cited studies to be a result of compromised autophagy. More recently and relevantly, disrupted/inhibited autophagy resulted in starch accumulation in leaves of *Arabidopsis thaliana* and *Nicotiana benthamiana* (Wang et al., 2013). Indeed, no excess of starch was found in our mutant when quantified enzymatically; however, the accumulation of starch in excessively large granules may not necessarily correspond to an overall increase in cellular starch content.

An additional piece of evidence is reflected in the results of our lipidomic profiling (**Figure 18**). Our knockdown cells accumulate TAGs, which may be well ascribed to defective autophagy (Singh et al., 2009). According to the cited study, reduced hydrolysis of TAGs by defective autophagosomes causes the former to accumulate. Our results and the interpretation we propose seem to contradict several studies that showed that the massive TAG and starch accumulation that occurs in nitrogen-deprived *Chlamydomonas* is accompanied by very pronounced autophagy (Wang et al., 2009). If TAG and starch accumulation go hand in hand with autophagy, why do we observe the two former phenomena in our supposedly autophagy-compromised cells? We postulate that the effects reported in the cited, and other, studies, indeed prerequisite nitrogen starvation, a dramatic onslaught that forces the cell to degrade proteins in order to replenish its amino-acid stock, this by means of autophagy. Basal autophagy, such as in our experiments, presumably behaves differently. As mentioned above, Singh et al. (2009) found that disrupted autophagy results in TAG accumulation in rat and mouse, and, conversely, that induced autophagy results in decreased TAG levels. This has been shown in *Chlamydomonas* as well: applying the autophagy inhibitor 3-methyladenine resulted in TAG accumulation in both nitrogen-deprived and control cells (Msanne,

2011), whereupon the author concluded that TAG accumulation in nitrogen-deprived cells may not be a direct result of autophagy.

Another observation combines our microscope images and our lipidomic profiling. A small fraction of our cells displayed a highly globulized phenotype (**Figure 12I**). This occurred in WT as well, but much more frequently in the VMP1 knockdown. These cells greatly resemble the lipid-body accumulating cells, following nitrogen deprivation, seen in Goodson et al. (2011; **Figure 24**). Presumably nitrogen deprivation occurred in a fraction of our cultures, resulting in massive accumulation of lipid bodies, which, incidentally, contain mainly TAGs (such cultures, it should be noted, were never used in any other experiment). The fact that this occurred much more frequently in the VMP1 knockdown reinforces the finding of TAG accumulation mediated by our analytical profiling, and again, contradicts, if indeed autophagy is compromised in our cells, the findings reported by Goodson et al. (2011).

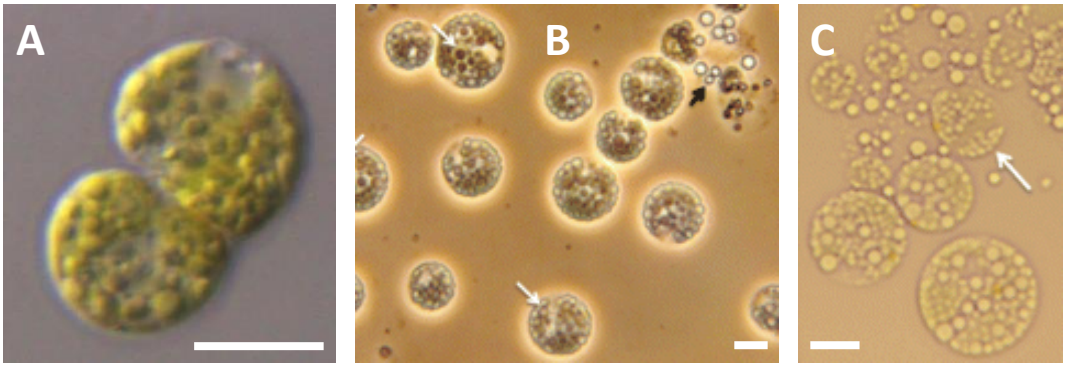

Figure 24. Globulized cells in VMP1 knockdown cells and in the literature. (A) a VMP1 knockdown cell (strain UVM11, this work; **Figure 12I**). (B) Wild-type cells (strain CC-4349) following a four-day nitrogen starvation. (C) The same cells as in B, but following an acetate boost. B and C taken from Goodson et al. (2011). Original images figures were cropped. Original figure numbers were Figure 5A (B) and Figure 4E (C). Scale bars = 5 μm. Scale bars did not originally appear in B and C. White arrows indicate starch.

TAG is not the only lipid class changed in our mutant; but it is the most coherently changed. The changes we observe in other classes of lipids may also be related to autophagy, especially in the context of lipids that are constituents of the autophagosome and autolysosome membranes. Out of six phosphatidylethanolamine (PE) species that we detected, four were reduced in the mutant (two considerably, two mildly), one was unchanged and one accumulated in the mutant. PE is the major lipid involved in the initial stages of autophagosome formation, and it conjugates with ATG8 (Nakatogawa et al., 2007). However, conclusions to be drawn from that must remain

tentative: it is not known how paucity or plethora of autophagosomes influence the overall levels of PE in the cell; it is also not known which other lipid classes are major components of autophagosomes and autolysosomes. Incidentally, PE has also been shown to be essential for cytokinesis: Chinese hamster ovary cells depleted of PE showed severe cytokinesis defects (Emoto and Umeda, 2000).

4.7 VMP1, autophagy and cytokinesis: a link between the three?

Further experiments are required in order to provide a more definite conclusion in regard to the autophagic capacity of our mutant: ATG8 is better used in its Western-blot rather than its qRT-PCR version as a marker for autophagy, and the matter-filled vacuoles that we identified as autolysosomes in our TEM images need to be molecularly defined using established markers. Lastly, numerous reasons can account for the accumulation of TAGs, indeed a common stress response in many organisms; a direct link between the accumulation that we observe and defective autophagy still requires establishment.

Our results show concurrence with observations in other organisms with regard to VMP1's involvement in autophagy, but also suggest a heretofore unreported involvement in cell division. It is interesting to note that despite the relatively high sequence conservation between the different VMP1 homologues, CrVMP1 occupies a phylogenetic branch distinct from the other six reported homologues (**Figure 1C**). Plausibly its sequence divergence is responsible for its added roles in *Chlamydomonas*. That said, the two hallmarks of our mutant phenotype, defective cytokinesis and defective autophagy, may be tightly linked to each other. Two recent reports provide such a link. In the first, inhibition of autophagy resulted in cytokinesis failure, multinucleation and aneuploidy in human cells (Belaid et al., 2013). According to this report, the cell uses autophagy to maintain correct levels of RhoA, a small GTPase protein critical for cytokinesis. The second report shows that inhibited autophagy in yeast results, under conditions of starvation, in aneuploidy, abnormal mitosis, and growth deficiency (Matsui et al., 2013). An even more direct link between cytokinesis and VMP1's specific role in autophagy is provided by phosphatidylinositol 3-phosphate (PI3P). The synthesis of this lipid at the preautophagosomal site is essential for autophagosome formation and is mediated by the enzyme PI3-kinase class III, which forms a complex with, among others, VMP1 (Molejón et al., 2013b). PI3K-III has been shown to form complexes that regulate cytokinesis, and that are very similar to the autophagy-related PI3K-III complexes. Downregulation of various components of the

PI3K-III complex resulted in impaired cytokinesis (Sagona et al., 2010; Thoresen et al., 2010). It is therefore possible that cytokinesis in our mutant is inhibited either as a result of impaired autophagy, whereby the VMP1 deficiency is solely the cause for said impairment; or that the VMP1 deficiency causes the cytokinesis defect in a more direct fashion, possibly through the disruption of PI3K-III complexes. Thus far, VMP1' strong involvement in cancer in humans, a disease whose hallmark is cell division gone awry, has been shown to be a result of the protein's roles in cell adhesion (Sauermann et al., 2008) and in autophagy (Pardo et al., 2010; Lo Ré et al., 2012). Our results may point toward a more direct role of VMP1 in cell division.

4.8 Summary and outlook

VMP1 has been researched before in a plant (*A. thaliana*; Wang et al., 2011) and in a microorganism (*D. discoideum*; Calvo-Garrido et al., 2008), and now: in a species that is both. In this study we generated VMP1-deficient *Chlamydomonas* and subsequently identified both a novel role for VMP1 and a new gene involved in *Chlamydomonas* cell division. CrVMP1-deficient cells exhibited disrupted cytokinesis and aberrant morphologies. Cell-biological and biochemical evidence suggest malfunctioning autophgay: mutant cells accumulated triacylglycerides and formed enlarged starch granules; they were devoid of autolysosomes although WT cells showed many; and they showed enlarged mitochondria. In addition, mutants underexpressed several genes involved in cell-cycle regulation and autophagy. Several issues remain to be addressed: what are CrVMP1's interaction partners and subcellular localization in *Chlamydomonas*? In what way does CrVMP1 influence cytokinesis so dramatically? Are the effects seen in the mutant a direct consequence of reduced CrVMP1 levels, or is rather a long cascade of events involved? We hope that follow-up studies will provide further elucidation.

5. References

Aguado C, Sarkar S, Korolchuk VI, Criado O, Vernia S, Boya P, Sanz P, de Córdoba SR, Knecht E, Rubinsztein DC (2010) Laforin, the most common protein mutated in Lafora disease, regulates autophagy. *Hum Mol Genet*, **19:** 2867–2876.

Allen RD (2000) The contractile vacuole and its membrane dynamics. *BioEssays*, **22:** 1035–1042.

Allen RD, Tominaga T, Naitoh Y (2008) The contractile vacuole complex and cell volume control in protozoa. In: Osmotic and Ionic Regulation: Cells and Animals. Edited by Evans DH, CRC Press, Boca Raton, FL, USA.

Altschul SF, Gish W, Miller W, Myers EW, Lipman DJ (1990) Basic local alignment search tool. *J Mol Biol*, **215:** 403–410.

Arvidsson S, Kwasniewski M, Riaño-Pachón DM, Mueller-Roeber B (2008) QuantPrime—a flexible tool for reliable high-throughput primer design for quantitative PCR. *BMC Bioinformatics*, **9:** 465.

Belaid A, Cerezo M, Chargui A, Corcelle-Termeau E, Pedeutour F, Giuliano S, Ilie M, Rubera I, Tauc M, Barale S, Bertolotto C, Brest P, Vouret-Craviari V, Klionsky DJ, Carle GF, Hofman P, Mograbi B (2013) Autophagy plays a critical role in the degradation of active RHOA, the control of cell cytokinesis, and genomic stability. *Cancer Res*, **73:** 4311–4322.

Bard F, Casano L, Mallabiabarrena A, Wallace E, Saito K, Kitayama H, Guizzunti G, Hu Y, Wendler F, DasGupta R, Perrimon N, Malhotra V (2006) Functional genomics reveals genes involved in protein secretion and Golgi organization. *Nature*, **439:** 604–607.

Benoliel AM, Pirro N, Marin V, Consentino B, Pierres A, Vitte J, Bongrand P, Sielezneff I, Sastre B (2003) Correlation between invasiveness of colorectal tumor cells and adhesive potential under flow. *Anticancer Res*, **23:** 4891–4896.

Bernstein E (1960) Synchronous division in *Chlamydomonas moewusii*. *Science*, **131:** 1528–1529.

Bertani G (1951) Studies on lysogenesis. I. The mode of phage liberation by lysogenic *Escherichia coli*. *J Bacteriol*, **62:** 293–300.

Betapudi V, Mason C, Licate L, Egelhoff TT (2005) Identification and characterization of a novel α-kinase with a von Willebrand factor A-like motif localized to the contractile vacuole and golgi complex in *Dictyostelium discoideum*. *Mol Biol Cell*, **16:** 2248–2262.

Betapudi V, Egelhoff TT (2009) Roles of an unconventional protein kinase and myosin II in *Amoeba* osmotic shock responses. *Traffic*, **10:** 1773–1784.

Bethesda Research Laboratories (1986) BRL pUC host: *E. coli* DH5α competent cells. *Focus*, **8:2** 9.

Bradford MM (1976) A rapid and sensitive method for the quantitation of microgram quantities of protein utilizing the principle of protein-dye binding. *Anal Biochem*, **72:** 248–254.

Briesemeister S, Blum T, Brady S, Lam Y, Kohlbacher O, Shatkay H (2009) SherLoc2: a high-accuracy hybrid method for predicting subcellular localization of proteins. *J Proteome Res*, **8:11** 5363–5366.

Briesemeister S, Rahnenführer J, Kohlbacher O (2010) YLoc: an interpretable web server for predicting subcellular localization. *Nucleic Acids Res*, **38:** W497–W502.

Burgess SJ, Tredwell G, Molnar A, Bundy JG, Nixon PJ (2012) Artificial microRNA-mediated knockdown of pyruvate formate lyase (PFL1) provides evidence for an active 3-hydroxybutyrate production pathway in the green alga *Chlamydomonas reinhardtii*. *J Biotechnol*, **162:1** 57–66.

Burkhard P, Stetefeld J, Strelkov S (2001) Coiled coils: a highly versatile protein folding motif. *Trends Cell Biol*, **11:2** 82–88.

Calvo-Garrido J, Carilla-Latorre S, Lázaro-Diéguez F, Egea G, Escalante R (2008) Vacuole Membrane Protein 1 is an endoplasmic reticulum protein required for organelle biogenesis, protein secretion, and development. *Mol Biol Cell*, **19:** 3442–3453.

Calvo-Garrido J, **Escalante R** (2010) Autophagy dysfunction and ubiquitin-positive protein aggregates in *Dictyostelium* cells lacking VMP1. *Autophagy*, **6:1** 100–109.

Camargo A, Llamas A, Schnell RA, Higuera JJ, Gonzalez-Ballester D, Lefebvre PA, Fernandez E, Galvan A (2007) Nitrate signaling by the regulatory gene *NIT2* in *Chlamydomonas*. *Plant Cell*, **19:** 3491–3503

Cao B, Porollo A, Adamczak R, Jarrell M, Meller J (2006) Enhanced recognition of protein transmembrane domains with prediction-based structural profiles. *Bioinformatics*, **22:3** 303–309.

Carpenter EP, Beis K, Cameron AD, Iwata S (2008) Overcoming the challenges of membrane protein crystallography. *Curr Opin Struct Biol*, **18:5** 581–586.

Chastellier CD, Quiviger B, Ryter A (1978) Observations on the functioning of the contractile vacuole of *Dictyostelium discoideum* with the electron microscope. *J Ultrastruct Res*, **62:3** 220–227.

Cole DG, Diener DR, Himelblau AL, Beech PL, Fuster JC, Rosenbaum JL (1998) *Chlamydomonas* kinesin-II-dependent intraflagellar transport (IFT): IFT particles contain proteins required for ciliary assembly in Caenorhabditis elegans sensory neurons. *J Cell Biol*, **141:4** 993–1008,

Cooper S (2004) Whole-culture synchronization cannot, and does not, synchronize cells. *Trends Biotechnol*, **22:6** 274–276.

Crespo JL, Díaz-Troya S, Florencio FJ (2005) Inhibition of target of rapamycin signaling by rapamycin in the unicellular green alga *Chlamydomonas reinhardtii*. *Plant Physiol*, **139:** 1736–1749.

Cuervo AM, Bergamini E, Brunk UT, Dröge W, Ffrench M, Terman A (2005). Autophagy and aging: the importance of maintaining "clean" cells. *Autophagy*, **1:3** 131–140.

Damer CK, Bayeva M, Hahn ES, Rivera J, Socec CI (2005) Copine A, a calcium-dependent membrane-binding protein, transiently localizes to the plasma membrane and intracellular vacuoles in *Dictyostelium*. *BMC Cell Biol*, **6:46**.

Damer CK, Bayeva M, Kim PS, Ho LK, Eberhardt ES, Socec CI, Lee JS, Bruce EA, Goldman-Yassen AE, Nalibof LC (2007) Copine A is required for cytokinesis, contractile vacuole function, and development in *Dictyostelium*. *Eukaryot Cell*, **6:3** 430–442.

Dieckmann CL (2003) Eyespot placement and assembly in the green alga *Chlamydomonas*. *BioEssays*, **25:4** 410–416.

Doberstein SK, Baines IC, Wiegand G, Korn ED, Pollard TD (1993) Inhibition of contractile vacuole function *in vivo* by antibodies against myosin-I. *Nature*, **365:** 841–843.

Du F, Edwards K, Shen Z, Sun B, De Lozanne A, Briggs S, Firtel RA (2008) Regulation of contractile vacuole formation and activity in *Dictyostelium*. *EMBO J*, **27:** 2064–2076.

Dusetti NJ, Jiang Y, Vaccaro MI, Tomasini R, Samir AZ, Calvo EL, Ropolo A, Fiedler F, Mallo GV, Dagorn JC, Iovanna JL (2002) Cloning and expression of the rat Vacuole Membrane Protein 1 (VMP1), a new gene activated in pancreas with acute pancreatitis, which promotes vacuole formation. *Biochem Biophys Res Commun*, **290:** 641–649.

Dziuba N, Ferguson MR, O'Brien WA, Sanchez A, Prussia AJ, McDonald NJ, Friedrich BM, Li G, Shaw MW,Sheng J, Hodge TW, Rubin DH, Murray JL (2012) Identification of cellular proteins required for replication of human immunodeficiency virus type 1. *AIDS Res Hum Retroviruses*, **28:10** 1329–1339.

Eichinger L, Pachebat JA, Glockner G, Rajandream MA, Sucgang R, Berriman M, Song J, Olsen R, Szafranski K, Xu Q, Tunggal B, Kummerfeld S, Madera M, Konfortov BA, Rivero F, Bankier AT, Lehmann R, Hamlin N, Davies R, Gaudet P, Fey P, Pilcher K, Chen G, Saunders D, Sodergren E, Davis P, Kerhornou A, Nie X, Hall N, Anjard C, Hemphill L, Bason N, Farbrother P, Desany B, Just E, Morio T, Rost R, Churcher C, Cooper J, Haydock S, van Driessche N, Cronin A, Goodhead I, Muzny D, Mourier T, Pain A, Lu M, Harper D, Lindsay R, Hauser H, James K, Quiles M, Madan Babu M, Saito T, Buchrieser C, Wardroper A, Felder M, Thangavelu M, Johnson D, Knights A, Loulseged H, Mungall K, Oliver K, Price C, Quail MA, Urushihara H, Hernandez J, Rabbinowitsch E, Steffen D, Sanders M, Ma J, Kohara Y, Sharp S, Simmonds M, Spiegler S, Tivey A, Sugano S, White B, Walker D, Woodward J, Winckler T, Tanaka Y, Shaulsky G, Schleicher M, Weinstock G, Rosenthal A, Cox EC, Chisholm RL, Gibbs R, Loomis WF, Platzer M, Kay RR, Williams J, Dear PH, Noegel AA, Barrell B, Kuspa A (2005) The genome of the social amoeba *Dictyostelium discoideum*. *Nature*, **435:** 43-57.

Emanuelsson O, Brunak S, von Heijne G, Nielsen H (2007) Locating proteins in the cell using TargetP, SignalP, and related tools. *Nat Protoc*, **2:** 953–971.

Emoto K, Umeda M (2000) Regulation of contractile ring disassembly by redistribution of phosphatidylethanolamine. *J Cell Biol*, **149:6** 1215–1224.

Fernandez E, Schnell R, Ranum LP, Hussey SC, SilXow CD, Lefebvre PA (1989) Isolation and characterization of the nitrate reductase structural gene of *Chlamydomonas reinhardtii*. *Proc Natl Acad Sci USA*, **86:** 6449–6453.

Fischer N, Rochaix JD (2001) The flanking regions of *PsaD* drive efficient gene expression in the nucleus of the green alga *Chlamydomonas reinhardtii*. *Mol Genet Genomics*, **265:** 888–894.

Fok AK, Clarke M, Ma L, Allen RD (1993) Vacuolar H^+-ATPase of *Dictyostelium discoideum*: a monoclonal antibody study. *J Cell Sci*, **106:** 1103–1113.

Fok AK, Aihara MS, Ishida M, Nolta KV, Steck TL, Allen RD (1995) The pegs on the decorated tubules of the contractile vacuole complex of *Paramecium* are proton pumps. *J Cell Sci*, **108:** 3163–3170.

Fukuda T, Roberts A, Plotz PH, Raben N (2007) Acid alpha-glucosidase deficiency (Pompe disease). *Curr Neurol Neurosci Rep*, **7:** 71–77.

Furukawa R, Fechheimer M (1994) Differential localization of α-actinin and the 30-kD actin-bundling protein in the cleavage furrow, phagocytic cup, and contractile vacuole of *Dictyostelium discoideum. Cytoskeleton*, **29:** 46–56.

Gabriel D, Hacker U, Köhler J, Müller-Taubenberger A, Schwarz JM, Westphal M, Gerisch G (1999) The contractile vacuole network of *Dictyostelium* as a distinct organelle: its dynamics visualized by a GFP marker protein. *J Cell Sci*, **112:** 3995–4005.

Garz A, Sandmann M, Rading M, Ramm S, Menzel R, Steup M (2012) Cell-to-cell diversity in a synchronized *Chlamydomonas* culture as revealed by single-cell analyses. *Biophys J*, **103:** 1078–1086.

Geng J, Klionsky DJ (2008) The Atg8 and Atg12 ubiquitin-like conjugation systems in macroautophagy. *EMBO Rep*, **9:9** 859–864.

Gerald NJ, Siano M, De Lozanne A (2002) The *Dictyostelium* LvsA protein is localized on the contractile vacuole and is required for osmoregulation. *Traffic*, **3:** 50–60.

Gilabert M, Vaccaro MI, Fernandez-Zapico ME, Calvo EL, Turrini O, Secq V, Garcia S, Moutardier V, Lomberk G, Dusetti N, Urrutia R, Iovanna JL (2013) Novel role of VMP1 as modifier of the pancreatic tumor cell response to chemotherapeutic drugs. *J Cell Physiol*, **228:** 1834–1843.

Goodson C, Roth R, Wang ZT, Goodenough U (2011) Structural correlates of cytoplasmic and chloroplast lipid body synthesis in *Chlamydomonas reinhardtii* and stimulation of lipid body production with acetate boost. *Eukaryot Cell*, **10:12** 1592–1606.

Gorman DS, Levine RP (1965) Cytochrome *f* and plastocyanin: their sequence in the photosynthetic electron transport chain of *Chlamydomonas reinhardtii*. *Proc Natl Acad Sci USA*, **54:** 1665–1669.

Grasso D, Sacchetti ML, Bruno L, Lo Ré A, Iovanna JL, Gonzalez CD, Vaccaro MI (2009) Autophagy and VMP1 expression are early cellular events in experimental diabetes. *Pancreatology*, **9:1** 81–88.

Grasso D, Ropolo A, Lo Ré A, Boggio V, Molejón MI, Iovanna JL, Gonzalez CD, Urrutia R, Vaccaro MI (2011) Zymophagy, a novel selective autophagy pathway mediated by VMP1-Usp9x- p62, prevents pancreatic cell death. *J Biol Chem*, **286:10** 8308–8324.

Guillard RRL (1960) A Mutant of *Chlamydomonas moewusii* lacking contractile vacuoles. *J Protozool*, **7:3** 262–268.

Guo L, Yang LY, Fan C, Chen GD, Wu F (2012) Novel roles of VMP1: Inhibition metastasis and proliferation of hepatocellular carcinoma. *Cancer Sci*, **103:12** 2110–2119.

Gutierrez L, Mauriat M, Guénin S, Pelloux J, Lefebvre JF, Louvet R, Rusterucci C, Moritz T, Guerineau F, Bellini C, Van Wuytswinkel O (2008) The lack of a systematic validation of reference genes: a serious pitfall undervalued in reverse transcription polymerase chain reaction (RT-PCR) analysis in plants. *Plant Biotechnol J*, **6:** 609–618.

Hara T, Takamura A, Kishi C, Iemura S, Natsume T, Guan JL, Mizushima N (2008) FIP200, a ULK-interacting protein, is required for autophagosome formation in mammalian cells. *J Cell Biol*, **181:** 497–510.

Harper JDI, Wu L, Sakuanrungsirikul S, John PCL (1995) Isolation and partial characterization of conditional cell division cycle mutants in *Chlamydomonas*. *Protoplasma*, **186:3–4**, 149–162.

Harper JDI (1999) *Chlamydomonas* cell-cycle mutants. *Int Rev Cytol*, **189:** 131–176.

Harris EH (2009) The *Chlamydomonas* Sourcebook. San Diego, CA: Academic Press.

Hartwell LH (1970) Periodic density fluctuation during the yeast cell cycle and the selection of synchronous cultures. *J Bacteriol*, **104:3** 1280–1285.

Heath RJW, Insall RH (2008) *Dictyostelium* MEGAPs: F-BAR domain proteins that regulate motility and membrane tubulation in contractile vacuoles. *J Cell Sci*, **121:** 1054–1064.

Helmstetter CE, Cummings DJ (1963) Bacterial synchronization by selection of cells at division. *Proc Natl Acad Sci USA*, **50:4** 767.

Hess FD, Bayer D (1977) Binding of the herbicide trifluralin to *Chlamydomonas* flagellar tubulin. *J Cell Sci*, **24:** 351–360.

Heuser J, Zhu Q, Clarke M (1993) Proton pumps populate the contractile vacuoles of *Dictyostelium* amoebae. *J Cell Biol*, **121:6** 1311–1327.

Heuser J (2006) Evidence for recycling of contractile vacuole membrane during osmoregulation in *Dictyostelium* amoebae—A tribute to Günther Gerisch. *Eur J Cell Biol*, **85:** 859–871.

Hirono M, Yoda A (1997) Isolation and phenotypic characterization of *Chlamydomonas* mutants defective in cytokinesis. *Cell Struct Funct*, **22:1** 1–5.

Hofmann K, Stoffel W (1993) Tmbase—A database of membrane-spanning protein segments. *Biol Chem Hoppe-Seyler*, **374:** 166.

Hummel E, Osterrieder A, Robinson DG, Hawes C (2010) Inhibition of Golgi function causes plastid starch accumulation. *J Exp Bot*, **61:10** 2603–2614.

Hummel J, Segu S, Li Y, Irgang S, Jueppner J, Giavalisco P (2011) Ultra-performance liquid chromatography and high resolution mass spectrometry for the analysis of plant lipids. *Front Plant Sci*, **2:54**.

Hutner SH, Provasoli L, Schatz A, Haskins CP (1950) Some approaches to the study of the role of metals in the metabolism of microorganisms. *Proc Am Philos Soc*, **94:** 152–170.

Iwamoto M, Allen RD, Naitoh Y (2003) Hypo-osmotic or Ca^{2+}-rich external conditions trigger extra contractile vacuole complex generation in *Paramecium multimicronucleatum*. *J Exp Biol*, **206:** 4467–4473.

Jung G, Titus MA, Hammer JA III (2009) The *Dictyostelium* type V myosin MyoJ is responsible for the cortical association and motility of contractile vacuole membranes. *J Cell Biol*, **186:4** 555–570.

Käll L, Krogh A, Sonnhammer ELL (2007). Advantages of combined transmembrane topology and signal peptide prediction—the Phobius web server. *Nucleic Acids Res*, **35:** W429–W432.

Kan Y, Pan J (2010) A one-shot solution to bacterial and fungal contamination in the green alga *Chlamydomonas reinhardtii* culture by using an antibiotic cocktail. *J Phycol*, **46:** 1356–1358.

Khalfan WA, Klionsky DJ (2002) Molecular machinery required for autophagy and the cytoplasm-to-vacuole targeting (Cvt) pathway in *S. cerevisiae*.*Curr Opin Cell Biol*, **14:** 468–475.

Kindle KL (1990) High-frequency nuclear transformation of *Chlamydomonas reinhardtii*. *Proc Nat Acad Sci USA*, **87:3**, 1228–1232.

Kirisako T, Ichimura Y, Okada H, Kabeya Y, Mizushima N, Yoshimori T, Ohsumi M, Takao T, Noda T, Ohsumi Y (2000). The reversible modification regulates the membrane-binding state of Apg8/Aut7 essential for autophagy and the cytoplasm to vacuole targeting pathway. *J Cell Biol*, **151:2** 263–276.

Koblenz B, Schoppmeier J, Grunow A, Lechtreck KF (2003) Centrin deficiency in *Chlamydomonas* causes defects in basal body replication, segregation and maturation. *J Cell Sci*, **116:13** 2635–2646.

Komsic-Buchmann K, Stephan LM, Becker B (2012) The SEC6 protein is required for contractile vacuole function in *Chlamydomonas reinhardtii*. *J Cell Sci*, **125:** 2885–2895.

Krogh A, Larsson B, von Heijne G, Sonnhammer EL (2001) Predicting transmembrane protein topology with a hidden Markov model: application to complete genomes. *J Mol Biol*, **305:** 567–580.

Kubo T, Kaida S, Abe J, Saito T, Fukuzawa H, Matsuda Y (2009) The *Chlamydomonas* hatching enzyme, sporangin, is expressed in specific phases of the cell Cycle and is localized to the flagella of daughter cells within the sporangial cell wall. *Plant Cell Physiol*, **50:3** 572–583.

Kunst A, Draeger B, Ziegenhorn J (1988), in Methods in Enzymatic Analysis, 3rd ed., Vol. 6, editor: Bergmeyer HU, 163–171. Weinheim, Germany: Chemie.

Kuwayama H, Obara S, Morio T, Katoh M, Urushihara H, Tanaka Y (2002) PCR-mediated generation of a gene disruption construct without the use of DNA ligase and plasmid vectors. *Nucleic Acids Res*, **30:** U14–U18.

Ladenburger EM, Korn I, Kasielke N, Wassmer T, Plattner H (2006) An Ins(1,4,5)P_3 receptor in *Paramecium* is associated with the osmoregulatory system. *J Cell Sci*, **119:** 3705–3717.

Lamb MR, Dutcher SK, Worley CK, Dieckmann CL (1999) Eyespot-assembly mutants in *Chlamydomonas reinhardtii*. *Genetics*, **153:2** 721–729.

Levine B (2005) Eating oneself and uninvited guests: autophagy-related pathways in cellular defense. *Cell*, **120:2** 159–162.

Levine B, Mizushima N, Virgin HW (2011) Autophagy in immunity and inflammation. *Nature*, **469:** 323–335.

Livak KJ, Schmittgen TD (2001) Analysis of relative gene expression data using real-time quantitative PCR and the 2(-delta delta C(T)) method. *Methods*, **25:** 402–408.

Lisec J, Schauer N, Kopka J, Willmitzer L, Fernie AR (2006) Gas chromatography mass spectrometry-based metabolite profiling in plants. *Nat Protoc*, **1:** 387–396.

Lo Ré AE, Fernández-Barrena MG, Almada LL, Mills LD, Elsawa SF, Lund G, Ropolo A, Molejón MI, Vaccaro MI, Fernandez-Zapico ME (2012) Novel AKT1-GLI3-VMP1 pathway mediates KRAS oncogene-induced autophagy in cancer cells. *J Biol Chem*, **287:** 25325–25334.

Lumbreras V, Stevens DR, Purton S (1998) Efficient foreign gene expression in *Chlamydomonas reinhardtii* mediated by an endogenous intron. *Plant J*, **14:** 441–447.

Lupas A, Van Dyke M, Stock J (1991) Predicting coiled coils from protein sequences. *Science*, **252:** 1162–1164.

Luykx P, Hoppenrath M, Robinson DG (1997a) Structure and behavior of contractile vacuoles in *Chlamydomonas reinhardtii*. *Protoplasma*, **198:** 73–84.

Luykx P, Hoppenrath M, Robinson DG (1997b) Osmoregulatory mutants that affect the function of the contractile vacuole in *Chlamydomonas reinhardtii*. *Protoplasma*, **200:** 99–111.

Maruyama Y, Yanagita T (1956) Physical methods for obtaining synchronous culture of *Escherichia coli*. *J Bacteriol*, **71:5** 542.

Matsui A, Kamada Y, Matsuura A (2013) The role of autophagy in genome stability through suppression of abnormal mitosis under starvation. *PLoS Genet*, **9:1** e1003245.

Mercanti V, Blanc C, Lefkir Y, Cosson P, Letourneur F (2006) Acidic clusters target transmembrane proteins to the contractile vacuole in *Dictyostelium* cells. *J Cell Sci*, **119:** 837–845.

Merchant SS, Prochnik SE, Vallon O, Harris EH, Karpowicz SJ, Witman GB, Terry A, Salamov A, Fritz-Laylin LK, Marechal-Drouard L, Marshall WF, Qu LH, Nelson DR, Sanderfoot AA, Spalding MH, Kapitonov VV, Ren Q, Ferris P, Lindquist E, Shapiro H, Lucas SM, Grimwood J, Schmutz J, Cardol P, Cerutti H, Chanfreau G, Chen CL, Cognat V, Croft MT, Dent R, Dutcher S, Fernandez E, Fukuzawa H, Gonzalez-Ballester D, Gonzalez-Halphen D, Hallmann A, Hanikenne M, Hippler M, Inwood W, Jabbari K, Kalanon M,

Kuras R, Lefebvre PA, Lemaire SD, Lobanov AV, Lohr M, Manuell A, Meier I, Mets L, Mittag M, Mittelmeier T, Moroney JV, Moseley J, Napoli C, Nedelcu AM, Niyogi K, Novoselov SV, Paulsen IT, Pazour G, Purton S, Ral JP, Riano-Pachon DM, Riekhof W, Rymarquis L, Schroda M, Stern D, Umen J, Willows R, Wilson N, Zimmer SL, Allmer J, Balk J, Bisova K, Chen CJ, Elias M, Gendler K, Hauser C, Lamb MR, Ledford H, Long JC, Minagawa J, Page MD, Pan J, Pootakham W, Roje S, Rose A, Stahlberg E, Terauchi AM, Yang P, Ball S, Bowler C, Dieckmann CL, Gladyshev VN, Green P, Jorgensen R, Mayfield S, Mueller-Roeber B, Rajamani S, Sayre RT, Brokstein P, Dubchak I, Goodstein D, Hornick L, Huang YW, Jhaveri J, Luo Y, Martinez D, Ngau WC, Otillar B, Poliakov A, Porter A, Szajkowski L, Werner G, Zhou K, Grigoriev IV, Rokhsar DS, and Grossman AR (2007). The *Chlamydomonas* genome reveals the evolution of key animal and plant functions. *Science*, **318:** 245–250.

Mizushima N, Yoshimori T, Ohsumi Y (2011) The role of ATG proteins in autophagosome formation. *Annu Rev Cell Dev Biol*, **27:** 107–132.

Molejón MI, Ropolo A, Lo Ré A, Boggio V, Vaccaro MI (2013a) The VMP1-Beclin 1 interaction regulates autophagy induction. *Scientific Rep*, **3:** 1055.

Molejón MI, Ropolo A, Vaccaro MI (2013b) VMP1 is a new player in the regulation of the autophagy-specific phosphatidylinositol 3-kinase complex activation. *Autophagy*, **9:6** 1–3.

Molnar A, Bassett A, Thuenemann E, Schwach F, Karkare S, Ossowski S, Weigel D, Baulcombe D (2009) Highly specific gene silencing by artificial microRNAs in the unicellular alga *Chlamydomonas reinhardtii*. *Plant J*, **58:** 165–174.

Moniakis J, Coukell MB, Janiec A (1999) Involvement of the Ca^{2+}-ATPase PAT1 and the contractile vacuole in calcium regulation in *Dictyostelium discoideum*. *J Cell Sci*, **112:** 405–414.

Montalvetti A, Rohloff P, Docampo R (2004) A functional aquaporin co-localizes with the vacuolar proton pyrophosphatase to acidocalcisomes and the contractile vacuole complex of *Trypanosoma cruzi*. *J Biol Chem*, **279:37** 38673–38682.

Msanne J (2011) Abiotic stress responses in photosynthetic organisms. University of Nebraska-Lincoln, PhD dissertation.

Nakatogawa H, Ichimura Y, Ohsumi Y (2007). Atg8, a ubiquiting-like protein required for autophagosome formation, mediates membrane tethering and hemifusion. *Cell*, **130:1** 18–20.

Neupert J, Karcher D, Bock R (2009) Generation of *Chlamydomonas* strains that efficiently express nuclear transgenes. *Plant J*, **57:** 1140–1150.

Nishihara E, Yokota E, Tazaki A, Orii H, Katsuhara M, Kataoka K, Igarashi H, Moriyama Y, Shimmen T, Sonobe S (2008) Presence of aquaporin and V-ATPase on the contractile vacuole of *Amoeba proteus*. *Biol Cell*, **100:** 179–188.

Nishino I, Fu J, Tanji K, Yamada T, Shimojo S, Koori T, Mora M, Riggs JE, Oh SJ, Koga Y, Sue CM, Yamamoto A, Murakami N, Shanske S, Byrne E, Bonilla E, Nonaka I, DiMauro

S, Hirano M (2000) Primary LAMP-2 deficiency causes X-linked vacuolar cardiomyopathy and myopathy (Danon disease). *Nature*, **406:** 906–910.

Noda T, Kim J, Huang WP, Baba M, Tokunaga C, Ohsumi Y, Klionsky DJ (2000) Apg9/Cvt7p is an integral membrane protein required for transport vesicle formation in the Cvt and autophagy pathways. *J Cell Biol*, **148:3** 465–480.

Nüsse M, Egner HJ (1984) Can nocodazole, an inhibitor of microtubule formation, be used to synchronize mammalian cells? *Cell Proliferation*, **17:** 13–23.

Ogata H, Goto S, Sato K, Fujibuchi W, Bono H, Kanehisa, M (1999) KEGG: Kyoto Encyclopedia of Genes and Genomes. *Nucleic Acids Res*, **27:** 29–34.

Ossowski S, Schwab R, Weigel D (2008) Gene silencing in plants using artificial microRNAs and other small RNAs. *Plant J*, **53:4** 674–690.

Pagni M, Ioannidis V, Cerutti L, Zahn-Zabal M, Jongeneel CV, Hau J, Martin O, Kuznetsov D, Falquet L (2007) MyHits: improvements to an interactive resource for analyzing protein sequences. *Nucleic Acids Res*, **35:** 433–7.

Pardo R, Lo Ré A, Archange C, Ropolo A, Papademetrio DL, Gonzalez CD, Alvarez EM, Iovanna JL, Vaccaro MI (2010) Gemcitabine induces the VMP1-mediated autophagy pathway to promote apoptotic death in human pancreatic cancer cells. *Pancreatology*, **10:1** 19–26.

Pérez-Pérez ME, Florencio FJ, Crespo JL (2010). Inhibition of target of rapamycin signaling and stress activate autophagy in *Chlamydomonas reinhardtii*. *Plant Physiol*, **152:** 1874–1888.

Pérez-Pérez ME, Crespo JL (2010). Autophagy in the model alga *Chlamydomonas reinhardtii*. *Autophagy*, **6:4**, 562–563.

Pérez-Pérez ME, Couso I, Crespo JL (2012). Carotenoid deficiency triggers autophagy in the model green alga *Chlamydomonas reinhardtii*. *Autophagy*, **8:3** 376–388.

Petersen TN, Brunak S, von Heijne G, Nielsen H (2011) SignalP 4.0: discriminating signal peptides from transmembrane regions. *Nature Methods*, **8:** 785–786.

Pfannenschmid F, Wimmer VC, Rios RM, Geimer S, Kröckel U, Leiherer A, Haller K, Nemcová Y, Mages W (2003) *Chlamydomonas* DIP13 and human NA14: a new class of proteins associated with microtubule structures is involved in cell division. *J Cell Sci*, **116:** 1449–1462.

Punta M, Coggill PC, Eberhardt RY, Mistry J, Tate J, Boursnell C, Pang N, Forslund K, Ceric G, Clements J, Heger A, Holm L, Sonnhammer ELL, Eddy SR, Bateman A, Finn RD (2012) The Pfam protein families database. *Nucleic Acids Res*, **40:** 290–301.

Qin H, Wang Z, Diener D, Rosenbaum J (2007) Intraflagellar Transport Protein 27 is a small G protein involved in cell-cycle control. *Curr Biol*, **17:** 193–202.

Quiviger B, Chastellier CD, Ryter A (1978) Cytochemical demonstration of alkaline phosphatase in the contractile vacuole of *Dictyostelium discoideum*. *J Struct Biol*, **62:** 228–236.

Radoshevich L, Murrow L, Chen N, Fernandez E, Roy S, Fung C, Debnath J (2010) ATG12 conjugation to ATG3 regulates mitochondrial homeostasis and cell death. *Cell*, **142:4** 590–600.

Rai A, Nöthe H, Tzvetkov N, Korenbaum E, Manstein DJ (2010) *Dictyostelium* dynamin B modulates cytoskeletal structures and membranous organelles. *Cell Moll Life Sci*, **68:16** 2751–2767.

Roessner U, Luedemann A, Brust D, Fiehn O, Linke T, Willmitzer L, Fernie A (2001) Metabolic profiling allows comprehensive phenotyping of genetically or environmentally modified plant systems. *Plant Cell*, **13:** 11–29.

Rohloff P, Montalvetti A, Docampo R (2004) Acidocalcisomes and the contractile vacuole complex are involved in osmoregulation in *Trypanosoma cruzi*. *J Biol Chem*, **279:50** 52270–52281.

Ropolo A, Grasso D, Pardo R, Sacchetti ML, Archange C, Lo Ré A, Seux M, Nowak J, Gonzalez CD, Iovanna JL, Vaccaro MI (2007) The pancreatitis-induced Vacuole Membrane Protein 1 triggers autophagy in mammalian cells. *J Biol Chem*, **282:51** 37124–37133.

Ruiz FA, Marchesini N, Seufferheld M, Govindjee, Docampo R (2001) The polyphosphate bodies of *Chlamydomonas reinhardtii* possess a proton-pumping pyrophosphatase and are similar to acidocalcisomes. *J Biol Chem*, **276:49** 46196–46203.

Sagona AP, Nezis IP, Pedersen NM, Liestøl K, Poulton J, Rusten TE, Skotheim RI, Raiborg C, Stenmark H (2010) PtdIns(3)P controls cytokinesis through KIF13A-mediated recruitment of FYVE-CENT to the midbody. *Nat Cell Biol*, **12:4** 362–371.

Saheb E, Biton I, Maringer K, Bush J (2013) A functional connection of *Dictyostelium* paracaspase with the contractile vacuole and a possible partner of the vacuolar proton ATPase. *J Biosci*, **38:** 509–521.

Sauermann M, Sahin Ö, Sültmann H, Hahne F, Blaszkiewicz S, Majety M, Zatloukal K, Füzesi L, Poustka A, Wiemann S, Arlt D (2008) Reduced expression of Vacuole Membrane Protein 1 affects the invasion capacityof tumor cells. *Oncogene*, **27:** 1320–1326.

Schägger H (2006) Tricine-SDS-PAGE. *Nat Protoc*, **1:** 16–22.

Schmidt-Nielsen B, Schrauger CR (1963) *Amoeba proteus*: studying the contractile vacuole by micropuncture. *Science*, **139:** 606–607.

Schmollinger S, Strenkert D, Schroda M (2010) An inducible artificial microRNA system for *Chlamydomonas reinhardtii* confirms a key role for heat shock factor 1 in regulating thermotolerance. *Curr Gen*, **56:** 383–389.

Schroda M (2006) RNA silencing in *Chlamydomonas*: mechanisms and tools. *Curr Genet*, **49:** 69–84.

Schwab R, Ossowski S, Riester M, Warthmann M, Weigel D (2006) Highly specific gene silencing by artificial microRNAs in *Arabidopsis*. *Plant Cell*, **18:5** 1121–1133.

Sesaki H, Wong EFS, Sui CH (1997) The cell adhesion molecule DdCAD-1 in *Dictyostelium* is targeted to the cell surface by a nonclassical transport pathway involving contractile vacuoles. *J Cell Biol*, **138:4** 939–951.

Shin J, Dunbrack RL Jr, Lee S, Strominger JL (1991) Signals for the retention of transmembrane proteins in the endoplasmic reticulum studied with CD4 truncation mutants. *Proc Natl Acad Sci USA*, **88:** 1918–1922.

Singh R, Kaushik S, Wang Y, Xiang Y, Novak I, Komatsu M, Tanaka K, Cuervo AM, Czaja MJ (2009) Autophagy regulates lipid metabolism. *Nature*, **458:** 1131–1135.

Sizova I, Fuhrmann M, Hegemann P (2001) A *Streptomyces rimosus* aphVIII gene coding for a new type phosphotransferase provides stable antibiotic resistance to *Chlamydomonas reinhardtii*. *Gene*, **277:** 221–229.

Small I, Peeters N, Legeai F, Lurin C (2004) Predator: a tool for rapidly screening proteomes for N-terminal targeting sequences. *Proteomics*, **4:6** 1581–1590.

Sohal RS, Sohal BH (1991) Hydrogen peroxide release by mitochondria increases during aging. *Mech Ageing Dev*, **57:** 187–202.

Spallanzani L (1799) Tracts on the Nature of Animals and Vegetables. Edinburgh.

Stavrou I, O'Halloran TJ (2006) The monomeric clathrin assembly protein, AP180, regulates contractile vacuole size in *Dictyostelium discoideum*. *Mol Biol Cell*, **17:** 5381–5389.

Stock C, Grønlien HK, Allen RD, Naitoh Y (2002) Osmoregulation in *Paramecium*: in situ ion gradients permit water to cascade through the cytosol to the contractile vacuole. *J Cell Sci*, **115:11** 2339–2348.

Strachan SD, Hess FD (1983) The biochemical mechanism of action of the dinitroaniline herbicide oryzalin. *Pestic Biochem Physiol*, **20:** 141–150.

Sueoka N (1960) Mitotic replication of deoxyribonucleic acid in *Chlamydomonas reinhardtii*. *Proc Natl Acad Sci USA*, **46:** 83–91.

Tani T, Tominaga T, Allen RD, Naitoh Y (2002) Development of periodic tension in the contractile vacuole complex membrane of *Paramecium* governs its dynamics. *Cell Biol Int*, **26:10** 853–860.

Tardif M, Atteia A, Specht M, Cogne G, Rolland N, Brugière S, Hippler M, Ferro M, Bruley C, Peltier G, Vallon O, Cournac L (2012) PredAlgo, a new subcellular localization prediction tool dedicated to green algae. *Mol Biol Evol*, **29:12** 3625–3639.

Terman A, Dalen H, Eaton JW, Neuzil J, Brunk UT (2003) Mitochondrial recycling and aging of cardiac myocytes: the rold of autophagocytosis. *Exp Gerontol*, **38:** 863–876.

Thimm O, Bläsing O, Gibon Y, Nagel A, Meyer S, Krüger P, Selbig J, Müller LA, Rhee SY, Stitt M (2004) MapMan: a user-driven tool to display genomics data sets onto diagrams of metabolic pathways and other biological processes. *Plant J*, **37:6** 914–939.

Thomas PD, Campbell MJ, Kejariwal A, Mi H, Karlak B, Daverman R, Diemer K, Muruganujan A, Narechania A (2003) PANTHER: a library of protein families and subfamilies indexed by function. *Genome Res*, **13:** 2129–2141.

Thoresen SB, Pedersen NM, Liestøl K, Stenmark H (2010) A phosphatidylinositol 3-kinase class III sub-complex containing VPS15, VPS34, Beclin 1, UVRAG and BIF-1 regulates cytokinesis and degradative endocytic traffic. *Exp Cell Res*, **316:20** 3368–3378.

Tian Y, Li Z, Hu W, Ren H, Tian E, Zhao Y, Lu Q, Huang X, Yang P, Li X, Wang X, Kovács AL, Yu L, Zhang H (2010) *C. elegans* screen identifies autophagy genes specific to multicellular organisms. *Cell*, **141:** 1042–1055.

Tooze SA, Yoshimori T (2010). The origin of the autophagosomal membrane. *Nat Cell Biol*, **12:** 831–835.

Ulrich PN, Jimenez V, Park M, Martins VP, Atwood III J, Moles K, Collins D, Rohloff P, Tarleton R, Moreno SNJ, Orlando R, Docampo R (2011) Identification of contractile vacuole proteins in *Trypanosoma cruzi*. *PLoS ONE*, **6:3**.

Vaccaro MI, Grassoa D, Ropolo A, Iovanna JL, Cerquetti MC (2003) VMP1 expression correlates with acinar cell cytoplasmic vacuolization in arginine-induced acute pancreatitis. Pancreatology, **3:** 69–74.

Vaccaro MI (2012) Zymophagy: selective autophagy of secretory granules. *Int J Cell Biol*, **2012:** 1–7.

Wang J, Virta VC, Riddelle-Spencer K, O'Halloran TJ (2003) Compromise of clathrin function and membrane association by clathrin light chain deletion. *Traffic*, **4:** 891–901.

Wang P, Hummel E, Osterrieder A, Meyer AJ, Frigerio L, Sparkes I, Hawes C (2011) KMS1 and KMS2, two plant endoplasmic reticulum proteins involved in the early secretory pathway. *Plant J*, **66:4** 613–628.

Wang Y, Yu B, Zhao J, Guo J, Li Y, Han S, Huang L, Du Y, Hong Y, Tang D, Liu Y (2013) Autophagy contributes to leaf starch degradation. *Plant Cell*, **25:4** 1383–1399.

Wang ZT, Ullrich N, Joo S, Waffenschimdt S, Goodenough U (2009) Algal lipid bodies: stress induction, purification, and biochemical characterization in wild-type and starchless *Chlamydomonas reinhardtii*. *Eukaryot Cell*, **8:12** 1856–1868.

Wen Y, Stavrou I, Bersuker K, Brady RJ, De Lozanne A, O'Halloran TJ (2009) AP180-mediated trafficking of Vamp7B limits homotypic fusion of *Dictyostelium* contractile vacuoles. *Mol Biol Cell*, **20:** 4278–4288.

Wigg D, Bovee EC, Jahn TL (1967) The evacuation mechanism of the water expulsion vesicle ("contractile vacuole") of *Amoeba proteus*. *J Eukaryot Microbiol*, **14:1** 104–108.

Xu P, Zhang Y, Kang L, Roossinck MJ, Mysore KS (2006) Computational estimation and experimental verification of off-target silencing during posttranscriptional gene silencing in plants. *Plant Physiol*, **142:** 429–440.

Yamasaki T, Miyasaka H, Ohama T (2008) Unstable RNAi effects through epigenetic silencing of an inverted repeat transgene in *Chlamydomonas reinhardtii*. *Genetics*, **180:** 1927–1944.

Ying Q, Liang L, Guo W, Zha R, Tian Q, Huang S, Yao J, Ding J, Bao M, Ge C, Yao M, Li J, He X (2011) Hypoxia-inducible microRNA-210 augments the metastatic potential of tumor cells by targeting Vacuole Membrane Protein 1 in hepatocellular carcinoma. *Hepatology*, **54:6** 2064–2075.

Yu CS, Chen YC, Lu CH, Hwang JK (2006) Prediction of protein subcellular localization. *Proteins: Structure, Function and Bioinformatics*, **64:** 643–651.

Zhao T, Wang W, Bai X, Qi Y (2009) Gene silencing by artificial microRNAs in *Chlamydomonas*. *Plant J*, **58:** 157–164.

Zhu Q, Clarke M (1992) Association of calmodulin and an unconventional myosin with the contractile vacuole complex of *Dictyostelium discoideum*. *J Cell Biol*, **118:2** 347–358.

Acknowledgements

Martin Steup Project outline, meticulous supervision, invaluable advice | **Hans-Gerd Löhmannsröben** Generous support and collaboration | **AG Steup,** in particular **Michael Sandmann** and **Julia Smirnova,** and **AG Willmitzer,** especially **Mariusz Bromke, Alvaro Cuadros-Inostroza, Andrea Leisse, Gudrun Wolter, Änne Eckardt, Antje Bolze,** and **AG Others: Carsten Hille, Juliane Neupert, Daniel Karcher, Gini Wendenburg, Jessica Jueppner, Flavia Vischi-Winck, Stefan Schmollinger, Samuel Arvidsson, Patrick Giavalisco, Susann Irgang** Immense technical advice, assistance, help, aid, succor, and support | **Anke Koch** Unrelenting encouragement | **Parents** Not so much for their unwavering support as for not disturbing me too much | **Rouhollah Mehrdad Barahimipour** Dedicated, benevolent, disinterested assistance | **Eugenia Maximova** Professional microscopy | **Michael Schroda, Sabeeha Merchant, Andre Scheffel** Discussions, insights, ideas, suggestions | **Rafael Perl-Treves** and **Hanokh Czosnek** Kindly agreeing to review my thesis | **Hans-Peter Eckle** Friend and mentor | **Lothar Willmitzer** Providing magnanimous sustenance to my ailing PhD | **Zip** Jew gone green (alga) | **Yarden** Böse gelbe Babykatze | **Yariv Brotman** Without whom.